A NOVEL APPROACH FOR VASCULARIZING TISSUE ENGINEERED CARDIAC SCAFFOLDS

A Dissertation

by

NICOLE AMRITA MEHTA

Submitted to the Office of Graduate and Professional Studies of
Texas A&M University
in partial fulfillment of the requirements for the degree of

DOCTOR OF PHILOSOPHY

Chair of Committee,	Fred J. Clubb Jr.
Co-Chair of Committee,	Doris A. Taylor
Committee Members	Lakeshia J. Taite
	Bradley R. Weeks
Head of Department,	Ramesh Vemulapalli

August 2019

Major Subject: Biomedical Sciences

ABSTRACT

Each year as cardiovascular disease continues to be one of the leading causes of death world wide, new treatment options are researched daily. For those whose cardiovascular disease progresses to end-stage heart failure, the gold standard remains transplantation. Those awaiting transplant however, far outweighs the available donor organs. One such potential to alleviate the donor shortage are decellularized cardiac scaffolds. These acellular scaffolds retain the native extracellular matrix and larger order branched vasculature. Retention of the native extracellular matrix creates an environment that is most optimal to support cell survival and differentiation. However, during the decellularization process the smaller microvasculature is mostly lost. The oxygen diffusion limitation in the body is around ~200 microns, and since the vast majority of tissues in the body are vascularized and accordingly need vascular supplies to remain viable, attention is turned to creating an environment that will increase the vascularization of said scaffolds. In order to increase said microvascular content, my dissertation study is focused on utilizing three angiogenic growth factors, Vascular endothelial growth factor A (VEGF-A), Platelet derived growth factor ββ and Angiopoietin 1 and creating a collagenous based system to deliver these growth factors to decellularized scaffolds and encourage vascular growth at a higher rate than would be seen otherwise.

First, a model *in vitro* system was created to simulate the decellularized scaffold environment for testing the growth factor delivery system. This was done by using a 3D decellularized extracellular matrix hydrogel derived from porcine left ventricles, and cross-

linked genipin. The gels were then characterized, and were seen to be able to support cell survival, proliferation, and even encourage trans-differentiation of human adipose derived stem cells towards a cardiac lineage. Then, research was focused on the testing of the growth factor release within a collagenous matrix. Release was found to mimic a pattern similar to *in vivo* angiogenesis over the course of 22 days. Analysis of angiogenic machinery, specifically the endothelial cell lumen formation complex, showed that critical lumen formation components were either upregulated or similar to controls, evidence that the presence of the growth factors do not aberrantly affect cellular behavior. Finally, endothelial cells were either seeded within the collagenous delivery system or on top of, that was then formed on top of the dECM hydrogels. Cells that had been encapsulated within the collagen invaded deeper into the dECM hydrogels faster than their control counterparts. The research done here provided the groundwork that this collagenous angiogenic growth factor delivery system may be used one day to increase the rate at which microvasculature can form in deceullarized scaffolds.

ACKNOWLEDGEMENTS

I would like to thank my committee Co-Chairs Dr. Fred Clubb, and Dr. Doris A. Taylor for their unwavering support in my pursuant of my degree, and their guidance. I would also like to thank my committee members Dr. Lakeshia Taite and Dr. Brad Weeks for their constant support and help. Thanks especially to the Muneoka lab for letting me use their equipment, and to our research assistant Nick Edenhoffer for his assistance. Finally, thanks to my mother and father for their encouragement and to my boyfriend Ryan Attridge.

Dr. Doris A. Taylor- Dr. Taylor I cannot thank you enough. You took a chance on me taking me on as your graduate student, and I have worked tirelessly for the past 4 years to make you not regret your decision! (I hope I have succeeded!) You have improved me significantly as a scientist, a writer, and a human being. I have never been pushed so hard by someone to do better, and have also never been as motivated by someone to do better. I have learned so much from you and I will cherish all the things I have learned forever. When I look back at my writing from when I first started with you it makes me laugh to see how far we have come. Thanks for being a strong female role model and always looking out for me. In a field where there are less than 2% females, it has been such an inspiration, and an honor to work under you. I hope that we can stay in contact, as you will forever be my mentor. One of the things that you have repeatedly said to me when I was nervous and getting ready to present something is “I got your back”- while that may seem trivial, it was a reminder to me that I wasn’t alone in this process and you were always looking out for me. I hope in times of hardship you are able to pull out your Doris the Stem

Cell book and remind yourself that you are a strong brilliant scientist- and the world looks up to you!

Dr. Fred J. Clubb Jr.- Dr. Clubb when I think back about how we first met, when I accidently cut in line in front of another student at a mentor lunch in 2013, I am astonished you still chose me as your student. You have been a constant source of positivity, mentorship, and friendship. I have learned so much under your wing about pathology, science, and life. In the times I felt like I was about to go thermonuclear about random things you were always there to be a calming and guiding mentor. You never questioned my desire to go to medical school and you always encouraged me to follow my dreams. Thanks for always instilling the mantra of "cooperate then graduate" to me. I feel like it applies to all life situations! Some of my favorite memories are of us all traveling to the ASAIO conferences and listening to your army and THI stories over a Guinness. You will be one of the most important influencers of my life and I hope we stay in contact throughout my career! (Cue Dr. Clubb to make a joke about his self-driving car taking him to the morgue)

Dr. Lakeshia Taite- Dr. Taite there aren't enough words in the dictionary to express my gratitude for your support throughout this Ph.D. You took the role of "lab mom" in addition to mentor, committee member, and research scientist. You were always able to help show the glass half full to me in every situation. I remember when I first started and I was so scared of all the questions you asked me, and felt like I was so naïve and destined for failure. What I didn't realize at the time was that you showed me how to be a scientist

from those questions. You showed me how to successfully answer any question I was asked with a thoughtful answer. You have a tremendous ability to guide and mentor students and I am so privileged to have experienced that mentorship. You always supported me on my journey, all the way till medical school applications. The fun times we had in the lab are some of my most cherished memories- from making gels, watching serial killers, to filming medical school applications, we had a great time all while doing great work. I know we will stay in contact forever, and I can't wait to see what good we can do for the world in the future! All I can say is, #Laminout.

Dr. Bradley Weeks- I cannot thank you enough for your kindness and guidance over the past 6 years. All the way from the beginning, I have enjoyed working with you and just talking with you in general. You always made me feel welcome and like I was a valued member of the lab. Some of my favorite memories of grad school include our funny conversations during evaluations and meetings. You have a knack for bringing the humor and the joy into every situation, even ones that are a huge bummer! I will always cherish those conversations we had, and especially the ones where we came up with random inventions (various selfie sticks, and who can forget photoshipe). Thanks so much for all the scientific conversations, and all the conversations that we had that turned into not only science, but life lessons.

Ryan Attridge- My love and best friend for 7.5 years. The journey we have been on together has been amazing, and I can't wait to continue it. If there is one person who takes credit for me being able to complete my Ph.D., it's you. You have been the one day after

day to tell me to not quit. On the days where I was ready to throw in the towel, it was you who always showed me the bright side of things. Even if it was you saying, “I’m sure it’s not that bad” those words always made me put things into perspective. The fact that you have stuck by me even through times when I was crying over P values and data shows a lot about who you are as a person. You have never questioned me on my academic journey, despite being on my 3rd degree and soon to be pursuing my fourth. You have also never judged me for being 26 and never having a real adult job yet (one day Ryan, one day). I love you so much and I am so happy that we get to spend our lives together. Oakley and Andy Mehta-Attridge- the most appreciation goes to my two sweet puppies, Oakley and Andy. Oakley, you have been my best friend and emotional support animal for 6 years. Whenever my blood pressure would rise, or I felt stressed out, I felt a sweet little furry head lay in my lap and saw a adorable little black dog with a wagging tail looking back up at me. If there is one thing in this world that truly got me through this, it’s you buddy. Thanks for always being there for me, for greeting me when I got home despite failing at experiments, with happiness. I love you so much, and my next field of research will be on cloning you because you will be my best friend forever! Andy, my little demon child puppy, I love your outlook on life. Even when you literally ate my dissertation outline, my MCAT study outlines, and destroyed my couch, you always did it with a sweet little look in your eyes. Despite you destroying my house I love you so much, as you are genuinely one of the goofiest and kindest souls I have ever interacted with. Thank you for teaching me to keep playing constantly, and to also put my important papers up high out of your reach. Thanks also go to my friends and colleagues and the department faculty and staff for making my time at Texas A&M University a great experience.

CONTRIBUTORS AND FUNDING SOURCES

This work was supported by a dissertation committee consisting of Professor Fred J. Clubb, Profressor Bradley Weeks, of the Department of Veterinary Pathobiology, and Doris A. Taylor [co-advisor], and Lakeshia Taite of the Department of Veterinary Physiology and Pharmacology.

All research was funded by the Center for Cell and Organ Biotechnology, specifically from the Texas Emerging Technology fund, and the Cardiovascular Pathology Laboratory.

In Chapter 1, all material was written and authored by N.A. Mehta.

In Chapter 2, all hypothesis, and study designs were developed jointly by N.A Mehta, L.J. Taite, and D.A Taylor. All experiments were conducted by N.A. Mehta. All analysis were performed by N.A. Mehta.

In Chapter 3, all hypothesis, and study designs were developed jointly by N.A Mehta, L.J. Taite, and D.A Taylor. Decellularization and DNA assays were performed by N.P. Edenhoffer. All other experiments and data collection was conducted by N.A Mehta. All statistical analyses were performed by N.A. Mehta.

All other work conducted for the dissertation was completed by the student independently.

NOMENCLATURE

EC	Endothelial Cell
HUVEC	Human Umbilical Vein Endothelial Cells
dECM	Decellularized Extracellular Matrix
3D	Three Dimensional
2D	Two Dimensional
GF	Growth Factor
VEGF	Vascular Endothelial Growth Factor
Ang1	Angiopoietin 1
PDGF-BB	Platelet Derived Growth Factor- Beta Beta
hADSC	Human Adipose Derived Stem Cell

TABLE OF CONTENTS

Page

LIST OF FIGURES

Page

LIST OF TABLES

Page

1 INTRODUCTION*

1.1 Whole Cardiac Tissue Bioscaffolds

1.1.1 Introduction

Cardiovascular disease continues to be the leading cause of death worldwide, with more patients progressing to heart failure each year [1-3]. Current treatments for heart failure are targeted at symptomatic improvements whereas newer investigative strategies are aimed at repairing injured myocardium or regenerating healthy myocardium, often via regenerative medicine approaches. Despite recent advancements in the field, few patients regain full cardiac function. Currently, the most effective treatment for patients with end-stage heart failure is cardiac allo-transplantation [4, 5]. However, the list of patients awaiting transplant far exceeds donor hearts available [6]. Therefore, developing alternative treatments for heart failure remains a top priority.

One potential therapy is the use of a bio-scaffold to replace or support damaged cardiac tissue. An acellular scaffold could be applied to the surface of the heart to prevent, or even reverse, dilatation, or could be dosed with cells and delivered at the site of injury to aid in the restoration of lost cardiac cells and promote healing. Ideal scaffold candidates should be compatible with all cell types found in the heart, provide mechanical strength as location demands, guide cells to organize properly, and deliver biochemical cues for appropriate cell function within the heart [7]. These scaffolds may be sourced from biologic or synthetic materials, each of which has advantages and disadvantages.

* Reprinted with permission from Springer Nature, "Whole Cardiac Tissue Bioscaffolds" by Mehta NA†, Tang-Quan KR†, LC Sampaio, DA Taylor, 2019, Springer Nature, United Kingdon. Copyright 2018 Nicole Mehta. † Denotes co-first authorship. https://doi.org/10.1007/978-3-319-97421-7_5

Synthetic materials are not always biodegradable and often lack the characteristics required for vascular and parenchymal cell attachment and infiltration [8], but can easily be crafted into virtually any size or shape.

In contrast, biologic scaffolds – typically derived from extracellular matrix (ECM) – retain biological cues necessary for cell migration, alignment, and differentiation but can be difficult to obtain in a sterile reproducible fashion and generally have low mechanical strength for cardiovascular application. The focus of this chapter is biologic scaffolds derived from whole hearts, typically via removal of cells, to yield the cardiac extracellular matrix (ECM).

In its intact state, the cardiac ECM is a complex system that contains a multitude of structural and non-structural proteins organized as a meshwork to hold cardiac cells (myocytes, fibroblasts, cardiac vascular cells, etc.) and to provide specific biological cues for their function. The ECM meshwork is comprised of collagens, elastin, laminin, fibronectin, proteoglycans, and glycoproteins [9-12] that are arranged into two specific compartments: basement membrane and interstitium (Figure 1.1)[13-17]. The basement membrane plays a critical role in tissue function by facilitating cell-cell communication and organization [19]. It primarily consists of laminin and non-fibrillar type IV collagen, that serves as an anchor for cells and is important for cell alignment. Proper cell alignment is especially critical in the heart, as it is necessary both for cell-cell electrical communication and for productive contraction required for adequate pumping [18]. In contrast with the basement membrane, the interstitium is comprised of fibrillar collagens, elastin, various proteoglycans, and glycoproteins. It underlies the basement membrane and

provides mechanical rigidity to the tissue. The combined cardiac ECM creates a unique environment that supports multiple cell types including endothelial cells (ECs), smooth muscle cells (SMCs), cardiomyocytes, cardiac fibroblasts, neurons, and cardiac progenitor cells, in a structural arrangement sufficient for proper cardiac function.

The unique architecture of the cardiac ECM is difficult to recapitulate de novo. Not only is the macrostructure complex, but the microstructure varies with each cardiac chamber and with the valves. Furthermore, the entire myocardium is thoroughly vascularized and contains extensive neural and electrical circuits. Building a solid organ of this complexity via 3-D printing, biomaterial chemistry, or other de novo methods remains difficult to date. Alternatively, some researchers have focused on deriving ECM-based scaffolds from whole hearts that are not suitable for transplantation.

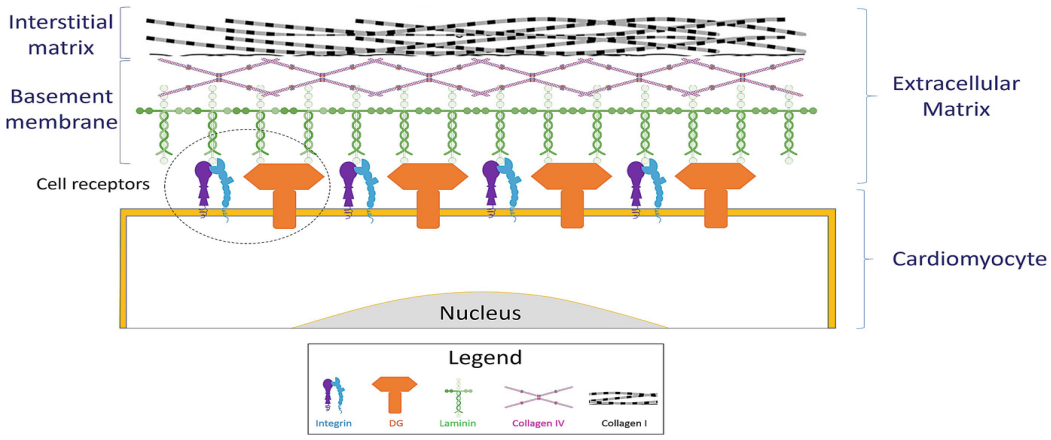

Figure 1.1: Extracellular Matrix Compartments. (1) Interstitial matrix with fibrillar collagens, elastin, proteoglycans, and glycoproteins; (2) basement membrane with non-fibrillar collagens and laminin. Cardiomyocytes attach to the basement membrane through integrins and dystroglycan (DG). Reprinted with permission from [19].

One technique widely under investigation to generate a cell-free scaffold with native-like 3D architecture is perfusion decellularization of whole hearts where cells are removed, leaving only the cardiac ECM components. This usually involves the lysis of cells in some fashion (e.g. freezing, chemical perfusate) followed by vascular and chamber perfusion to wash out cell debris, leaving behind the ECM as a scaffold (Figure 1.2). ECM bioscaffolds would be an ideal candidate for tissue engineering of a whole heart, in that

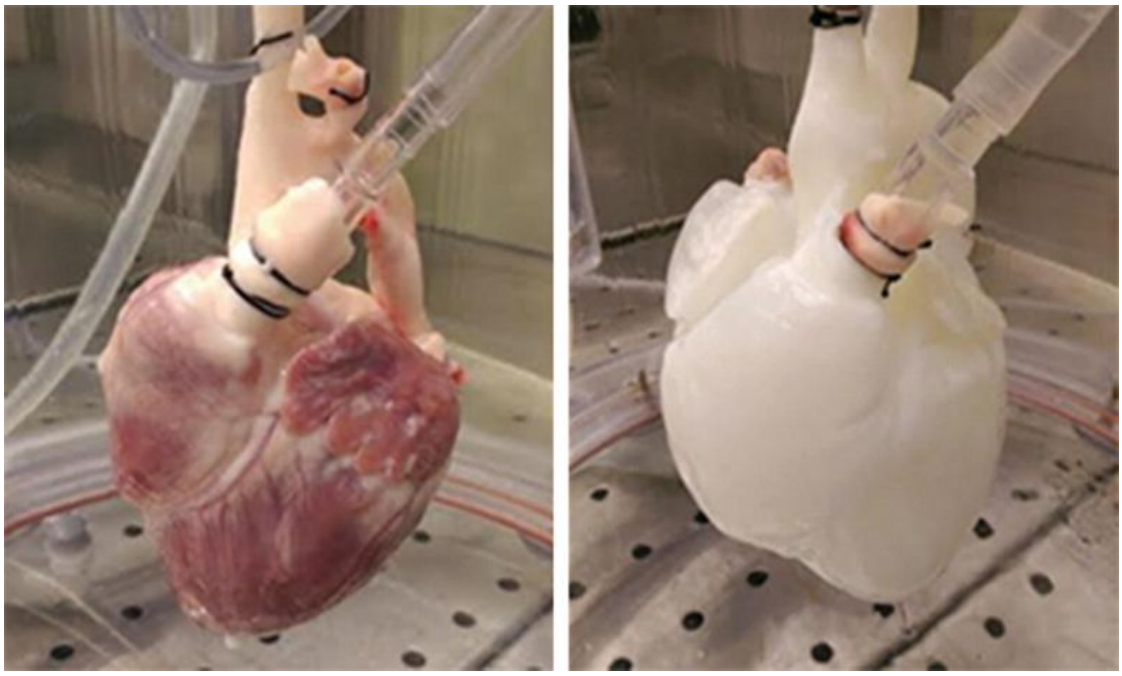

Figure 1.2: Decellularized Porcine Heart. Decellularized porcine heart (right) adjacent to a cadaveric heart porcine heart.

they can be derived from both xenogeneic sources [20] and from hearts otherwise not suitable for transplant; they retain the native vascular conduits and the native ECM macro- and micro-architecture; they preserve intrinsic biochemical cues (e.g. stereochemistry of the matrix, surface ligand density) that guide the alignment and orientation of cells seeded onto the scaffold [21, 22]; and they can theoretically be repopulated using a recipient's cells, allowing for creation of an autologous organ.

The first successful perfusion decellularization of a whole heart was achieved by our group in 2008 [23]. We successfully showed that a rat or pig heart could be decellularized, and a rat heart could subsequently be partially re-cellularized, matured *in vitro*, or transplanted *in vivo* [23]. Since then, the decellularization of whole hearts has advanced, with new methods and techniques developed to decellularize and recellularize ECM bioscaffolds. This chapter will define the current approaches for decellularization and recellularization of whole hearts and discuss methodologies for utilizing cardiac tissue bioscaffolds.

1.1.2 Decellularization

Decellularization of the heart is carried out by chemical [23-26], enzymatic [27-29], or physical [30] means with varying degrees of cell removal [31]. Chemical-based decellularization changes osmotic gradients to initiate cell membrane lysis and removal. Enzymatic decellularization cleaves cell membranes, cell-cell attachments, cell-ECM attachments, or nucleic acid ECM attachments with specific enzymes to remove cells or cell remnants from the organ. Physical methods of decellularization use techniques such as tissue freeze-thawing cycles to lyse cell membranes. Each of these is followed by a cell debris washout either via immersion or perfusion. Immersion involves the submersion of the organ, with or without agitation and then repeated solution changes to remove cellular debris. It can be viewed as an outside-in wash. Perfusion-based decellularization was developed in the Taylor lab. It is solution-agnostic, takes advantage of the native vasculature or other tissue conduits, and is the method of choice for solid, whole organs [23, 32, 33]. In the heart, perfusion is often performed via the aorta in a fashion that allows full perfusion through the coronary tree.

With any method of decellularization, the primary goal remains preservation of the native ECM composition, stiffness, and overall structure. However, each method of decellularization disrupts the ECM to varying degrees, and care must be taken to minimize ECM damage, while also eliminating cellular content. The standard for determining complete decellularization has been established as: 1) less than 50 ng of double stranded DNA (dsDNA) per mg dry weight of ECM, 2) less than 200 base pair DNA length, and 3) no nuclei visible upon staining using either hematoxylin and eosin (H&E) or DAPI (4',6-

diamidino-2-phenylindole) staining [34] garreta [35].

1.1.2.1 Chemical Decellularization

Chemical-based decellularization reagents are primarily comprised of ionic and non-ionic detergents, acids and bases, and hypertonic or hypotonic solutions. These chemicals lyse cell membranes and wash out cellular and nuclear materials by changing osmotic gradients [36]. Detergent-based decellularization has been proven to be the most effective method for removing cellular content from many tissues but must be used at low concentrations to reduce the disruption to the ECM ultrastructure and preserve glycosaminoglycan (GAG) concentrations [37-39]. Sodium dodecyl sulfate (SDS) is one of the most widely used anionic detergents for cardiac scaffold generation, as it can effectively wash out cytoplasmic proteins and nuclear debris from the thick myocardium to a greater degree than other detergents [23, 40]. However, SDS can be difficult to remove from the ECM since it is an anionic surfactant and remains bound to ECM proteins. This leads to further undesired alterations in the decellularized ECM scaffold biochemistry and structure. Another detergent often used in conjunction with SDS is Triton X-100, a non-ionic detergent shown to remove cellular contents and to aid in the washout of residual SDS from the ECM [23, 41]. While Triton X-100 treatment results in a cell-free heart valve, it is less effective in clearing the myocardium and aortic wall of cellular remnants [29].
Our group previously compared four different chemical-based decellularization techniques, including SDS, Triton X-100, enzymes, and polyethylene glycol. We found that a combination of SDS and Triton X-100 was the most effective for removing cells while

preserving the ECM. This technique has been successfully carried over into larger sized hearts, such as a porcine and human hearts [23-26, 30, 42].

1.1.2.2 Enzymatic Decellularization

Enzyme-based decellularization breaks nucleic acid bonds or cell-matrix attachments, which can be washed out from the native tissue. Nucleases, such as RNase and DNase, are used to cleave RNA and DNA into shorter strands and render the nuclei indistinguishable [43]. Since these nucleases target intracellular contents, they are often used alongside another decellularization technique, such as high pressure used in physical decellularization, to be effective [34]. Another common enzyme used in decellularization is trypsin, a serine protease that hydrolyzes proteins at the C-terminus of lysine or arginine, except when either is followed by proline. Trypsin is often used in cell culture to remove adherent cells from culture plates [44, 45]. When used in a decellularization protocol, trypsin cleaves peptide bonds that hold cells to the ECM. Other solutions, such as Triton X-100 or sodium deoxycholate, then follow the trypsin step to wash out remaining cellular material from the scaffold [46, 47]. Less common enzymes used in decellularization include collagenase, dispase, and alpha-galactosidase [34]. Just as was seen with detergents, enzyme concentrations that are too high or applied for too long can disrupt the ECM ultrastructure, strip the ECM of GAGs, and remove important glycoproteins such as laminin and fibronectin [41]. The balance between matrix preservation and nuclear and cellular clearance must be achieved for the successful generation of a usable acellular ECM bioscaffold.

1.1.2.3 Physical Decellularization

Multiple physical methods of decellularizing tissues have been employed such as agitation, freeze/thawing, and pressure application with supercritical fluids. These physical methods are typically followed with washing steps to remove any residual cellular debris. Wainwright et al. published a study that utilized freeze/thaw cycles for lysing cell membranes as the first step in decellularization [30][30]. After freeze/thaw cycles, a combination of enzymes and detergents was used to accomplish full decellularization of a porcine heart after only 10 hours [30][30]. The freeze/thaw method thus shortened the total decellularization time by lysing cell membranes prior to enzymatic and chemical decellularization. Another physical method is agitation, in which the whole heart is immersed in a decellularization reagent, followed by shaking on a mixer or a stir plate, to physically lyse cell membranes. Immersion decellularization of the whole heart often damages the external surface of the organ by the time full decellularization of inner constituents is achieved. Agitation helps diffuse reagents deeper into thick tissues, and in combination with the perfusion of the aorta, has effectively decellularized cardiac scaffolds [48].

The application of pressure in conjunction with supercritical fluids such as CO_2 that has already been used for smaller tissue pieces could potentially be used to decellularize whole organs. Supercritical CO_2 has a critical temperature of 31.1°C and a pressure of 7.40 MPa, making it a biocompatible solution that does not require copious washing steps [49]. The fluid and pressure burst open cell membranes and remove cellular contents. Supercritical CO_2 has not been applied to the whole heart yet, but its success in other tissues and smaller

pieces of the heart makes it a promising decellularization agent for creating whole cardiac bioscaffolds [50, 51].

Another approach to physical-based decellularization was recently published by our group, where we found that inversion of a porcine heart during detergent perfusion led to lower DNA content, higher collagen and elastin content, and higher heart shape index (Figure 1.3) [33]. The heart shape index was defined as the ratio of the horizontal length to the vertical length of the rectangle that fit the anterior-view of the decellularized hearts. Since higher inflow rates were necessary to maintain a pressure of 60 mmHg in the upright perfusion position, the inverted orientation of the heart during decellularization led to less aortic valve damage and improved coronary artery perfusion. Therefore, this new physical decellularization method appears superior to previously described methods used for porcine hearts [33].

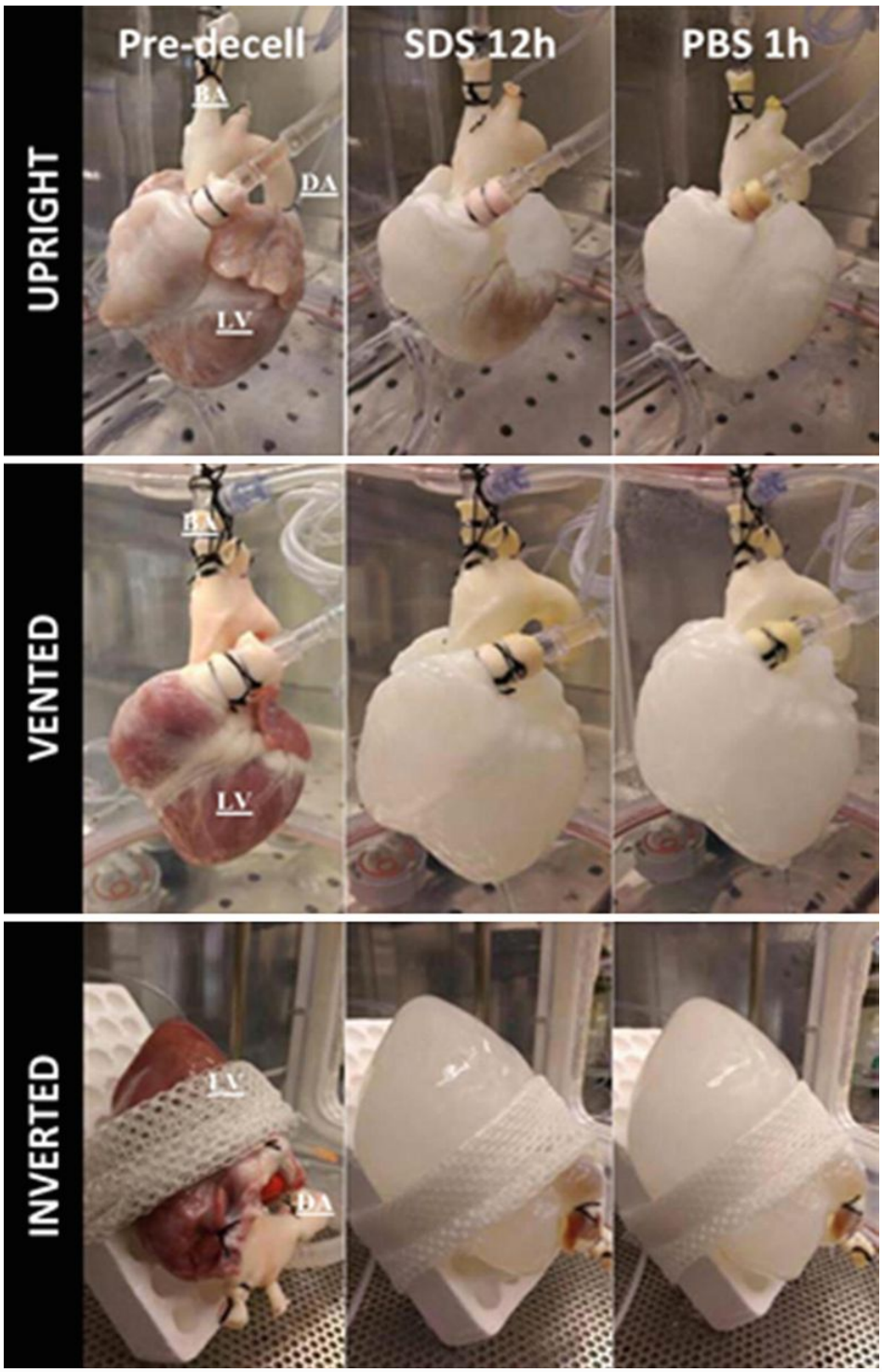

Figure 1.3: Different Orientations of the Heart During Decellularization. Orientation affects the decellularization efficacy; inverted orientation (bottom) leads to higher collagen and elastin content, as well as aortic valve preservation. *LV* Left ventricle, *DA* descending aorta, *BA* brachiocephalic artery, *SDS* sodium dodecyl sulfate, *PBS* phosphate-buffered saline. Reprinted with permission from [33].

As demonstrated by the above discussion of various decellularization methods, none has been accepted as the field or industry standard. Currently, different groups have practices that differ slightly from each other. Along with different methodologies comes numerous values for the measure of decellularization efficacy. While most methods will leave the decellularized scaffold with less than 50 ng/mg of dsDNA per mg dry weight and no nuclei on histological analysis, the variation from heart to heart is still controversial [52]. What these differences mean for recellularization and eventual application of the scaffold *in vivo* has not been fully elucidated, but ongoing research is bringing about new insights into the recellularized ECM bioscaffold.

1.1.3 Recellularization

Recellularization involves the seeding of vascular, parenchymal, and support cells into a previously decellularized scaffold. Parameters important for recellularizing the heart include cell type, cell concentrations, and seeding strategies. The variable cell composition within the heart presents a challenge when establishing the ratio of each cell type needed to recellularize the scaffold [53-55]. Research groups have recellularized murine and porcine hearts with murine or human cells, and a handful of labs have published results from human hearts recellularized with human cells [56, 57]. These reports employed different recellularization techniques: perfusion, direct injection, and a combination of perfusion and direct injection. This section discusses each recellularization strategy and its application in engineering whole cardiac tissue from decellularized ECM (dECM).

1.1.3.1 Direct Injection

The direct injection of cells into the heart involves using a syringe and needle to inject cells suspended in media into the area of interest. The use of a needle presents a concern that the ECM is damaged during the injection process. Additionally, since cells are injected into one specific location, and migration is often limited, cell density is not uniform throughout the ECM. In the first published study of a recellularized human heart, 500 million cardiomyocytes derived from human BJ fibroblast RNA-induced pluripotent stem cells (BJ RiPS) were injected using five intramyocardial direct injections between the left anterior descending artery and the left circumflex artery [24][24]. Upon histological analysis after two weeks, the 5 cm^3 injection region of the tissue showed approximately 50% cell

repopulation, confirming that uniform cell density is still lacking after recellularization via direct injection [57].

A shortcoming of recellularizing a scaffold via direct injection is the loss of cells during the injection, contributing to low numbers of cells observed in the parenchyma of the cardiac dECM bioscaffold in various studies [26, 57, 58]. Steps can be taken to mitigate the loss of cells, such as adding sutures to the sites of injection, as was done in the recellularization of the human heart; however, full cellularity of the parenchyma was still not achieved in this study. As functional cardiac tissue requires enough viable cells for gap junction formation and cardiomyocyte contractility in the parenchyma, it is critical to have complete cellular coverage in the recellularized heart. Research is ongoing to develop improved injection techniques for complete cell coverage of whole heart bioscaffolds.

1.1.3.2 Perfusion

Perfusion-based recellularization utilizes the native vascular conduits in the heart as a pathway to deliver cells. Perfusion-based recellularization is accomplished by cannulating one of the major vessels leading to the heart, most often the aorta, which allows for access to coronary arteries. Perfusion usually involves two steps: delivery of the cells where flow occurs, followed by a period of "rest" to allow cells to adhere. The adhesion of cells to the matrix is critical in all recellularization protocols but is particularly important when perfusion occurs shortly after delivery. If cells are not allowed sufficient time or provided sufficient conditions to adhere to the ECM, cells will be "washed out" of the ECM during

reperfusion, and incomplete recellularization will occur. This loss of cells would therefore result in a need for larger cell numbers for any recellularization process.

In 2011, Ng et al. cannulated the aorta of a decellularized mouse heart to deliver human embryonic stem cells (hESCs) and human mesendodermal-cells derived from hESCs to the vasculature of the heart via perfusion [59]. After the heart was in static culture for 14 days, researchers found that the stem cells expressed endothelial cell (EC) markers in the vasculature, suggesting that site-specific cues were retained in the matrix and contributed to progenitor cell differentiation. In a similar manner, Lu et al. repopulated murine hearts with cells from an embryoid body, via retrograde coronary perfusion [60]. Cells then differentiated within the recellularized dECM into cardiomyocytes and smooth muscle cells (SMCs), resulting in spontaneous contractions, new vessel formation, and responsiveness to isoproterenol, a beta-adrenergic agonist, and E4031, an antiarrhythmic agent. Although contraction occurred, evidence of arrhythmias suggested the cells were immature and that gap junction formation between cardiomyocytes was incomplete. These studies provided further confirmation that the coronary vascular tree is intact after decellularization and can be used to deliver cells to various areas of the matrix.

Due to the unidirectional flow, perfusion recellularization can result in higher cell density in large vessels that are proximal to the infusion site – upstream of smaller vessels. Yasui et al. perfused a mixture of 100 million cardiomyocytes, fibroblasts, and ECs antegrade through the coronary tree of a decellularized rat heart[61]. The variety of cells seeded into the matrix resulted in a non-homogeneous distribution of cells, with a higher concentration

of cells found closer to large vessels and near well-perfused vascular beds. However, spontaneous contractions of the heart started 2-3 days after recellularization and continued for the length of the 30 day culture period, suggesting that although cell distribution was uneven, enough cellularity was achieved through perfusion to allow the partial formation of gap junctions.

To compare injection and perfusion side-by-side, Kitahara et al. recellularized one group of porcine dECM bioscaffolds by injection and a second group by perfusion, using 1.5×10^7 porcine mesenchymal stem cells (pMSCs) in each [26]. Recellularized hearts were then heterotopically transplanted into recipient pigs. The perfusion-recellularized heart did not show patent coronary arteries during intraoperative coronary angiography, as was observed in the scaffold recellularized by injection. Interestingly, none of the perfused cells were observed in vessel lumens upon scaffold excision, while thrombi and inflammatory cells were evident in the parenchyma. Cells already present vs. those recruited into the parenchyma were not separately identified in the study. The injected pMSCs were seen in the parenchymal space in clusters and not homogeneously distributed. This observation confirmed that both methods could be used to revascularize and reseed portions of the cardiac dECM bioscaffolds, but both result in non-uniform distribution of cells throughout the matrix when compared directly.

1.1.3.3 Perfusion and Injection

Perfusion and injection is a combined approach to recellularizing the whole heart, delivering cells both with a needle into the parenchyma and to both parenchyma and

vasculature via perfusion. Our group routinely uses a combination of perfusion and intramyocardial injections to recellularize rat and pig hearts [23, 32]. Previously, we established a closed-circuit retrograde perfusion system through the aorta to infuse rat aortic endothelial cells (RAECs) directly into the patent aorta of a decellularized rat heart [23]. Histological evaluation showed adhesion of RAECs on the endocardial surface and within the vasculature of the heart. When five injections containing a mixture of neonatal cardiomyocytes, fibrocytes, ECs, and smooth muscles cells were delivered into the anterior left ventricle, a high degree of cell retention at injections sites was observed (>80%), which led to cell coupling and electrical activity propagation. By day 8, the areas of confluent cellularity were about 1 mm thick, and throughout the thickness of the ventricular wall, cell viability was greater than 95%. Although a high density of cells was maintained near the injection sites, density decreased with distance from the needle track. In another study by our group, rat hearts were re-endothelialized via three different methods: direct aortic perfusion of cells, perfusion of cells into the brachiocephalic artery (BA), or a combination of venous and arterial cell perfusions through the inferior vena cava (IVC) and BA; the combination of venous and arterial perfusion resulted in enhanced distribution of endothelial cells within the vasculature. We found that re-endothelialization of the heart's vasculature by EC perfusion improved the contractility of cardiomyocytes injected into the myocardium [62]. This improved function is not surprising since endothelial cells have been previously shown to promote cardiomyocyte organization and survival [63]. Along with the method of delivery (injection or perfusion), the order in which cells are delivered into the matrix therefore plays a role in their survival and function.

Our findings of improved cell viability and contractility from a combination of perfusion and injection recellularization have been confirmed in the whole porcine heart as well. In a study by Weymann et al., 5-6 x 10^6 human umbilical vein endothelial cells (HUVECs) were first perfused through the aorta, and then five injections of 8-9 x 10^6 neonatal rat cardiomyocytes (NRCMs) were injected intramurally into the anterior left ventricle of the decellularized porcine heart [64]. The recellularized porcine hearts were found to have platelet endothelial cell adhesion molecule-1 (PECAM-1) positive cells in the large and small coronary arteries, with minimal gaps in cell coverage. The seeded cardiomyocytes exhibited intrinsic electrical activity after 10 days in culture, but average recellularization of the scaffold was 50% around the sites of cell injection, and significantly decreased farther away from the injection sites. The electrical activity of the injected cells, as measured by multi-electrode array, demonstrated that areas of functionality could be achieved in a large whole organ, but a larger number of cells may be necessary to get complete cell coverage.

To summarize, successful recellularization of decellularized cardiac bioscaffolds will require essentially recapitulating a native heart by replacing cells in the vasculature, parenchyma, valves, etc. This will require achieving uniform cell density in the parenchyma while also promoting vascularization. High cell numbers are required to achieve complete cell coverage, and this is especially true with larger human-sized hearts. While direct injection requires the insertion of a needle with a diameter large enough for cells to pass into the scaffold, this technique allows cells to be delivered to a specific location in the myocardium. Perfusion-based recellularization allows cells to reach almost

every part of the heart by taking advantage of the native vasculature and cavities. Order of cell delivery is also important, as re-endothelialization of the vasculature prior to parenchymal recellularization increased retention of other cell types and improved function of the organ [23, 32]. Additional studies are required for conclusive statements on the order of recellularization, especially if a progenitor cell type is delivered to whole cardiac bioscaffolds.

1.1.4 Clinical Applications and Potential of Cardiac ECM Bioscaffolds

Clinical applications of decellularized whole heart scaffolds are numerous. Decellularized and/or recellularized matrices have the potential to replace heart valves [65], to create cardiac patches [66], or eventually to be used for whole heart transplantation. In fact, several acellular bioscaffolds have been FDA approved for use *in vivo* for cardiac repairs. However, the use of whole cardiac scaffolds is still being optimized, and several challenges must be addressed for *in vivo* applications. Figure 1.4 provides the workflow diagram for creating functional tissues from dECM matrices for various clinical applications.

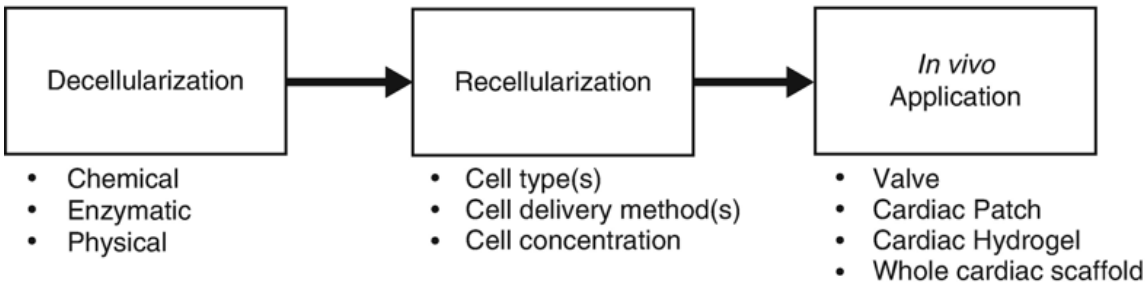

Figure 1.4: Workflow for Creating Functional Cardiac Tissue. Specficially, from decellularized bioscaffolds. Important considerations are method of decellularization, optimizing recellularization, and finally creating a product that matches the desired application.

Thrombus formation is one of the challenges of using whole cardiac dECM *in vivo*. Animal studies have shown that fully decellularized cardiac scaffolds transplanted into a

pig retained blood vessel diameter and shape, including the right coronary artery [26]. Unfortunately, these dECM scaffolds induced platelet activation, which led to inflammation and thrombosis formation. Incomplete endothelialization of scaffolds also induces thrombus formation, so complete endothelial cell coverage must be achieved for surfaces in contact with blood. Remnants of cellular and nuclear content in these scaffolds also may induce thrombus formation and inflammation. In addition, decellularization solutions that have not been completely rinsed out of the scaffold can prevent successful recellularization and engraftment into the recipient. Thorough cleaning before transplantation must be accomplished and standardized for decellularized scaffolds to be used widely *in vivo*.

1.1.4.1 Heart Valves

A valve homograft from a human cadaver to a human recipient is ideal for biocompatibility, but the shortage of organ donors is still a problem worldwide. To address this issue, mechanical and bioprosthetic heart valves (BHVs) have been used. BHVs from porcine or bovine tissue are FDA approved valves that have been sterilized and rendered biologically inactive by glutaraldehyde fixation [67]. One of the advantages of BHVs over mechanical valves is that anticoagulants are not required [68]. However, BHV calcification is commonly observed in patients, likely due to the glutaraldehyde-fixation process, increased valve stiffness, and heightened immune competence of the recipient [69]. A non-fixed decellularized heart valve could be ideal for recipients to avoid failures associated with both BHVs and mechanical valves. *In vivo* studies of decellularized valves recellularized with endothelial cells and myofibroblasts showed no thrombus formation

when implanted into juvenile sheep [70] In some studies, decellularized valves implanted into sheep have also seen positive long term outcomes, where animals were alive 9 months post implantation with functioning valves [71, 72].

Several decellularized allograft cardiac valves have already been FDA approved. CryoValve SG® (CryoLife Inc., Kennesaw, GA), the only approved human acellular pulmonary heart valve, and SynerGraft® (CryoLife Inc.) have both seen excellent long term success when implanted in humans [73, 74].

1.1.4.2 Cardiac Patches

A cardiac patch provides necessary support and biochemical cues for restoring cardiac function for diseases ranging from atrial and ventricular defects to left ventricular dysfunction. Cardiac patches can be generated in different ways, whether it be a decellularized bioscaffold, injectable gel, or a printed bioscaffold. Additionally, these patches may be either acellular or recellularized, sourced from non-cardiac tissues, and can be formed into various shapes and sizes relevant to the designed study and therapeutic intervention. Patches may also be from xenogeneic sources, as these scaffolds have been shown to be biocompatible with human cells, which allows for further patient specific customization due to variable wall thicknesses in different species [75]. Even without cells, an acellular scaffold derived from cardiac or non-cardiac tissues, can provide mechanical support to the failing heart, repair major blood vessels, and promote intracardiac repair. Bioscaffolds used for heart recovery and repair are not limited to cardiac tissues. In one study, acellular dermis was used to repair a left ventricular aneurysm [76]; however, cell

engraftment was not studied in this patient. Using urinary bladder-derived ECM, researchers observed spindle-shaped cells in the matrix after one month, showing a non-cardiac derived tissue can support cardiac-shaped cells [77]. Furthermore, acellular scaffolds inactivated with chemical treatment still retained properties that made them a hospitable environment for cells [78].

In other studies, components of the decellularized cardiac ECM were sufficient to cause an increase in regenerative capacity *in vivo*. In a cross-species study, zebrafish hearts were decellularized and lyophilized into a cardiac ECM powder [79]. This powder was resuspended in saline and applied to a mouse heart with a permanent ligation of the left anterior descending coronary artery (LAD). The results of the study were encouraging as the decellularized zebrafish ECM suspension could enable endogenous regeneration of the murine heart after acute myocardial infarction.

A few of these matrices have been FDA approved and are currently used *in vivo* with positive clinical outcomes. PhotoFix® (CryoLife Inc., Kennesaw, GA), a bovine pericardium patch, is used for patching vascular structures and intracardiac repair [80]. Similarly, CorMatrix® (Aziyo, Roswell, GA), derived from porcine small intestinal submucosa, is used for repairing atrial and ventricular septal defects, vascular abnormalities, and cardiac tumors [81]. Several other matrices are also in the pipeline for FDA approval for human use.

1.1.4.3 Hydrogels

Cardiac ECM hydrogels have recently emerged as a new technology in the field of regenerative medicine. These gels are created by using a novel method for retaining the native ECM components by turning a decellularized scaffold into a hydrogel.

1.1.4.4 Injectable Gel

The Christman group pioneered the technique for forming a hydrogel from decellularized porcine left ventricular myocardium [75, 82]. The majority of the dECM myocardial gel protocols utilize chemical detergents such as SDS or Triton X-100, while some groups recently have used supercritical CO_2 as a method to decellularize myocardial pieces [83-87]. After the myocardium is decellularized, it is enzymatically digested down using either pepsin in hydrochloric acid (HCl) or acetic acid (AA) for a period of 48-72 hours [88, 89] [90-92]. This digested dECM is then polymerized into a hydrogel by bringing the solution

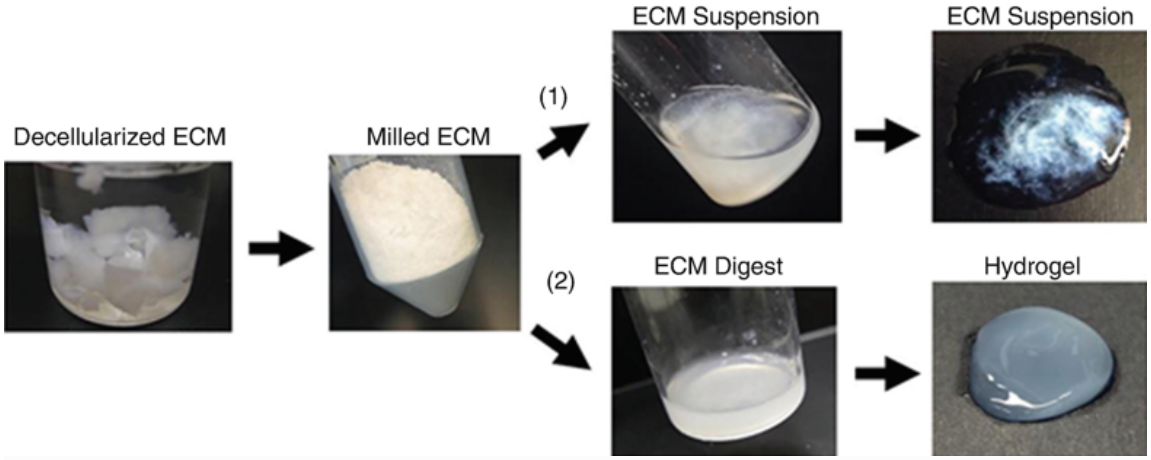

Figure 1.5: Process for the Development of Extracellular Matrix (ECM) Hydrogels. After decellularization, resulting tissue is lyophilized and milled into a fine powder. This powder is then added to a solution to form a suspension (1, top right) or digested using enzymes to form a hydrogel (2, bottom right). Reprinted with permission from [93].

to physiologic pH and salt concentrations at 37°C (Figure 1.5). The mechanical strength of these ECM hydrogels, however, are not high (<1kPa), and several researchers have explored methods to increase their mechanical strength.

To make the ECM hydrogels stiffer, different groups have added materials such as chitosan, polyethylene glycol (PEG), fibrin, and silk to make a hybrid hydrogel [92, 94-97]. These materials often bind to the matrix using photo cross-linkers to polymerize gels. The addition of an inert biocompatible polymer, such as PEG, into the ECM hydrogel to provide mechanical stiffness has been researched by the Christman group [94], where PEG crosslinked gels within 4 minutes and sustained a high cell viability. Addition of an inert biocompatible polymer is advantageous, in that the concentration of the ECM proteins is not disrupted, as would be for collagen or hyaluronic acid. Different groups have used other crosslinkers to increase the mechanical strength of these gels; for instance, genipin, a non-cytotoxic naturally derived chemical from gardenia fruit, has been used to render a hydrogel that has mechanical properties similar to native cardiac tissue [96] The hydrogels can also be delivered *in vivo* using a catheter and crosslinked *in situ* with positive results of maintained cardiac function, no induced arrhythmias, and pro-angiogenic properties when applied to an area of myocardial infarction [89-91, 98].

Currently there are no FDA-approved ECM hydrogel products, but VentriGel™ (Ventrix, Inc., San Diego, CA), a myocardial ECM hydrogel derived from porcine left ventricles, is currently in a Phase 1 Clinical trial and is set to complete in September 2018 [99]. Although there are limited clinical data on cardiac ECM hydrogels, this field has a high

potential for growth, allowing researchers to take the lead in developing new applications for clinically viable therapies.

1.1.4.5 Bioprinting

3D bioprinting involves the controlled construction of an object made layer-by-layer [100]. This allows the user to print objects of any shape and size for a desired application. Bioprinting is accomplished using different printing methods such as extrusion-based, inkjet-based, and laser-based printing [101]. The inks used with these printers range from synthetic to biologic in origin, known as a "bioink". The candidate for a bioink must maintain the desired shape and be able to withstand the addition of layers during the print process. This ink must also foster an environment suitable for cellular growth and possibly differentiation.

ECM hydrogels have been used as bioinks for 3D printing [102, 103] and hold great promise, as these gels already retain *in vivo* ECM constituents. As a bioink, ECM hydrogels can support cell differentiation and survival better than traditional bioinks, encouraging differentiation to a specific cell type based on the tissue source [104] In a comparative study, rat myoblasts showed higher expression of cardiogenic differentiation genes when cultured on bioprinted cardiac dECM than on collagen hydrogels, showing evidence that the bioink retains tissue-specific cues [104] To crosslink dECM hydrogels for printing, different photo cross-linkers have been researched such as riboflavin (vitamin b2), a non-cytotoxic alternative to other photo crosslinking agents [96, 103]. Riboflavin with the ECM alone does not crosslink rapidly but can produce cytocompatible materials

with a mechanical strength similar to native cardiac ECM [102, 103] 3D bioprinting is thus a promising technology, as customizable structures may be created. However, an existing limitation is that these structures must be intricately vascularized to support complex tissues and organs. Further research and design development is necessary to bioprint whole organs with a vascular network out of ECM-derived hydrogels.

1.1.5 Conclusion

Cardiac tissue bioscaffolds continue to be of great interest in the field of regenerative medicine due to their ability to take various forms – a whole scaffold, cardiac patch, or hydrogel, along with their numerous therapeutic applications for cardiovascular disease. New technologies such as cardiac ECM hydrogels hold promise as a potential bioink and as an *in vivo* patch; however, 3D printed structures do not innately contain vascular conduits, while decellularized matrices do. Decellularization of the whole heart in 2008 paved the way for whole bioscaffolds to be used *in vivo* and eventually in clinical trials. As recellularization and other bioengineering technologies improve, the uses and applications of cardiac bioscaffolds continue to grow. Furthermore, for standardized manufacturing of these recellularized dECM matrices, guidelines must be established to manufacture consistently safe and effective bioscaffolds for clinical applications. Although many unknowns exist before whole cardiac bioscaffolds become a clinical reality, current research shows tremendous potential. As new discoveries happen every day, the field moves closer to making whole cardiac bioscaffolds clinically feasible.

1.2 Vascularizing Decellularized Tissues

1.2.1 Overview

The tissue engineering of whole organs has become an expansive multi-faceted field of research with the goal of discovering and implementing methods to replace or regenerate diseased organs. The demand for organ transplant continues to increase while the donor lists remain steady, necessitating alternatives to traditional allogeneic transplants. The field encompasses research in various organ systems, each of which has a unique set of required parameters that must be satisfied to be successful. The common concern, which increases the complexity of all of these systems, is the requirement of a vascular system capable of supplying nutrients to the tissues. Acellular tissues are currently heavily studied as biocompatible scaffolds, as these tissues can potentially be recellularized with autologous stem cells, lowering the possibility of rejection. However, the process of decellularizing tissues to render them acellular often destroys microvasculature, causing the remaining tissue a non-viable treatment option, as the vascular content is insufficient to supply adequate nutrient for long-term survival. Thus, tissue engineering has begun to explore ways to vascularize acellular constructs to create vascular networks adequate for sufficient perfusion to implanted tissues.

1.2.2 Introduction

The ever-expanding field of regenerative medicine relies heavily on the development of biocompatible scaffolds capable of supporting cell adhesion, growth, and signaling. One of the most promising discoveries within regenerative medicine has been the decellularization of tissues and whole organs, which renders biologic matrices that are inherently compatible

with cells and retain the composition and ultrastructure of the extracellular matrix (ECM). Decellularization removes the cellular components of a tissue, leaving behind an acellular ECM scaffold that retains native tissue architecture [23, 62, 105-108]. This method has been applied to a multitude of different tissues within the body including the bladder, heart, trachea, liver, and kidney [62, 109-111]. The scaffold that remains after the removal of cellular contents may be repopulated with various cell types to create an engineered tissue or organ suitable for transplant. The goal is to use a transplant patient's autologous stem cells to repopulate the decellularized scaffold, which might decrease the possibility of transplant rejection [107]. Additionally, the process of removing the cellular components from the scaffolds, and thus the components that cause an immunogenic response, may allow the use of xenografts in human organ transplants [11, 39, 112]. Due to the potential use of xenografts with reduced immune response, fully decellularized scaffolds may be a future "off the shelf" treatment for many different diseases, as tissues could be decellularized, stored, and re-seeded with cells as needed, increasing the availability of organs for transplant. Although these scaffolds seemingly provide an optimal scaffold to build an organ, they do not retain a vascular network that can support metabolically active tissues.

Sufficient vascularization remains a top challenge in the successful engineering of tissues and whole organ replacements [40, 113-116]. While acellular scaffolds retain the network of vascular conduits throughout the decellularized tissue, the process of decellularization mostly destroys the majority of microvasculature [62]. Due to oxygen diffusion limitations within tissues, the absence of a dense capillary network will render the resulting implants

non-viable [117]. Additionally, the rate of vascular growth within the body is much slower than the immediate metabolic demand that a transplanted tissue requires [118, 119]. Thus, various methods of how to increase the vascular content within decellularized scaffolds is a focus of current research.

Vascularization of decellularized scaffolds poses two different challenges; the acellular scaffold must: 1) be fully re-endothelialized, and 2) promote outgrowth of new vascular structures from the existing ones to increase the density. To encourage neovascularization within decellularized scaffolds different methodologies that have been implemented including, loading angiogenic growth factors into micro/nano particles,

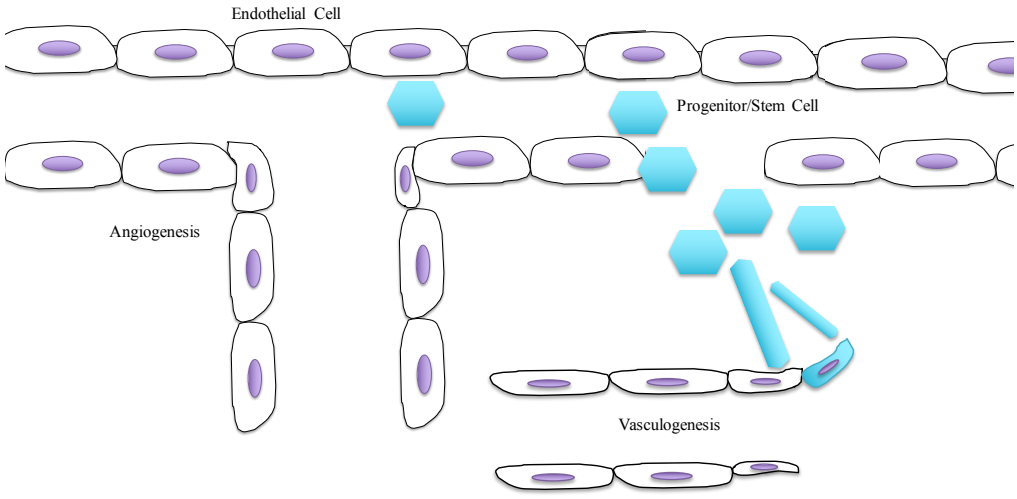

Figure 1.6: Angiogenesis vs. Vasculogenesis. Angiogenesis (right), the outgrowth of new vessels from existing vessels, and Vasculogenesis (left), the growth of new vasculature from progenitor/stem cells.

including cell types known to encourage vascular growth such as endothelial cells or fibroblasts, bolus injections of growth factors into specific areas, and encapsulation of angiogenic growth factors into hydrogels. All of these methods aim to re-endothelialize the scaffolds, and increase the rate of neovascular growth (Figure 1.6). The following review will summarize various methods that are currently employed to encourage re-endothelialization and subsequently encourage vascular growth, as well as provide insight into the state of the field of regenerative medicine where the future of the field is.

1.2.3 Re-endothelialization of Acellular Scaffolds

As the decellularized scaffold retains the majority of the vascular architecture, the main technique that has been used to encourage vascular growth in these constructs has been seeding these scaffolds with endothelial cells (ECs); known as re-endothelialzation. The vasculature of decellularized scaffolds must be seeded with ECs, as scaffolds without the presence of ECs have been shown to be leaky and thrombogenic [62]. Additionally, complete cell coverage of the vessels is necessary in order to replicate the function of the endothelium *in vivo.* There are multiple cell types that may be utilized in the re-endothelialization of the vasculature, with each cell type having different efficacy on the regrowth of functional vessels. Elucidating the optimal cell type for re-endothelialization that can encourage the growth of new vessels as well as provide complete endothelial coverage of vessels is critical and necessary for a functional vascular network. Additionally, research should be conducted regarding the supporting cell types present in a vessel such as pericytes, as they play an important role in the vessels as a producer of growth factors and as a regulator of capillary blood flow [120].

1.2.3.1 Stem Cells

Stem cells may be an optimal cell source to vascularize a decellularized matrix due to their capacity for self-renewal and ability to differentiate into multiple cell types. These cells can either be differentiated by *in vitro* exogenous growth factors, or *in situ* by both growth factors and signals from the ECM. Stem cells have been used in engineering tissues such as decellularized kidneys, in which embryonic stem cells were shown to differentiate into ECs within the remnant vascular architecture [22]. In the study by Ross *et al*., murine embryonic stem cells were injected into an arterial cannula within acellular scaffolds, with no added growth factors into the media. Scaffolds were then sectioned and stained positive for an EC specific lectin, BsLB4 and vascular endothelial growth factor receptor 2 (VEGFR2) [121]. BsLB4 is an EC specific lectin that is used as an indicator of EC differentiation [122]. The VEGFR2 is a receptor specific to vascular endothelial growth factor (VEGF), and is primarily expressed on vascular EC surfaces and significant in angiogenesis [123]. The presence of these signals were found to be most apparent within the vasculature and glomeruli in the kidneys, indicating that the embryonic stem cells were not only differentiating into ECs but also differentiating in areas where vasculature had previously been. Investigators believe that the cells differentiated in the correct location due to the retention of site-specific signals within a decellularized matrix [22]. In a separate study conducted by Lu *et al*., induced pluripotent stem cells (iPSCs) were differentiated into cardiomyocytes, smooth muscle cells, and ECs, which were subsequently used to repopulate decellularized mouse hearts [124]. Through a cannulated aorta, iPSCs were perfused through the heart. After 7 days, vessel-like structures were seen within these re-cellularized hearts, indicative of cell differentiation into ECs [27]. These

results indicated that one stem cell type could differentiate into smooth muscle cells, cardiomyocytes, and ECs. The findings from Lu *et al*. provided further evidence that the ECM niche within an acellular scaffold retains the cues necessary to promote cell differentiation. The use of iPSCs as a cell source for regenerative medicine holds tremendous promise, as these cells could in the future be autologously derived, and differentiate into various cell types. Despite the promising ability to direct iPSCs into any cell type, iPSCs are cultured at a low rate, and require increased time to produce an adequate amount that would be needed to sufficiently re-endothelialize a scaffold [125]. As we have previously reported, stem cells are more resistant to hypoxia than cells that have differentiated further, potentially allowing higher survival rates in an environment such as a decellularized matrix [62, 126]. However, these cells also have the risk to become tumorigenic due to transgene insertion [127]. Although stem cells have promising characteristics as a cell source for the re-endothelialization and the subsequent vascular growth of scaffolds, they still need to be directed into differentiating into the EC lineage, adding a layer of complication.

1.2.3.2 Endothelial Progenitor Cells

Endothelial progenitor cells (EPCs) can be sourced from peripheral blood, adipose tissue, and bone marrow [128, 129]. EPCs are involved in the creation of new vessels *in vivo*, the expansion of existing vessels, and additionally have the capability to form new vessels *in vitro* [128, 130]. Using EPCs for re-endothelialization of the decellularized tissues has shown to repopulate the vasculature and form vessels similar to the native tissues in organs such as liver, heart, bladder, and kidney [110, 129, 131]. In a study of adipose derived

endothelial progenitor cells (ADEPCs) on their angiogenic potential within decellularized bladder scaffolds, Dai *et al*., found that the ADEPCs showed EC like characteristics through the expression of cell markers such as CD31 and eNOS [132]. Additionally, these cells (ADEPCs) could form capillary-like structures within Matrigel, indicating their angiogenic capability, from a potential autologous source [129]. Bone marrow derived endothelial progenitor cells have also been used to re-endothelialize a liver scaffold [129]. EPCs were seeded into the liver scaffold via the portal vein and cultured for 3 days before being analyzed. Scaffolds stained positively for CD31, and a cross section of the vasculature showed that ECs had covered the vessel structures [129]. Authors did note, however, that the re-endothelialization was seen more in the larger vessels versus the smaller vessels, and hypothesized that this was due to differences in media pressure gradients. In a study conducted by Maniu *et al.*, Wharton's jelly mesenchymal stem cells (MSCs), were differentiated into EPCs through exposure to different growth factors such as VEGF, IGF, EGF, and bFGF, and cultured for 4 weeks. Cells were then analyzed for EC cell markers, CD31, CD105, as well as EPC cell markers CD34, and CD133, all indicative of EPC differentiation [133]. Additionally, they also exhibited decreased expression of MSC marker CD90, further indication of MSC to EPC differentiation. EPCs were then seeded onto a decellularized umbilical cord section and cultured for 4 days. EPCs were shown to successfully integrate into the decellularized human umbilical cord vein, lining the vessel. These results showed that the Whartons jelly derived EPCs could be a potential source of ECs for reendothelialization of a decellularized tissue [133]. The ability to differentiate MSCs into EPCs would allow EPCs to be obtained more easily, as they could be derived from adipose tissue, and in greater numbers.

An advantage of utilizing progenitor cells is that these cells are closer to full differentiation of a particular lineage, potentially eliminating the possibility of trans-differentiation. These cells could also be autologously derived, potentially decreasing a host immune response. However, although isolation from peripheral blood is possible, the circulating numbers of EPCs are low, so sufficient growth is difficult. While the EPC has shown to successfully endothelialize a scaffold, as well as grow vasculature, the difficulty in isolation of these cells from the blood could potentially prove to be a major deterrent as the larger use of this cell might be impractical. However, the promising studies indicating that WJ-EPCs and adipose derived EPCs are a potential EC source, lead to the possibility of these cells being useful endothelialization candidates. There is, however, limited information and further studies must be performed on the long-term capabilities and angiogenic potential of the EPC in a recellularized scaffold.

1.2.3.3 Adult Endothelial Cells

Adult Endothelial cells have been used to re-endothelialize many decellularized tissues. As our previous work has shown, rat aortic endothelial cells (RAECs) infused into the vasculature through both venous and arterial ends of a rat heart can repopulate the vessels and decrease the incidence of thrombus formation [62]. Human umbilical vein endothelial cells (HUVECs) have been used to repopulate rat acellular kidneys [1]. While these HUVECS were shown to repopulate the vasculature, the vascular resistance was high compared to native vessels, potentially due to a lack of a mature vessel structure [134]. Although the risk of differentiation in committed cell lineages are lower, they also have the

capacity to enter senescence sooner than stem cells, and may have a decreased ability to proliferate at rates similar to stem cells.

1.2.3.4 Co-Seeding of Cells

The co-seeding of ECs with other vascular cells, such as smooth muscle cells (SMCs), into a decellularized matrix can help recapitulate the native vascular environment more accurately. The co-seeding of these cells have been shown to facilitate growth of neo-vasculature at significantly higher levels compared to ECs alone in tissues such as decellularized small intestinal mucosa [135]. The rationale for the co-seeding of these cells is that the SMCs will differentiate into the smooth muscle that normally surrounds the vasculature. The co-culture of cells has also been shown to increase vascular density in a study by Sarig *et al.* in which hMSCs were co-cultured with HUVECs and found that ECs tended to proliferate in areas where the hMSCs were differentiating into supporting vascular cells [40]. The presence of the hMSCs greatly increased the amount of capillary growth [40]. An advantage of seeding scaffolds with ECs in addition to other cell types is that these support cells (smooth muscle cells) will secrete additional angiogenic growth factors that will directly influence the ECs. This will lead to the continued production of growth factors and would provide the micro environmental cues necessary for continued growth of mature vasculature, and rapid host integration.

The determination of the correct cell type for re-endothelialization remains a challenge. The acellular lumen must have full cellular coverage, otherwise vessels become leaky and thrombogenic. Many factors must be taken into consideration when determining the most

optimal cell type. To re-endothelialize a scaffold requires a large amount of cells, and often there is low cell adherence, which must be taken into account. Additionally, the source of the cells is crucial for prevention of an adverse immune response and potential graft rejection. Unfortunately, the seeding of cells alone thus far has not proven to grow a vasculature that is dense enough to support the tissue. The vascular lumens must be re-endothelialized, and then rapidly grow additional microvasculature and anastomose with a host vasculature in order to survive. Because of this, in conjunction with delivery of the cells, different methodologies to deliver different angiogenic cues have been explored, to help encourage the rate of vascular growth in decellularized tissues.

1.2.4. Bioactive Molecule Delivery

Bioactive molecules such as angiogenic growth factors (GFs) are signaling molecules that influence ECs to grow new vasculature. These GFs may be delivered to cells in different ways; by physically being bound to the matrix, using a hydrogel, using microparticles, or in a single bolus delivery (Figure 1.7). The bolus delivery of GFs refers to the perfusion/injection/delivery of GFs all at one time, without any temporal control in the way of delivery and can result in quick degradation of the GFs [136]. Multiple growth factors may be delivered at once with this method, or staggered throughout the time of cell culture. With uncontrolled delivery of growth factors into an acellular matrix, there is a potential for inconsistent dosage to certain areas of matrix, which could lead to non-uniform cellular growth [137]. Additionally, the over dosage of certain growth factors could have detrimental effects to a scaffold and surrounding tissues. Finally, many growth factors have a short half-life, resulting in even further reduction of the GF efficacy [138].

In order to use GFs efficiently, they must be delivered in a fashion that allows for cellular exposure in a controlled manner that leads to consistent dosage, and controlled timing. Below, we discuss different ways GFs are being used to encourage neovessel growth in decellularized matrices.

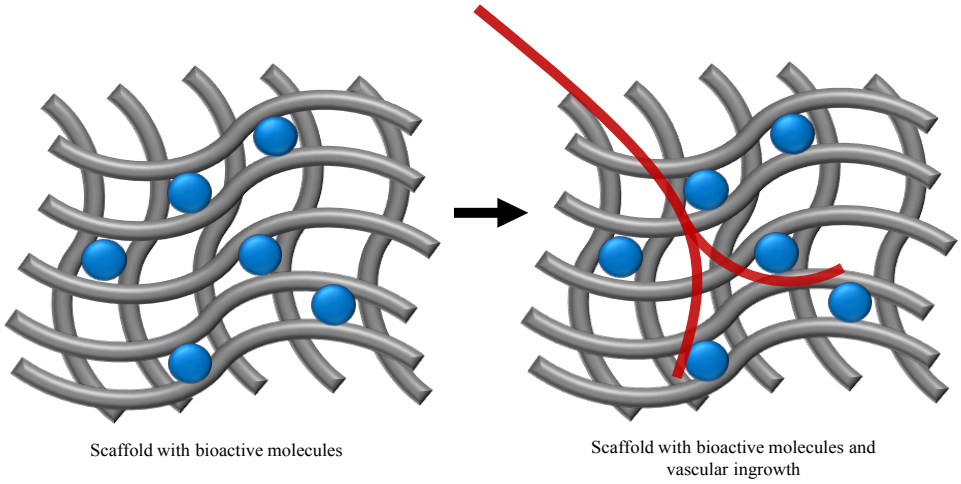

Figure 1.7: Bioactive Molecule Delivery in Scaffolds. Left, Scaffold with encapsulated or chemically bound bioactive molecules. Right, vessel ingrowth into the scaffold from the influence of the bioactive molecules.

1.2.4.1 Matrix Based Delivery

Matrix based delivery of bioactive molecules refers to the physical attachment/ encapsulation of a GF to the matrix itself. This may be beneficial, as it may lead to the sustained release of a GF over time, as cells are exposed to the GFs as they invade the matrix. In a study by Ogawa *et al.*, they tested the incorporation of single growth factor,

basic fibroblast growth factor (bFGF), into the matrix, by rehydrating a lyophilized bladder acellular matrix (BAM) with the GF. The group saw an increased density of vasculature the bFGF BAM when incorporated into murine subcutis, compared to controls [109]. Dai *et al.* continued studying the BAM, specifically the effects of the addition of VEGF and platelet derived growth factor BB (PDGF-BB). On the BAM, lyophilized matrices were rehydrated with GFs and incubated for 12 hours prior to implantation into a rabbits with partially resected bladders [139]. The experimental groups (with GFs) showed significantly more vascular structures with greater vessel cross sectional area than control groups. Interestingly, the group noted that there was increased vessel growth in the outer regions of the patches that did not extend to the inner areas of the patches. They hypothesized that this was due to the slow rate of host vascular ingrowth [139]. Loai *et al.* investigated the incorporation of VEGF at varying concentrations into a BAM, with the addition of hyaluronic acid (HA) [140]. The group looked at the implantation of a BAM with BAM+VEGF+HA, only HA, and only a BAM into a portion of a porcine bladder. After both 4 and 10 weeks, the BAM+VEGF+HA group was seen to have the highest amount of recellularization compared to the other groups. Additionally, they saw an increase in the amount of CD31+ (a marker of vasculature) staining present in the BAM+VEGF+HA group. They found that there was evidence of increased angiogenesis within VEGF containing scaffolds, and that the presence of hyaluronic acid increased the amount of CD31+ vessel density, compared to scaffolds without VEGF [140]. In a study conducted by Hilfiker *et al.*, a portion of a porcine small intestine was decellularized to form a biological vascularized matrix (BioVaM) [141]. The matrix segment was then coated with a matrix-associated protein CCN1 a protein that has been shown to promote adhesion,

migration, and proliferation of ECs [38]. The CCN1 was attached to the matrices by perfusing 100 ng/ml of the protein through the BioVaM, and subsequently removing the unbound CCN1 after overnight incubation. Human cord blood endothelial cells (hCBEC) were used and perfused into the BioVaM structures, and incubated and cultivated for 4 days [38]. The group noted that compared to the BioVaM structures that did not have the CCN1, the matrices showed an increase in the adhesion of the hCBEC, and retention. Additionally, authors found that there were longer vessel structures seen in the CCN1 groups, as well as seeding wide interconnected vascular structures after 14 days in culture, compared to the non-CCN1 groups. The group believes that part of the increased adhesion of the hCBEC arises from the integrin binding of CCN1 and the cells [38]. It is noted that there was not complete re-endothelialization within these scaffolds after 14 days in culture. Further study must be conducted on this system, as well as perhaps the inclusion of an additional signaling molecule.

1.2.4.2 Hydrogel Based Growth Factor Delivery

Hydrogels are hydrophilic polymeric materials that have been widely used in the field of tissue engineering [142, 143]. These polymeric materials have the ability to retain large amounts of water due to their hydrophilic nature [142-144]. Hydrogels can be made with either biologic or synthetic materials, and are often biocompatible [142]. Naturally derived hydrogels are especially attractive as these retain the properties most similar to the ECM, are biocompatible, and biodegradable [143, 144]. The biodegradability of a naturally derived hydrogel enables the possibility of using hydrogels as a bioactive molecule release mechanism, which has been widely used [143]. The porosity and release rate of a bioactive

molecule can be manipulated by altering densities of these materials, as needed for each application [143]. These characteristics of hydrogels render them a tool to encapsulate bioactive molecules such as angiogenic GFs, to be used for tissue engineering purposes. The application of hydrogels in decellularized tissues has been mostly limited, but has been widely studied in other tissue engineering applications. In a study performed by Kanematsu *et al*., collagen was chosen as a GF delivery vehicle, and hepatocyte growth factor (HGF), PDGF-BB, VEGF, insulin like growth factor-1 (IGF-1) and heparin binding epidermal growth factor (HB-EGF) were incorporated into the scaffold [137]. The researchers found that there was an initial large release of growth factors from the scaffolds as measured by radioactive tagging, and then sustained release of the growth factors for a period of up to 30 days, depending on the growth factor. Additionally, the matrix itself was shown to be degrading at rates that were similar to matrix degradation rates [137].

Although hydrogels have beneficial characteristics that may make them ideal candidates for growth factor delivery to decellularized tissues, there has been limited application and more research must be completed in order to determine the efficacy of delivery with a hydrogel.

1.2.4.3 Particle Based Growth Factor Delivery

The encapsulation of growth factors within micro- or nanoparticles enables the spatial and temporal controlled release of the growth factors into scaffolds, and has been used in different tissue engineering applications. Particles that are made out of biodegradable materials are ideal, as the body's rate of degradation would translate to rate of molecule

release. These micro- or nanoparticles can lead to longer sustained release of bioactive molecules, compared to a molecule directly added into the matrix. Particles may be synthesized from various synthetic materials, such as poly (lactic-co-glycolic acid) (PLGA), or natural materials such as alginate or chitosan [145-147]. Synthetic materials can be beneficial as they are easily obtained and manipulated, but natural biomaterials may elicit a decreased immune reaction.

Geng *et al*. loaded PLGA nanoparticles with VEGF, and injected them into BAMs, which were then implanted into porcine bladders. At weeks 4 and 12 post injection, there were significantly higher densities of micro-vessels within bladders containing nanoparticles compared to the control groups, as shown by CD31 positive structures [147]. Additionally, they saw sustained VEGF release that lasted for up to 3 months [45]. The authors also noted that with the incorporation of their particles, they saw less contraction of the implanted bladder. The contraction of implanted segments is not ideal, as it changes the structure and potentially function of an implanted graft.

Heparin is a linear polysaccharide that has been used in conjunction with a variety of bioactive molecules due to its ability to bind and prevent degradation of growth factors [148-150]. Heparin can also adsorb to the matrix surface. In a study by Wu *et al.,* heparin was used in conjunction with Chitosan, a natural biomaterial, to form nanoparticles that were immobilized onto a decellularized bovine jugular vein [44]. VEGF was then complexed to these scaffolds, by VEGF binding to the heparin/chitosan particles within the bovine jugular vein scaffold.

Capillary density was shown to significantly increase within scaffolds with VEGF incorporated nanoparticles *in vitro* and *in vivo* [148]. Wu also noted that *in vivo,* the vasculature that grew from the scaffolds appeared to aggregate with the tissues surrounding the implant, suggesting they anastomosed with host vasculature.

A unique possibility with particles is the ability to administer more than one bioactive molecule at a time, and at different times. These could be customized to create an environment more suitable for growth of more mature vessels, as it could be made to mimic angiogenic signaling patterns [147]. Particles have been previously made by Mooney *et al.* to deliver multiple GFs in a sequential manner in a collagen scaffold. The group worked on the co-administration of fibroblast growth factor (FGF) and angiopoietin-1 (Ang1), two growth factors important in angiogenesis and the stabilization of vessels [151, 152]. This enables the early release of factors that initiate the growth of vessels, followed by the release of factors that encourage maturation and long-term stabilization of vessels. The application of particle based molecule release in decellularized scaffolds needs to be further researched. In particular, particles made out of existing ECM material may be an especially promising category.

1.2.5 Conclusions and Future Directions

Using the native tissue architecture of a decellularized organ and repopulating the vasculature of the scaffold while encouraging neovascular growth holds promise of being the most clinically translatable method to create a vascularized tissue engineered construct. Because these scaffolds retain existing vascular architecture, when used *in vivo* dECM

scaffolds may anastomose with the host's vasculature more effectively. However, encouraging neovascular growth is the rate-limiting step to creating a viable tissue engineered construct. While steps have been made and different techniques have been developed, there has still not been a scaffold made with an adequate amount of vasculature for immediate use. Many different systems have been utilized to help encourage growth of vasculature in the matrices, but each is associated with advantages and disadvantages. The recapitulations of the angiogenic processes are difficult, as these are complex *in vivo* signaling processes. In order to replicate these processes, angiogenic growth factors should be delivered to the scaffolds in a sequential, temporally controlled manner to mimic *in vivo* angiogenesis signaling and theoretically leading to the growth of more vascular structures. In addition to using the most optimal cell type, a method to deliver angiogenic molecules using a material such as a hydrogel, could potentially be a promising way to re-endothelialize and encourage new vascular growth from a decellularized scaffold. Because of the ability to customize a hydrogel to a desired release profile, bioactive molecules could be delivered in a fashion that could help encourage sustained vessel growth. Scaffolds could also be pre-vascularized in this manner, lessening the amount of time required to provide a patient with an "off the shelf" tissue. There has been extensive research performed in hydrogel-based growth factor delivery in tissue engineering, but limited application in the field of decellularized tissues. Further research is necessary to create a fully vascularized decellularized scaffold and a clinically relevant treatment method.

2 CARDIAC DECELLULARIZED EXTRACELLULAR MATRIX UNIQUELY AFFECTS STEM CELL DIFFERENTIATION

2.1 Overview

As cardiovascular disease, including myocardial infarctions, continues to be the leading cause of death worldwide therapeutic interventions aim to reinforce or replace injured myocardium to regain the contractile function of the tissue. One approach is by using a cardiac patch, placed in areas of damaged myocardium to act as a mechanical support. In this study, we explored how a candidate cardiac patch material, cardiac decellularized extracellular matrix (dECM) hydrogels, are affected by changing cardiac dECM hydrogel formation, and how these changes affect the resulting hydrogel and consequently cell behavior.

To accomplish this, dECM was enzymatically digested for increasing amounts of time (24 - 72 hours) and crosslinked with genipin to form hydrogels with a range of mechanical properties. Time to gelation, material elasticity, and enzymatic degradation were quantified; hydrogels formed from dECM solutions enzymatically digested for 24 hours formed gels faster, were stiffer, and degraded at a slower rate. Biocompatibility was assessed by maintaining human cardiomyocytes, umbilical vein endothelial cells, and cardiac fibroblasts, on the hydrogel formulations. Finally, the effect of dECM on human adipose derived stem cell differentiation down a cardiac lineage was evaluated, including the roles of the β4 and β5 integrin subunits. Gels formed from dECM solutions digested for 24 hours increased cardiomyocyte-specific gene expression compared to dECM with

longer digestion times. Our study provides further evidence that tissue specific dECM hydrogels retain tissue specific cues that promote differentiation of stem cells, and may be suitable to stimulate stem cell differentiation and vascularization within a cardiac patch.

2.2 Introduction

Available treatment options for cardiovascular disease vary from drug therapy, interventional devices, and if necessary, transplantation [153]. One of the leading and most debilitating causes of heart failure stems from myocardial infarction (MI). Acute MI results from a loss of blood flow, and the accompanying oxygen, to an area of the heart, causing that area to become ischemic [154]. If perfusion is not restored within the first few hours, the often irreversible tissue damage leads to cell necrosis and causes an inflammatory reaction in the surrounding tissues which can induce further injury and affect the function of non-ischemic myocytes [155, 156]. This progressive degradation leads to deterioration of cardiac function and eventual heart failure [156]. Current treatment options for heart failure include pharmacologic interventions, cardiac resynchronization therapies, surgical interventions, and mechanical circulatory support (left ventricular assist devices; LVADs) [157-160]. Mechanical circulatory support is used to offload either the left or the right ventricle, and can be used as a bridge to transplant, or a bridge to recovery in certain cases [161]. It can also, however, cause serious complications such as pump thrombosis, stroke, and infection [158], [162], [163]. The large majority of patients with heart failure continue to decline despite therapeutic interventions [164, 165]. Currently, the most effective treatment for patients in end-stage heart failure remains a heart transplant; however, the list of recipients in need far exceeds donor organ availability [6, 158, 160].

Alternative newer regenerative medicine based treatments for heart failure include the application of cardiac patches to a localized area of damage in order to halt the progression of heart failure [166]. These tissue engineered cardiac structures reinforce the area damaged by ischemia with the aim of preventing further decline, while also promoting angiogenesis [40]. Different approaches have been proposed for the design of cardiac patches, including both biologic and synthetic materials [66, 167]. Ideally, these patches should mimic cardiac tissues as closely as possible in their mechanical properties, biochemical composition, and biocompatibility. The complex structure of the myocardium is challenging to engineer *ex vivo*, and thus acellular myocardial scaffolds have become an increasingly popular option in cardiac tissue engineering [11, 19, 23, 30, 62, 66, 168-173].

Acellular cardiac scaffolds can be derived from cadaveric human, pig, rabbit, or rat donor hearts [23]. The decellularization process removes cellular components from the tissue scaffold, leaving crucial acellular protein matrix scaffold behind [23, 40, 174] and significantly decreasing the possibility of immunogenic reactions [175]. The ECM components that remain can serve as a scaffold for cell attachment, proliferation, and migration [176]. Depending on the processing of the matrix, the scaffold may be used to provide stable mechanical support to maintain the architectural elements of the original tissue or can serve as an injectable therapy to be applied directly to the site of damaged tissue [113, 169-171]. These decellularized ECM (dECM) scaffolds retain the complex, tissue-specific mixtures of proteins and polysaccharides that guide cellular behavior and thus provide an enhanced microenvironment compared to purified protein scaffolds formed from collagen and fibrin [11, 34, 169, 176-178]. In 2008, our laboratory successfully

pioneered the use of perfusion to decellularize a whole organ [23], and we demonstrated successful recellularization of rat hearts that could be transplanted *in vivo* [62]. Since then, the field of decellularization has expanded and encompasses not only whole organs, but also dissected tissues that are further processed into powders or particles. These products have been reconstituted into various types of biomaterials [75, 179-182], including dECM hydrogels [35, 84, 88, 103, 183-186].

Myocardial matrix hydrogels, derived from decellularized left ventricular myocardium, can be formed under physiologic conditions through the self-assembly of matrix proteins. These hydrogels have been shown to be bioactive and improve cardiac function in both rat and porcine models of MI [75, 88, 187]. The tailoring of material properties such as mechanical stiffness, degradation profiles, and hydrogel composition can extend the range of potential biomaterial applications. Both physical (UV light) and chemical (carbodiimides, glutaraldehyde) crosslinking methods have been used to increase the mechanical stiffness of ECM-based biomaterials [103, 188-190]. Recent work has also shown that genipin, a naturally derived iridoid derivative found in the fruit of the gardenia (*Gardenia jasminoides*) [191-199] is a less cytotoxic crosslinker for various biologic-based scaffolds including chitosan [199-202], chondroitin sulfate [191], collagen [193, 196-198], gelatin [203], dECM [195, 204, 205], and hybrids of dECM with other materials [96]. Studies have also demonstrated that genipin-crosslinked scaffolds have improved mechanical properties and tunable enzymatic degradation profiles compared to non-crosslinked dECM scaffolds [96, 195, 204].

The exact composition and structure of the ECM is tissue-specific and varies due to the evolving cellular and environmental cues present during tissue development. The protein composition of the ECM has been shown to mediate several cellular processes such as adhesion, proliferation and differentiation [206]. In particular, collagen, fibronectin, and laminin have been implicated in significant roles during cardiac differentiation, and integrin subunits that predominantly interact with these three proteins, β1, are most highly expressed in cardiomyocytes [207, 208]. Integrins are heterodimeric membrane glycoproteins comprised of α and β subunits, which bind and recognize ECM proteins. Bidirectional integrin signaling influences both intracellular activity and extracellular affinity for ECM ligands [15]; however, the exact cues necessary to direct stem cell fate are not easily identified due to the complexity of the native cell environment [206]. Previous studies have shown that specific integrins, such as the β1 subunit and it's associated α subunits, are key facilitators of cardiac cell differentiation [207, 209, 210], [206, 211], and that the inhibition of other β subunits increases the activity of β1 integrins [212]. Thus, in our current study, I utilize decellularized porcine myocardium hydrogels to investigate two major factors that influence mesenchymal stem cell differentiation: 1) ECM protein and peptide composition, and 2) β1 integrin activity. I hypothesize that alterations in hydrogel protein content, achieved by variations in the enzymatic digestion of dECM would lead to crosslinked matrices of similar mechanical properties, but distinct environmental cues. dECM was digested over a range of different time courses following decellularization and the resulting digests were crosslinked with varying amounts of genipin. The mechanical properties and enzymatic degradation rates were assessed, as was the ability of these crosslinked hydrogels to sustain cardiac cell adhesion, viability, and

proliferation, and to guide mesenchymal stem cell differentiation toward a cardiac lineage. The impact of increased β1 integrin activity was assessed through the inhibition of β4 and β5 integrin-mediated activity. The data presented herein is intended to further explore the utility of crosslinked cardiac matrix as a suitable microenvironment for cardiac differentiation and an eventual scaffold for cardiac repair.

2.3 Specific Aims

Specific Aim 1: Create a 3D dECM hydrogel to be used as an *in vitro* model to simulate *in vivo* conditions.

Specific Aim 1.1: *Create hydrogels made out of porcine left ventricular decellularized extracellular matrix of dECM and characterize the material made.* I hypothesize that the digestion of the dECM will affect the material strength and cell behavior of the resulting hydrogels, such that an increased about of digestion time will aberrantly affect cell behavior and increase material strength.

Specific Aim 1.2: *Characterize the effect of increasing digestion time on stem cell behavior and differentiation.* I hypothesize that adipose derived stem cells will express cardiac markers on all dECM hydrogels regardless of the length of digestion times, but that the increasing digestion time will lead to a decrease in expression of cardiac genes.

Specific Aim 1.3: *Elucidate the effect that the material composition has on the differentiation of adipose derived stem cells towards a cardiac phenotype.* I hypothesize that by blocking the integrins beta 4 and beta 5, known fibronection and laminin receptors, the expression of cardiac genes will decrease since fibronectin and laminin have been implicated in cardiac differentiation.

Overall Goal for Specific Aim 1: Create a 3D environment of decellularized extracellular matrix that can be used to validate my system to be created in Aim 2 to increase vascularization in a decellularized environment.

2.4 Materials and Methods

All chemicals were purchased from Sigma Aldrich (St. Louis, MO) unless otherwise indicated.

2.4.1 Cardiac dECM Preparation

Porcine hearts were obtained from a USDA certified slaughterhouse (K&C Processing, Navasota, Texas). Left ventricular (LV) free wall tissue was excised and rinsed in deionized (DI) water. Tissue samples were then trimmed to remove residual chordae tendinae, valve leaflets, papillary muscles, adipose tissue and, most epicardial surfaces from the exterior portion, leaving primarily LV myocardium. Sections were either frozen at -20°C in sterile phosphate buffered saline (PBS) or decellularized immediately. For decellularization, LV wall sections were cut into small pieces approximately 36 - 64 mm^3 (Fig. 2.1A), which were then suspended in a hypertonic 500 mM sodium chloride (NaCl) solution for 2 h at 500 rpm. Samples were filtered using a sterilized fine mesh metal filter then transferred into a hypotonic 20 mM NaCl solution for 2 h at 500 rpm, followed by another filtration. Tissues were subsequently exposed to a 1% sodium dodecyl sulfate (SDS solution in PBS containing 2500 U of penicillin/streptomycin (Thermo Fisher, Waltham, MA), then stirred at 500 rpm for 24 h. Solutions were changed every 24 h for a period of 5 days until the solutions remained clear and the tissue took on the characteristic opaque appearance of decellularized cardiac matrix (Fig. 2.1B). The dECM was rinsed

several times with water to ensure SDS removal, then exposed to a 1 kU/ml solution of DNAse in DI water for 2 h. After additional rinsing with DI water, the dECM was frozen to -20°C, lyophilized, and pulverized with a mortar and pestle. The resulting dECM powder was digested with pepsin (1 mg/ml) in 0.1 M hydrogen chloride (HCl) for either 24 h, 48 h, or 72 h, at which point the product was neutralized to pH 7.4 and stored at -20°C until use.

2.4.2 DNA Quantification

Residual double-stranded DNA (dsDNA) in dECM samples was quantified using Hoechst 33258 (Molecular Probes, Eugene, OR), which emits blue fluorescence when bound to dsDNA. dECM samples of approximately 20 mg each were analyzed for DNA content prior to freezing and lyophilization in order to gauge the efficiency of the SDS-mediated decellularization process. dsDNA content of dECM samples was compared to that of fresh tissue samples harvested from the same organ. Prior to the assay, samples were digested at 55°C overnight in a 10% solution of proteinase K in PureLink Genomic Digestion buffer (PureLink Genomic DNA Mini Kit; Invitrogen, Carlsbad, CA). Following digestion, a phenol-chloroform extraction was used to recover dsDNA. Briefly, samples were diluted in 10 M Trizma hydrochloride (Tris HCl, pH 8.5) and mixed with a 25:24:1 solution of phenol/chloroform/isoamyl alcohol. After subsequent mixing and centrifugation, the top (aqueous) layer was recovered and the bottom layer was subjected to an additional dilution, mixing, and centrifugation to recover any remaining dsDNA. The recovered aqueous solution was further diluted in an equivalent volume of a 24:1 mixture of chloroform and isoamyl alcohol, which was again thoroughly mixed and centrifuged. The resulting

aqueous layer was recovered as the purified nucleic acid product. An ethanol precipitation was then performed by adding ammonium acetate at a final concentration of 0.75, 1 µl of glycogen, and 2.5 times the total sample volume of 100% ethanol. Samples were incubated at 20°C and then centrifuged for 20 min at 4°C. The resulting pellet was washed 3 times in 80% ethanol and resuspended in 10 mM Tris HCl. Samples were further diluted in TE buffer (10 mM Tris, 1 mM ethylenediaminetetraacetic acid; EDTA) and mixed with an equal amount of Hoechst 33258 dye dissolved in TNE buffer (10 mM Tris, 1 mM EDTA, 2 M sodium chloride, 2 mM sodium azide). Sample fluorescence intensity was measured a POLARstar Omega plate reader (BMG Labtech, Inc., Cary, NC) and compared to calf thymus standards.

2.4.3 Genipin-Induced dECM Hydrogel Crosslinking

Digested dECM at a concentration of 6 mg/ml was crosslinked with genipin using either 5mM, 7.5 mM, or 10 mM total genipin. As genipin produces a fluorescent crosslink as a result of reactions with free amine groups, fluorescence was used as a tool to quantify crosslinking completion. dECM-genipin mixtures were pipetted into the wells of a 96-well plate and incubated for 24 hours at 37°C. Crosslinking was monitored using a POLARstar Omega plate reader (BMG Labtech, Inc., Cary, NC) measuring fluorescence over 24 h (λ_{ex} = 584 nm and λ_{em} = 620 nm). Hydrogel precursor solutions were plated into a 96-well plate and inserted into the plate reader, which was pre-warmed to 37°C. As genipin produces a fluorescent crosslink as a result of reactions with free amine groups, fluorescence was used as a tool to quantify crosslinking completion. Fluorescence intensity data was collected every hour for the duration of the experiment.

A colorimetric ninhydrin assay was performed in order to determine the concentration of free amines in genipin-crosslinked hydrogels, thus measuring the extent of the crosslinking reactions [59, 70]. Briefly, ninhydrin solution was added to crosslinked hydrogels suspended in sodium citrate buffer, as well as standard solutions of known amine concentrations. The samples and standards were then placed in a boiling water bath for 15 min and then allowed to cool for 30 min. Sample absorbances were measured at a wavelength of 570 nm using a POLARstar Omega plate reader (BMG Labtech, Inc., Cary, NC). In addition, methanol content was assessed over the duration of genipin-induced gel crosslinking using a methanol assay kit (BioVision Inc., Milpitas, CA). The assay uses an enzymatic mechanism to quantify methanol production through generation of a colorimetric signal. Hydrogels were crosslinked with genipin as described previously in 96 well plates. During the crosslinking reaction, liquid samples were removed from each well at specific time points (2.5 h, 8 h, 15 h, and 24 h) to assess the amounts of methanol produced as the crosslinking progressed. Samples and pure methanol standards were mixed with the methanol assay buffer, developer, enzyme mix, and the methanol probe as per the manufacturer's instructions, incubated at 30°C for 30 min, and absorbance were measured at a wavelength of 450 nm using a POLARstar Omega plate reader (BMG Labtech, Inc., Cary, NC).

2.4.4 Rheological Properties

Genipin crosslinked gels were pre-formed using the protocol described above. The viscoelastic properties of the hydrogels were analyzed using a rheometer (Physica MCR 301; Anton Paar, Graz, Austria) with an 8 mm parallel plate geometry and a 1 mm gap

between plates. A dynamic frequency sweep was performed (0.25-100 rads s^{-1}) at 2.5% strain to determine the storage modulus (G') and the loss modulus (G''). All measurements were performed at room temperature.

2.4.5 Enzymatic Degradation

Genipin-crosslinked dECM hydrogels were formed using the previously described protocol, except gels were crosslinked in 2 ml microcentrifuge tubes. Type 1 Collagenase (Thermo Fisher) was dissolved in Hank's Buffered Saline solution (HBSS; Thermo Fisher) containing 0.9 mM calcium chloride ($CaCl_2$) at a concentration of 150 U/ml. Following an initial weight measurement of each fully crosslinked gel, 0.5 mls of collagenase solution was added into each gel-containing microcentrifuge tube and the hydrogel weights were monitored over a period of thirty days by removing the liquid and weighing the remaining gel at each time point.

2.4.6 Cell Viability

Genipin crosslinked dECM hydrogels were formed as described previously in 96 well plates. Hydrogels were then rinsed with PBS three times for 1 h, followed by two subsequent 1-h cell culture media washes and an overnight media wash to ensure that residual genipin and the low levels of methanol generated during crosslinking were removed (Figure 2.2, Reaction 2). Following the rinse steps, gels were sterilized by irradiation with ultraviolet (UV) light overnight in a laminar flow hood. Three types of cardiac and vascular cells were assessed for viability on the dECM hydrogels: human cardiac fibroblasts (CFs, passage 2-3; Cell Applications, San Diego, CA), human neonatal

cardiomyocytes (CMs; Sciencell; Carlsbad, CA), and human umbilical vein endothelial cells (HUVECs, passage 4; Lonza, Walkersville, MD). Cells were seeded at a density of 20,000 cells/gel and cultured for 24 h on hydrogel surfaces. A Live/Dead cell viability assay (Thermo Fisher) was then used to assess the numbers of live and dead cells on each gel. In brief, cells were stained with a combination of calcein-AM, ethidium homodimer-1, and 4,6-diamidino-2-phenylindole (DAPI), resulting in green-fluorescent live cells and red-fluorescent dead cells, respectively. Cells were imaged using an EVOS FLoid Cell Imaging Station (Thermo Fisher), and the number of live and dead cells were quantified.

2.4.7 Human Adipose Stem Cell Differentiation

Human adipose stem cells (hADSCs; passages 2-3; Lonza) cultured in human adipose-derived stem cell growth media (Lonza, Walkersville, MD) were seeded onto 7.5 mM genipin-crosslinked dECM hydrogels, non-crosslinked dECM, Type I porcine collagen gels or TCPS at a density of 7,500 cells per well. Hydrogels were crosslinked as previously described in 96-well plates and rinsed to remove residual genipin and methanol as described above. Cells were cultured for either 3 days, or 1, 2, or 3 weeks in a humidified incubator with 5% CO_2 at 37°C, and the culture media was changed every 48 hours. Following the specified culture period, RNA was extracted and isolated from the cells using TRIzol Reagent (Invitrogen) according to the manufacturer's protocol. Samples were stored at -80°C until reverse transcription was performed. For reverse transcription, the *Power* SYBR® Green Cells-to-C_T™ kit (Invitrogen) was used according to manufacturer's protocols. Briefly, for each reaction, 25 µls of 2X SYBR® RT Buffer, 2.5 µls RT Enzyme Mix, and 12.5 µls nuclease-free water were added to each well along with 10 µls of the

RNA sample. Samples were heated for 60 minutes at 37°C, followed by 5 minutes at 95°C for enzyme inactivation using a C1000 Touch Thermal Cycler (Bio-Rad, Hercules, CA), and then cooled to 4°C. cDNA samples were stored at -20°C until use.

2.4.8 Quantitative Real-Time PCR (qRT-PCR)

Relative gene expression was quantified by qRT-PCR using a CFX348 Touch Real-Time PCR Detection System (Bio-Rad). Briefly, using the *Power* SYBR® Green Cells-to-C_T kit (Invitrogen), a master mix was made for each primer set consisting of the following: 5 µls *Power* SYBR® Green PCR Master Mix, 0.04 µls each of forward and reverse primers (Integrated DNA Technologies), 2.96 µls of nuclease-free water, and 2 µls of cDNA for a final volume of 10 µls. Samples were run at 95°C for 10 minutes, followed by 40 cycles of 95°C for 15 seconds and 60°C for 1 minute. Gene expression was normalized to the housekeeping gene eukaryotic translation elongation factor 1 alpha 1 (eEF1A1). The resulting data was analyzed as fold expression change of our experimental groups relative to collagen controls using the $-\Delta\Delta C_T$ method for non-integrin blocked groups, and for integrin blocked groups relative to their non-blocked counterparts.

2.4.9 Functional Blocking Studies

In order to determine the influence laminin and fibronectin have on the differentiation of hADSCs, 7,500 passage 3 hADSCs were incubated in media containing either 10 µg/ml of laminin receptor antibody (anti-integrin beta 4; Abcam, Cambridge, MA), 10 µg/ml of fibronectin receptor antibody (anti-integrin beta 5; Abcam), or both (10 ug/ml each). Cells were then seeded onto genipin-crosslinked dECM hydrogels and cultured for either 3 days,

or 1, 2, or 3 weeks. The antibody-containing culture media was changed every 2-3 days. Following the specified culture times, RNA was collected using the above-described RNA isolation protocol and relative gene expression was quantified as described previously.

2.4.10 Immunohistochemistry Studies

In order to determine the protein expression of genes analyzed using qPCR, immunohistochemistry analysis was conducted for the following markers- NKX2.5 (Thermo Fisher), cardiac troponin T (cTnI, Thermo Fisher), connexin 43 (Thermo Fisher), and sarcomeric alpha sctinin (Abcam). Briefly, hADSCs that were seeded on gels were rinsed with PBS, then fixed with 4% PFA for 15 minutes. Following fixation, gels were cryoprotected in 10%, 20%, and 20% sucrose/PBS solutions, remaining in each concentration until the gel sunk to the bottom of the tube. Gels were then mounted in cryomount OCT (VWR), and snap frozen using liquid nitrogen, and stored at -80°C until use. Gels were sectioned at 7 μm in a Leica CM3500 cryotome, using a Cryojane® Tape transfer system and stored at -20°C until use. Sections to be stained were brought to room temperature, permeabilized in 0.2% triton-PBS for 15 minutes, rinsed in PBS, then blocked in 5% BSA for 1 hour at room temperature. Following blocking, antibodies listed above were incubated on the slide overnight at 4°C. Slides were rinsed in PBS, and secondary antibodies, FITC-anti rabbit, or FITC-anti mouse (Abcam, or Thermofisher) were applied to the slides for 1 hour at room temperature. Slides were rinsed in PBS 3 times for 5 minutes each, and counterstained with DAPI to visualize the nuclei. Sections were mounted using Pro-Long Diamond Antifade Mountant (Thermo Fisher) and visualized using fluorescent microscopy.

2.4.11 Statistical Analysis

The statistical analysis of all data was performed using GraphPad Prism 7 (GraphPad Software Inc, La Jolla, CA, USA). Data are presented as mean ± standard deviation. Statistical comparison between groups were performed using either students unpaired t-test (viability studies) a one-way analysis of variance (ANOVA) with Tukey's multiple comparison test (rheological studies) or a two-way ANOVA with Tukey's multiple comparison test (all other studies). *p* values less than or equal to 0.05 were considered statistically significant.

2.5 Results

2.5.1 Evaluation of Decellularization Efficiency

To visualize the efficiency of decellularization, the opaque myocardial tissue pieces (Figure 2.1B) were evaluated for residual dsDNA content. Residual dsDNA content was 2.474 +/- 0.211% dsDNA, compared to its non-decellularized tissue counterpart. Additionally, the standard of less than 50 ng dsDNA/mg tissue was met, and recorded to be ~37.38 ng/mg tissue (Figure 2.1C).

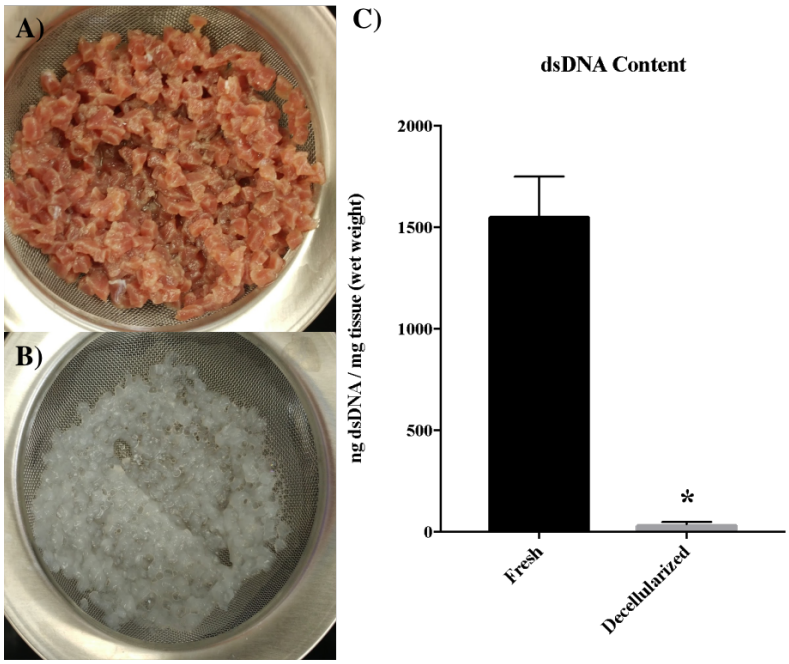

Figure 2.1: Decellularization Efficiency. (A) Cadaveric porcine left ventricular tissue prior to decellularization. (B) Decellularized porcine left ventricular tissue. (C) dsDNA content of decellularized ventricular tissues as compared to fresh control tissues. Data represent mean ± SD; n = 6, *p <0.05 vs control group.

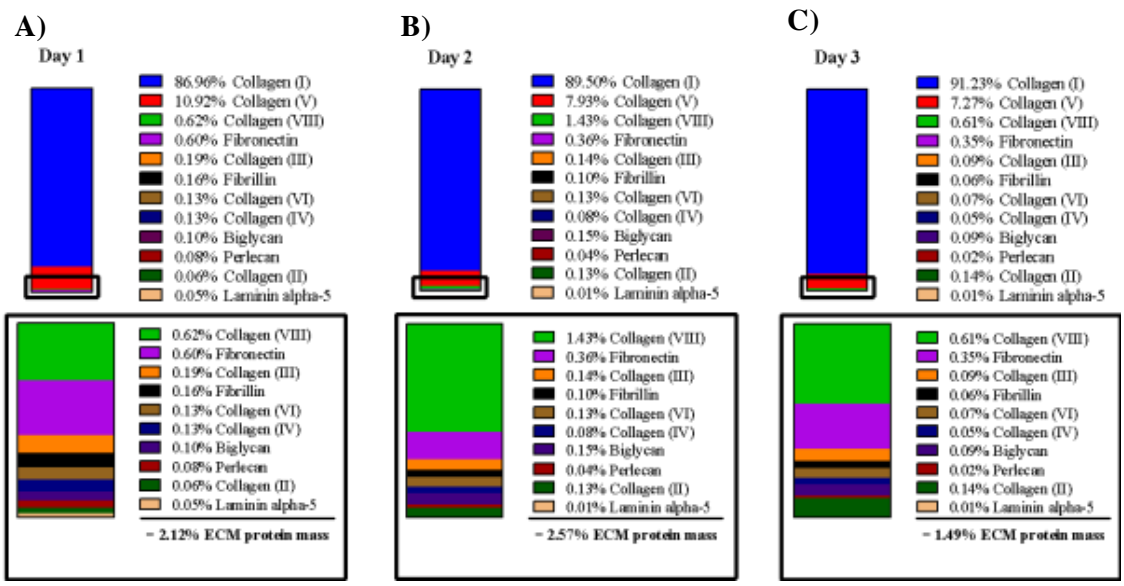

Fig. 2.2: Protein Composition of dECM. A) 24 hours of pepsin digestion, B) 48 hours of pepsin digestion, and C) 72 hours of pepsin digestion. ECM protein mass compositions are different across the different days of pepsin digestion.

2.5.2 Crosslinking Behavior of dECM Hydrogels

Genipin crosslinking with free amine residues forms a fluorescent byproduct that emits at 620 nm, which can be used to track the progress of the crosslinking reaction (Fig. 2.4). Control gels without genipin exhibited no fluorescence intensity change (Fig. 2.3A). Peak fluorescence intensity across all groups was achieved at ~5 hours after initial mixing with genipin and the signal plateaued thereafter. dECM hydrogels+ genipin that had been formed from dECM solutions digested for only 24 hours in pepsin peaked at a higher fluorescence intensity across all three concentrations of genipin and maintained a higher plateau at around ~300 nm (Fig. 2.3B,C,D).

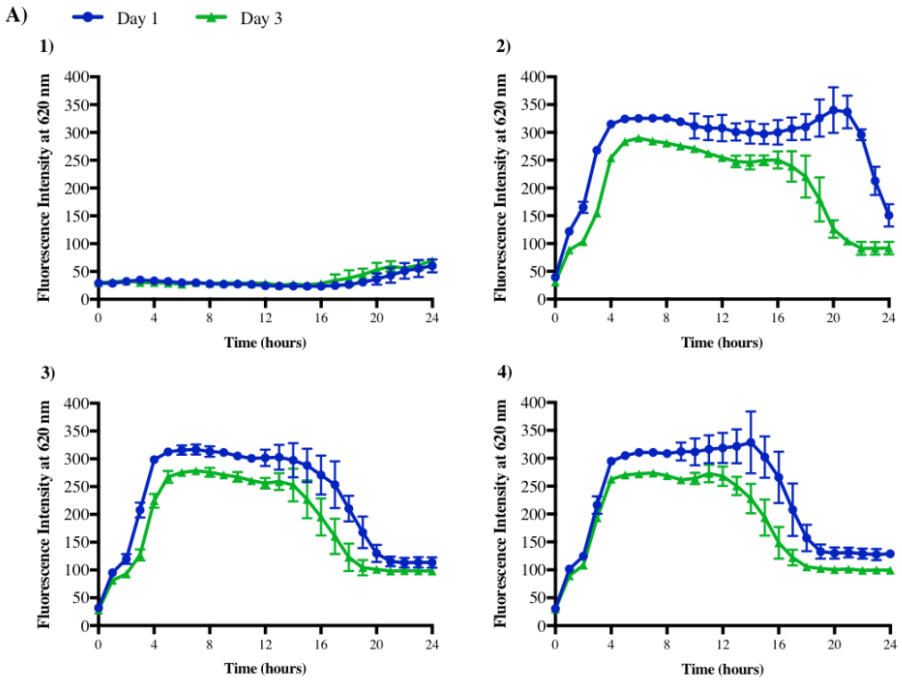

Figure 2.3: Gelation of Genipin-Crosslinked dECM Hydrogels. Observed by tracking the fluorescence intensity of by-products of genipin crosslinking at 37°C (λ_{ex} = 584 nm, λ_{em} = 620 nm). (1) dECM + 0 mM genipin, (2) dECM + 5 mM genipin, (3) dECM + 7.5 mM genipin, and (4) dECM + 10 mM genipin. Across all groups, gels formed from dECM digested for 1 day in pepsin peaked at a faster rate and reached higher fluorescence intensity values overall. Data represent mean ± SD; n = 6 per digest day group.

Thus, these data present evidence that dECM hydrogels crosslinked with solutions made from 24 hour of digested dECM hydrogels ($p<0.05$) crosslinked faster, and may produce more fluorescent crosslinks due to the availability of sites for crosslinking. Additionally, these data show that full crosslinking is assumed to be complete by ~5 hours, as the fluorescent signal plateaued at this point.

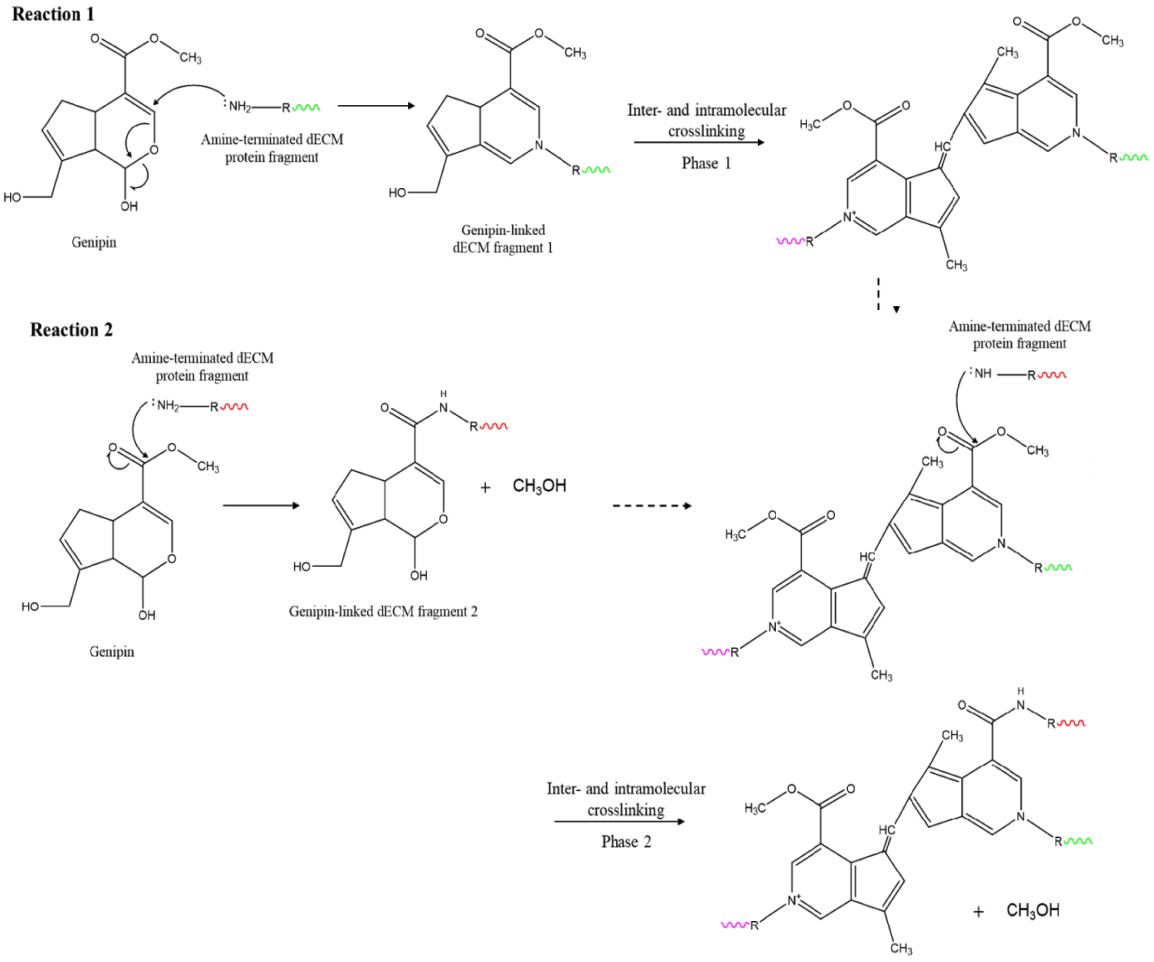

Figure 2.4: Schematic of Genipin Crosslinking. Depicts crosslinking reaction involving genipin and dECM peptide fragments. Reaction 1 involves the nucleophilic attack of genipin by a primary amine, leading to the formation of genipin-linked protein fragment that undergoes initial crosslinking as indicated by the Phase 1 crosslinking reaction. Reaction 2 is slower and involves the nucleophilic substitution of a genipin ester group to form a secondary amide link to available dECM fragments, resulting in the release of methanol. Dashed arrows indicate how further reactions of the products from Reaction 1 and Reaction 2 lead to additional crosslinking (Phase 2) of genipin-linked dECM fragments.

2.5.3 Characterization of Material Strength

To evaluate the strength of the cross-linked dECM hydrogels, storage and loss modulus (G', G") was recorded. Interestingly, gels that were formed from with both 7.5 and 10 mM genipin exhibited a higher storage modulus for gels that were formed from dECM digested

for 24 hours vs. 72 hours (7.5 mM: 314.65 +/- 26.11 rads/s vs. 523.95 +/- 58.265; 10 mM: 627.36 +/- 52.704 rads/s, vs. 356.31+/- 49.29; Fig. 2.5A) ($p<0.05$). Gels cross-linked with 5 mM of genipin did not show any differences based on digestion times.

Degradation of the hydrogels by collagenase was evaluated over 30 days. During the first five days after initial weights were recorded, linear regression was performed to analyze the degradation rate of change. The rate of degradation of the gels formed from either 24 or 72 hour digested dECM was different for the 5 mM and 10 mM genipin + dECM hydrogel groups ($p<0.05$). The rate of degradation was slower in gels formed from 24 hour digested dECM, and all concentrations of genipin showed similar results (Figure 2.5B,C).

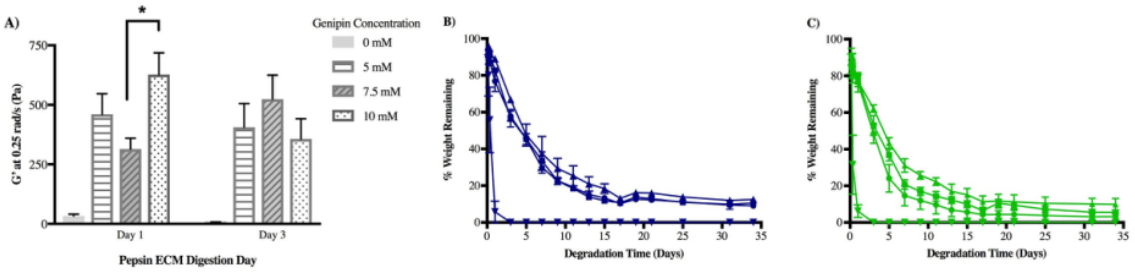

Figure 2.5: Rheological Properties of Genipin-Crosslinked dECM Hydrogels. (A) Assessed by performing frequency sweeps of hydrogels formed using dECM obtained after 1, 2, or 3 days of pepsin digestion, and increasing amounts of genipin concentration. At 0.25 rads/s genipin-crosslinked dECM hydrogels made shows significant increases in storage modulus with increasing genipin concentration for 7.5 mM and 10 mM gels, while genipin-crosslinked dECM hydrogels made from 3 days of pepsin digestion showed no significant changes with varying amounts of genipin. Data represent mean ± SD; n = 3 per digest day group, *$p < 0.05$. (B), (C) Collagenase-mediated degradation profiles of dECM hydrogels that were made from dECM solutions digested with pepsin for either (B) 1 day, or (C) 3 days, and then crosslinked with either 0, 5, 7.5, or 10 mM of Genipin. Gels that were formed from 1 day of pepsin digestion degraded more slowly than gels that were formed from 2 days or 3 days of digestion, but gels formed with varying amounts of genipin all showed similar degradation profiles. All groups were degraded in the presence of collagenase at 37°C. Data represent mean ± SD; n = 3 per digest day group.

2.5.4 Viability of Cardiac Cells

To determine the biocompatibility of the crosslinked digested ECM, multiple cardiac cell type viability was assessed using a live/dead stain, which showed that overall cell viability remained high. HUVEC cell viability was 98.38% +/-2.24% across all three genipin concentrations and digestion days (Fig. 2.6A). Cardiac fibroblasts showed over 100% live cell count across all three genipin concentrations and digestions days, indicative of proliferation as well (Fig. 2.6B). Interestingly, cardiomyocytes seeded on gels that were formed from dECM that had been digested in pepsin for only 24 hours and crosslinked with either 7.5 or 10 mM genipin showed the highest average cell viability, however, only a difference was observed in the 5 and 10 mM genipin groups between digestion times (Fig. 2.6C). This was attributed to the material composition of the gel; as the digestion

time was only 24 hours in pepsin, the protein fragments should be larger and therefore may be more similar to *in vivo* protein composition.

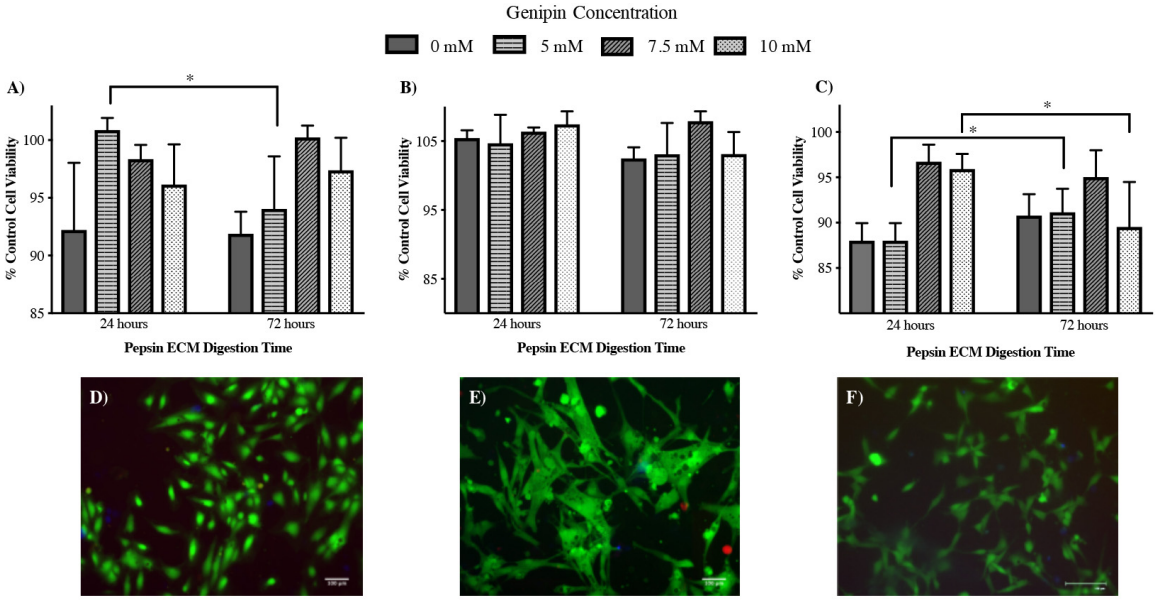

Figure 2.6: Cell Viability in Genipin-Crosslinked dECM Hydrogels. (A, D) HUVECs, (B, E) cardiac fibroblasts, and (C, F) cardiomyocytes on genipin-crosslinked dECM hydrogels. A) HUVECs seeded on 24 hour digested dECM showed higher viability compared to 72 hour digested dECM. B) No statistically significant differences were observed between hydrogels made from different pepsin digestion days for cardiac fibroblasts. C) Cardiomyocyte viability was significantly higher for cells cultured on 7.5 and 10 mM genipin-crosslinked dECM hydrogels as compared to 0 mM and 5 mM genipin-crosslinked dECM hydrogels. Cardiomyocytes seeded on hydrogels digested in pepsin for 24 hours showed higher cell viability than 72 hour digested counterparts for the 5 mM and 10 mM genipin groups. Data represent mean ± SD; n = 4 per digest day group, $*p < 0.05$.

2.5.5 Differentiation of ADSCs Towards Cardiac Phenotype

The differentiation of ADSCs towards a cardiomyocyte lineage with and without blocking of β4 and β5 integrins by quantitative PCR (qPCR) showed certain cardiac specific gene expression upregulated. qPCR showed significant upregulation of cTnI, and sarcomeric

alpha actinin in the β4 and β5 integrin blocked groups compared to all other groups (*p<0.001)* (Fig. 2.7). Additionally, expression of both MLC2 atrial and MLC2 ventricular isoforms of myosin light chain, was significantly up-regulated by 3 weeks compared with the genipin + dECM groups (*p<0.001)* (Figure 2.8, 2.10). Cells seeded only on genipin + dECM groups showed no expression of MLC2 until 2 weeks in culture, with a statistically significant difference seen 3 weeks post cell seeding ($p<0.05$) (Fig. 2.10). Expression of cTnI was not detected in qPCR until 2 weeks post cell seeding, and increased gradually over, with no differenes between groups (Fig 2.7. B, Fig 2.10). Sarcomeric alpha actinin expression increased as time went on (Fig 2.7. C), and the β4 + β5 integrin blocked groups

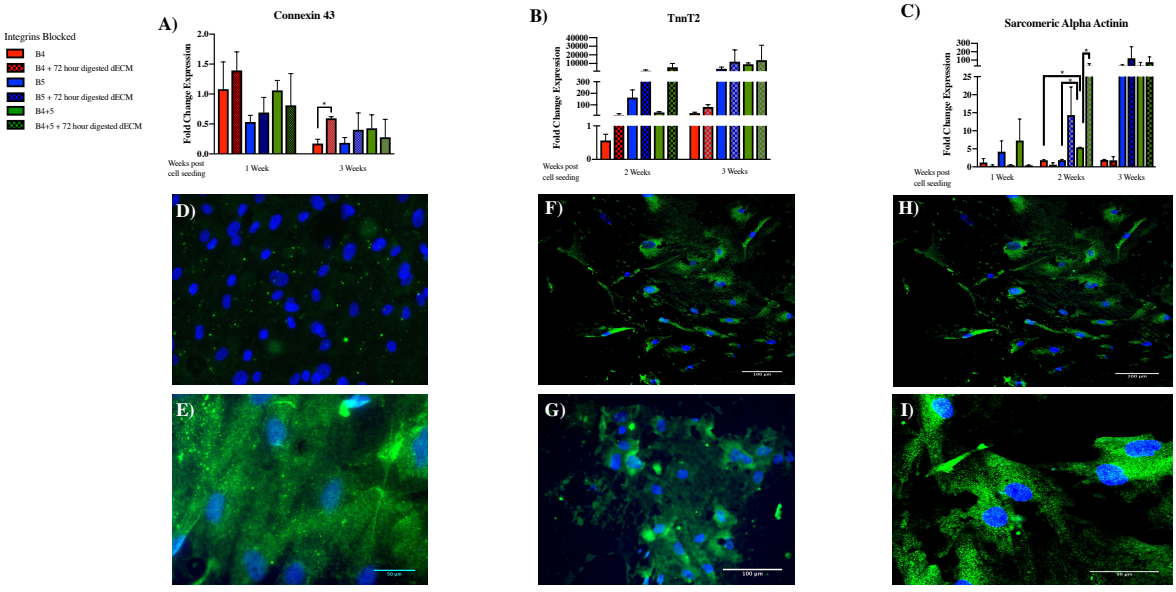

Figure 2.7: Expression of Cardiac Genes in Genipin-Crosslinked dECM Hydrogels. 7.5 mM dECM hydrogels digested for 24 or 72 hours, and either B4, B5, or B4+5 integrins blocked. Connexin 43 expression on 24 hour pepsin digested dECM +7.5 mM Genipin gels 1 week post cell seeding D) and 3 weeks post cell seeding E). TnnT2 expression on 24 hour digested dECM 1 week post cell seeding F) and 3 weeks post cell seeding G). Sarcomeric Alpha Actinin staining on 24 hour digested dECM 1 week post cell seeding H), and 3 weeks post cell seeding I). Data represents mean +/- SD. N=3 for each time-point and each group.

seeded on 72 hour digested dECM + genipin, after 2 weeks were significantly higher than all the other groups (p <0.05).

2.5.6 Activation of β1 integrin on hADSCs

To determine whether the increase in cardiac gene expression was due to the activation of the β1 integrin by the β4 and β5 integrins, a β1 integrin blocking antibody was incubated with hADSCs prior to seeding on genipin + dECM hydrogel surfaces. After 1 week in culture, activated β1 integrin was measured on cell surfaces (HUTS-4). The amount of positive HUTS-4 staining on β4+β5 blocked hADSCs that had been seeded on hydrogels digested for only 24 hours (44.02% +/-3.39) was significantly higher than cells seeded on gels made from dECM digested for longer (27.37% +/-4.92, *p<0.05)* (Fig. 2.11 D, H). To see whether blocking β1 integrin would eliminate the activation of the integrin, or if the β4 and the β5 integrin alone could activate β1, all three integrins were blocked in different

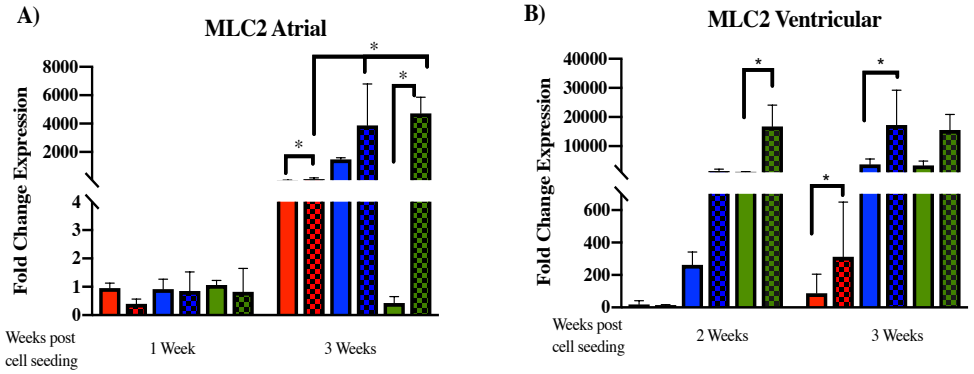

Figure 2.8: Expression of MLC2A and MLC2V. 7.5 mM dECM hydrogels digested for 24 or 72 hours, and either B4, B5, or B4+5 integrins blocked. A) MLC2 atrial isoform expression showed significant up-regulation in gene expression compared to unblocked controls 3 weeks post cell seeding. B) MLC2 ventricular isoform was not detected until 2 weeks post cell seeding, and was significantly higher than its unblocked counter part. Data represents mean +/- SD. N=3 for each time-point and each group.

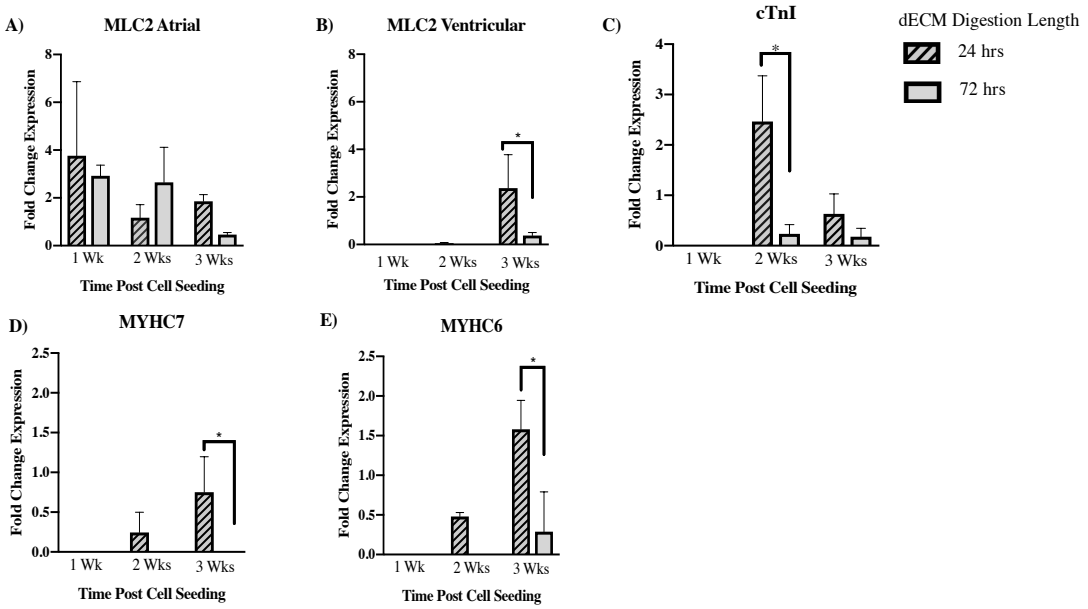

Figure 2.9: Expression of Cardiac Genes on Control dECM Hydrogels. 7.5 mM dECM hydrogels digested for 24 or 72 hours no integrins blocked. A) MLC2 ventricular isoform expression showed significant up-regulation in gene expression on 24 hour digested dECM compared to controls 72 hour digested dECM 3 weeks post cell seeding. B) MLC2 atrial isoform was not statistically different between digestion groups. C) cTnI expression was not detected until 2 weeks post cell seeding, and was significantly higher after 2 weeks in the 24 hour digested group. D) MYHC6 was not detected in 72 hour digested dECM E) MYHC7 expression was not detected in 72 hour digested dECM groups throughout seeding.

combinations (β1+β4, β1+β5, and β1, β4, and β5). Interestingly, across all three groups β1 activation was detected (Fig. 2.11 B, C, E, F). This suggests the intracellular connectivity between the β integrin subunits, and further implicates their role in cardiac differentiation.

2.6. Discussion

As ADSCs are an emerging and promising potential source for cardiovascular disease treatment, more studies into the differentiation of ADSCs into cardiomyocyte like cells have been conducted [213]. Previous studies have shown the capacity of ADSCs to

differentiate into different cardiac lineages such as cardiomyocyte, fibroblast, endothelial, and smooth muscle [213, 214]. Indeed, studies have seen varying amounts of effective differentiation efficiency, with conflicting results on cardiomyocyte integrity. While there are differing opinions on the efficacy of the differentiation of the cells, there nevertheless remains the clinical data showing that ADSCs are anti-inflammatory, pro-angiogenic, and may be beneficial when injected post- MI.

Recently, new technologies have been developed that may be used to help encourage the differentiation of ADSCs towards cardiomyocytes, such as the processing of decellularized tissues into hydrogels. These gels have been shown to retain the intrinsic cues necessary to differentiate mesenchymal cells towards a cardiac lineage [215]. The environment provided by the dECM hydrogel enables cells to be exposed to similar conditions as *in vivo;* as the majority of the ECM components are retained through processing [75]. When coupled with a crosslinker with low cytotoxicity, dECM gels can also provide cells with an environment that is more mechanically similar to *in vivo* conditions as well. In addition to the capability to differentiate stem cells towards tissue specific lineages, these gels may also be used as a potential delivery vehicle for bioactive factors, which could then be used to further drive differentiation [216]. As currently there are cardiac hydrogels, VentriGel (Ventrix, San Diego CA) in Phase I clinical trials, further investigation into how the processing of the tissue affects the final product, and subsequently cell behavior is necessitated. Further, because of the similar *in vivo* environment that the dECM hydrogels possess, elucidating how to differentiate stem cells more efficiently utilizing this technology is valuable. In this study, we aimed to expand upon previous studies

characterization of cardiac dECM hydrogels and investigate how differential processing of the dECM affects the final material characteristics and downstream applications such as differentiation of ADSCs into cardiomyocyte like cells. We further elaborated on the differential composition of the resulting hydrogels by utilizing *in vivo* integrin signaling pathways known to be important in the differentiation of cells early in cardiac development.

We found that the length of time that the dECM is digested not only affects the material properties, but also cell behavior. As the length of digestion is increased, and proteins are broken down into smaller fragments, the mechanical strength of the material should be altered due to the presence of more available crosslinking sites. However, our results indicated a different finding; after just 24 hours of digestion the highest G' was observed in the 10 mM genipin group, compared to 72 hours of digestion (Figure 2.5A). This was attributed to the size of the proteins that were available and the accessibility of the genipin to the protein. In the 5 mM genipin group, there were no differences noted between dECM digestion times. This lack of difference was hypothesized to be due to the concentration of the genipin relative to the available sites for crosslinking, which can affect the final material elasticity. The stiffness of a material has been shown previously to heavily influence stem cell differentiation, such as mesenchymal stem cells [217, 218]. Stiffness alone can help determine whether a cell will differentiate towards an osteogenic or a neurogenic lineage. Although the observed differences in G' were minimal, we can attribute some of the differences seen in our cell differentiation to the different G' measurements of the dECM + genipin hydrogels.

In addition to mechanical stiffness as a driving force of differentiation, protein composition of the extracellular matrix can influence cell signaling and consequently differentiation. Indeed certain proteins such as laminin and fibronectin have been implicated for their role in cardiac differentiation, with laminin in particular being important [219]. In proteomic analysis of the different digestion times, fibronectin, an important component of the ECM known for its role in cardiovascular development, decreased by approximately 40% when the digestion time was extended to 72 hours (compared to 24 hours; Fig 2.2). Although the fibronectin remained a small percentage of the overall protein composition of the dECM at both digestion times, even the slightest change in material composition can influence the behavior of cells and influence differentiation of stem cells. Another protein, Collagen V has been recently implicated in its role in cardiac differentiation. Indeed, the detected Collagen V decreased from 10.92% in 24 hour digested dECM hydrogels, to 7.27% after 72 hours of digestion. This disparity in Collagen V may help explain the differences noted in cardiac gene expression in our control hydrogels, which has shown to have a pro-cardiogenic effect (Figure 2.9)[220]. Because of the role of proteins in cell differentiation, we wanted to consider whether this difference in material composition could actually be the cause of the different cell behavior seen in the qPCR data, and did so by blocking the cell's ability to recognize certain proteins via integrins.

Based on previous studies completed, we believed that by blocking the β4 and β5 integrins we would be aberrantly affecting the cell differentiation. Instead, we found that by blocking the activity of β4 and β5 integrins, we increased the expression of certain cardiomyocytes specific genes (Fig. 2.7). This was hypothesized to be from a possible

increase in activation β1 integrin, and therefore it activity, which is critical to cardiomyocyte development. We found that by inducing increased β1 activity, we induced increased expression of both atrial and ventricular isoforms of myosin light and heavy chain proteins, and cardiac troponin I. For other genes, such as gap junction protein connexin 43, only slight increases in expression were seen when compared to cells whose integrins were unblocked. This was attributed to previous work that had found that β1 integrin function negatively regulates connexin expression, and if β1 integrin activity is supposedly increased in our model, then it follows that expression would not be increased (Fig 2.7)[209, 221]. Interestingly, early genes known to be critical to cardiac development such as GATA4 and NKX2.5 were expressed either very low, or were not detectable in qPCR analysis. NKX2.5 however, was detected via immunohistochemistry. Because low to no early cardiac gene expression was detected, we believe this gave evidence of the possible role of the integrins in the expression of more mature cardiomyocyte markers.

Previous studies have shown the crosstalk between integrin's and the significance that crosstalk can have on cell migration, adhesion and behavior [208]. The signaling that occurs via integrin's typically is induced by ligand binding, i.e. ECM, and is termed "outside in" signaling [208]. However, integrin cytoplasmic domains may also be altered by active non-integrin receptors, known as "inside-out" signaling, which can cause integrin's to be switched from an inactive state to a high affinity state [208]. In a study performed by Bernstein et al, the blocking of αVβ5 integrin indeed increased β1 activity, while also decreasing β1 integrin binding to the matrix [212]. Conversely, the authors

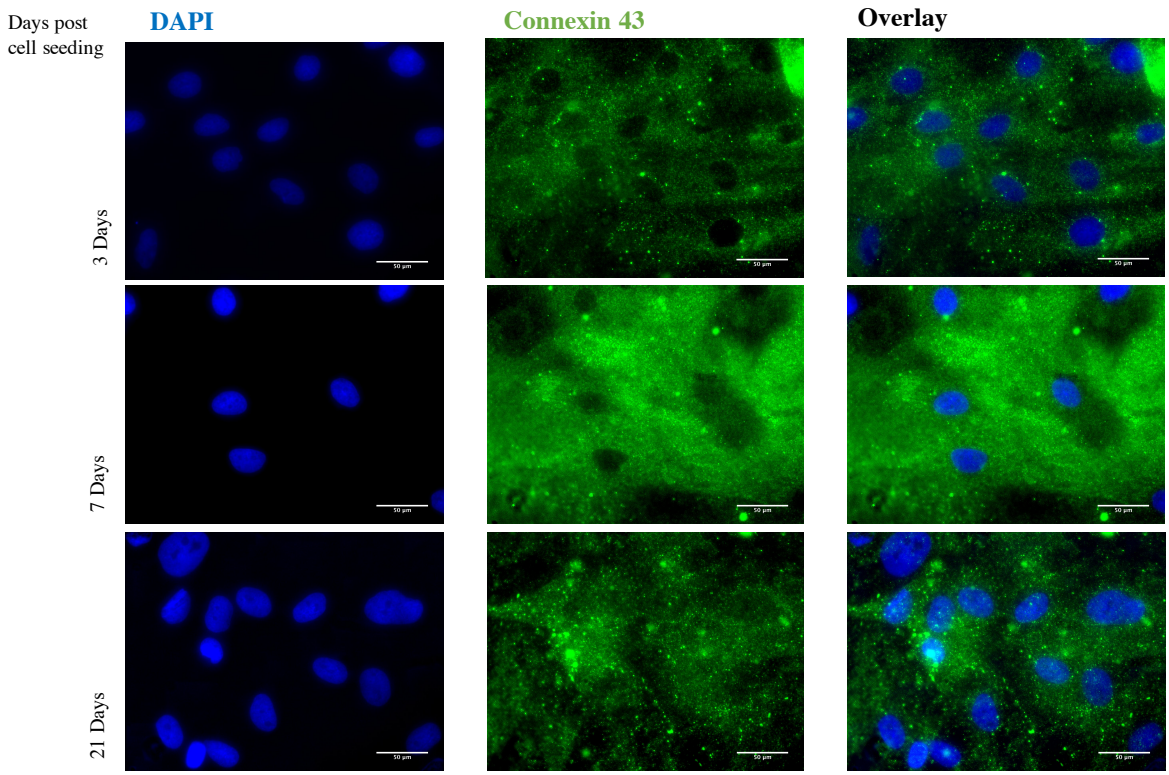

Figure 2.10: Expression of Connexin 43 on Cell Surfaces. Gap junction protein (green) and nuclei (blue) on the surface of hADSCs seeded onto dECM hydrogels +genipin that had been digested for 72 hours only. Distinct areas of connexin expression are more obvious over time within these images as seen as distinct brighter green fluorescence.

found that when the levels of β5 integrin increased, β1 integrin binding to collagen/fibronectin matrix increased, while β1 integrin activity decreased [212]. This not only suggests the interconnected relationship that the β integrin's possess, but also provides preliminary evidence that intracellular signals help to dictate other integrin confirmations. In our study, we found that by blocking β4 + β5 integrin, and with β1 integrin blocked, active β1 integrin was still seen via immunohistochemistry (HUTS 4; Fig. 2.11). Interestingly, hADSCs that were seeded on gels made from 24 hour digested

dECM appeared to show a higher overall amount of active β1 integrin compared to the 72 hour digested dECM (Fig. 2.11).

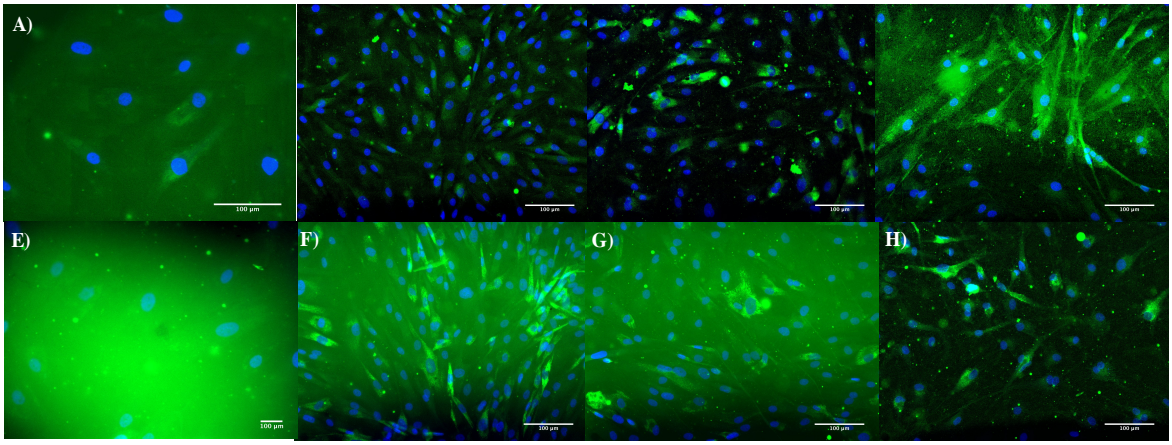

Figure 2.11: Activated B1 Integrin. Expression in hADSCs seeded on 24 hour digested dECM hydrogels + 7.5 mM genipin (HUTS4, Green, DAPI, Blue) (A, B, C, D), or 72 hour digested dECM hydrogels + genipin (E, F, G, H), 1 week post cell seeding. A) 7.5 mM Genipin + 24 hour digested dECM, B) B4 integrin blocked, C) B5 integrin blocked, D) B4+5 integrin blocked. E) 7.5 mM Genipin +72 hour digested dECM, F) B4 integrin blocked, G) B5 integrin blocked, H) B4+5 integrin blocked.

2.7 Conclusion

In this work, we demonstrated that the digestion time of decellularized extracellular matrix hydrogels affects cell and final hydrogel behavior. Additionally, we researched how the digestion time and resulting protein composition influences adipose derived stem cell differentiation towards a cardiomyocyte lineage. Adipose derived stem cells expressed certain cardiac specific genes 2 and 3 weeks post cell seeding, with cells seeded on 24 hour digested dECM exhibiting significantly higher expression than those seeded on 72 hour digested dECM of cardiomyocyte-specific markers. Because protein composition affects cell differentiation during development, it would be advantageous to utilize a dECM hydrogel and customize it through digestion to induce differentiation to a specific cell lineage [222, 223]. Here, we showed that not only the protein composition, but also the integrin signaling affects the ability of adipose derived stem cells to trans-differentiate. By blocking both the β4 + β5 integrins, we hypothesized that the increase in cardiac marker expression was due to the increased activation of the β1 integrin, and showed this through immunohistochemistry staining. This work suggests that integrin signaling and ECM composition in combination play a large role in the trans-differentiation of stem cells towards a cardiomyocyte lineage, and that further studies into the roles of these integrins in development is warranted.

3 OPTIMIZATION OF SUSTAINED SEQUENTIAL ANGIOGENIC GROWTH FACTOR DELIVERY FROM COLLAGEN HYDROGELS

3.1 Overview

In tissue engineering, many challenges exist on the path to creating scaffolds that may be used as an *in vivo* tissue replacement or graft. Few however, are as large as the vascularization of said scaffolds for use in regenerative medicine. Scaffolds must be able to support metabolically active tissues, or have the ability to support vascular growth into the scaffolds from host tissues. Recently decellularized scaffolds have been utilized in tissue engineering as they retain native extracellular matrix and vascular conduits are retained until the 2/3 order of branching. Microvasculature, however, is degraded in this process and therefore still cannot long term support metabolically active tissues. In this study, I have developed a collagenous-based angiogenic growth factor delivery system for use in decellularized scaffolds. By combining potent angiogenic growth factors such as vascular endothelial growth factor A (VEGF-A), Platelet derived growth factor ββ (PDGF- ββ) and Angiopoietin 1 into a collagen scaffold release of said molecules is controlled by charge and molecular weight. I show that the use of these growth factors increases cell migration and positively influences angiogenesis machinery such as the endothelial cell lumen formation complex. Then, by using a 3D dECM hydrogel as *in vitro* model of a decellularized scaffold environment, I show evidence that these growth factors would positively encourage endothelial cell migration and subsequent invasion into said scaffolds. This research lays the groundwork for future studies in utilizing the collagenous encapsulated growth factors into decellularized scaffolding's vascular beds.

3.2 Introduction

In tissue engineering, vascularization of biomaterials continues to be one of the leading challenges. Often, the biomaterials used are synthetic or natural in origin, and are not inherently vascularized. When applied to an *in vivo* environment these materials are expected to engraft with local tissue and be invaded by vascular cells. However, because of the slow *in vivo* angiogenic growth rate, different methodologies to increase the vascular growth rate into/out of a scaffold by modulating the scaffold to be a more angiogenic conductive environment have been explored. Recently, decellularization has emerged as a new technique to create scaffolds for tissue engineering that retains the native vasculature conduits. In 2008, our lab pioneered the decellularization of whole heart scaffolds, and showed that when the cellular contents were removed, the vascular conduits still remained up to the 2 and 3rd order of branching [23, 62]. Because of the retention of existing vasculature endothelial cells can be utilized to then repopulate these conduits- potentially solving the need for methods to increase the vascularization of tissue-engineered specimens. However, the microvasculature within these scaffolds is degraded by decellularization, which renders them not able to support a metabolically active tissue long-term [224].

Different ways to approach the low level of microvasculature regrowth within decellularized scaffolds shave been explored including chemical modification to the scaffold, utilizing both stem and progenitor cells, and bioactive molecule delivery [225]. Typically, re-endothelialization of an acellular scaffold is accomplished via perfusion and the scaffolds are perfused with stem cells, endothelial progenitor cells, or adult endothelial cells [226]. While some groups have seen success using a combination of both stem that

can differentiate into supporting cell types and adult endothelial cells, the rate of microvasculature growth is still insufficient. Chemical modifications to the scaffold itself have included the use of chemicals such as heparin that has been immobilized to a scaffold, or heparin gel coating on the scaffold surface to help with endothelial cell adhesion [227, 228]. In decellularized scaffolds this chemical modification has been coupled with bioactive molecules known for their role in angiogenesis, such as VEGF, to help increase the amount of vasculature that is formed within a scaffold, and also encourage vascular cell in growth to the scaffold.

Angiogenesis is a multifaceted process in which new vascular vessels form from pre-existing vessels [229, 230]. This process begins with the proliferation of endothelial cells (ECs), the formation

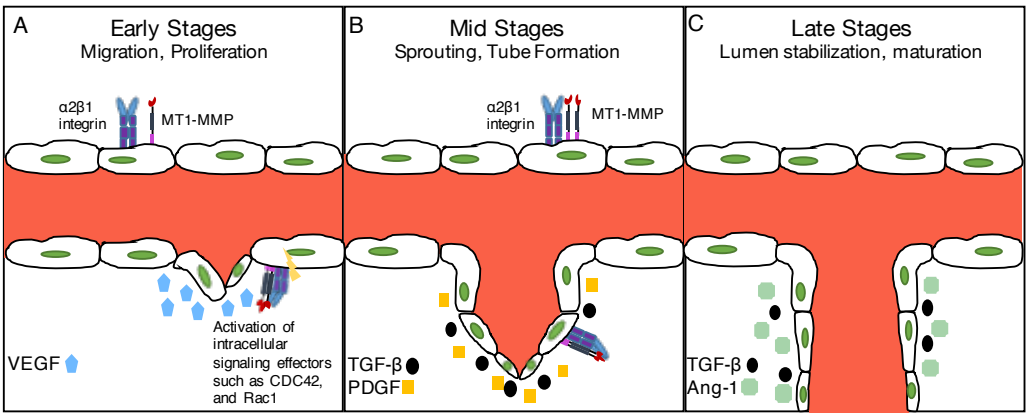

Figure 3.1 Angiogenesis Steps; A) Early- influence of VEGF on the proliferation of ECs, and work of MT1-MMP and α2β1 to help control the migration of the cells. B) Tube formation and sprouting of ECs; PDGF aides in chemotaxis and tube formation. C) Late-lumen stabilization facilitated by Ang-1 and TGF β

of primitive tubules by these cells, connection of adjacent tubes, and finally lumen formation and stabilization of the tubes, leading to a mature microvessel (Figure 3.1).

Throughout this process, specific signaling molecules are expressed at different time points as the new vessel grows. VEGF-A is an initiator of angiogenesis and causes the initial proliferation of ECs. Following the early stages of angiogenesis, a cascade of different signaling molecules is expressed, including PDGF. PDGF acts to stimulate EC proliferation, migration, tube formation, and also stimulate the secretion of VEGF from ECs [11]. In later stages of angiogenesis, Ang-1 promotes survival of ECs and vessel stabilization [11].

One of the most critical steps in angiogenesis is the initiation of lumen formation by ECs, which is facilitated by a variety of cellular components that function in a coordinated fashion (Figure 3.2). Membrane-type 1 matrix metalloproteinase (MT1-MMP) is a

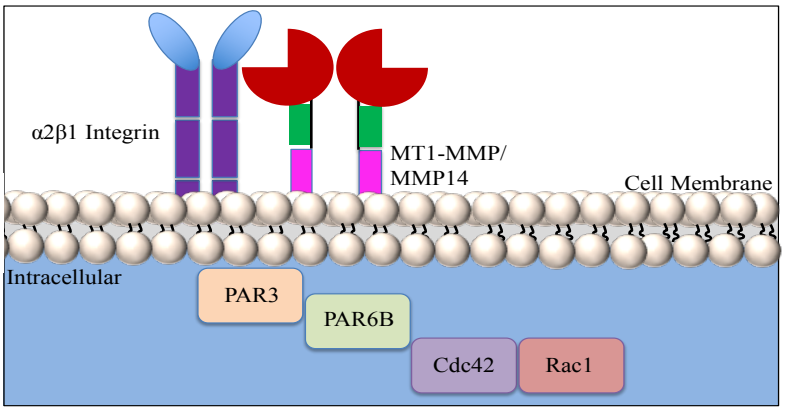

Figure 3.2: EC Lumen Formation Complex.

collagenase critical in the formation of EC lumen formation [231-233]. Additionally, MT1-MMP is necessary to amplify signals of various angiogenic growth factors, such as VEGF by causing an increase in receptor expression and cell surface localization [132, 231, 233, 234].

MT1-MMP works in conjunction with the α2β1 integrin to initiate a signaling cascade within endothelial cells [232, 235-237]. MT1-MMP also activates the rho-GTPase Cdc42 [235, 237, 238]. This GTP-ase acts as a downstream effector of MT1-MMP, and its proper activation and expression is crucial to the formation of endothelial cell lumens [235-238]. The activation of Cdc42 leads to the activation of the Src, B-Raf, C-Raf, and Erk1/2 causing the rearrangement of the actin cytoskeleton and affecting cell polarity machinery, which is important for cell migration [235, 237-239]. Confirmation of the activation and expression of these cellular components will confirm that the system I have designed is recapitulating the signaling events within angiogenesis, and ensuring the formation of a higher density of vasculature. The successful revascularization of decellularized organs must facilitate the onset of the MT1-MMP/ Cdc42 signaling cascade to recapitulate microvasculature lost during the decellularization process.

Here, I created a system to increase vascularization within tissue-engineered specimens by taking cues from nature and utilizing angiogenic growth factors encapsulated within collagen scaffolds as a GF delivery vehicle that may be eventually used one day within tissue engineered specimens. Three GFs (VEGF-A, PDGF, and Ang1) will be encapsulated

within collagen, and have been chosen based on their role in angiogenesis at various stages of vessel formation and maturation (Figure 3.1). The GFs that have been chosen include vascular endothelial growth factor-A (VEGF-A), which induces EC proliferation and maturation [240, 241]. Platelet derived growth factor (PDGF) a GF that has been shown to enhance viability and migration [242], and Angiopoietin-1 (Ang-1), which contributes to blood vessel maturation and stabilization [243], encouraging the final maturation of blood vessels. The encapsulation of these GFs within collagen will allow for their controlled release, which should promote EC organization into complete monolayers with appropriate junction formation. The system is designed to release GFs over a period of time, to allow for sufficient time for EC proliferation and formation of microvascular structures. The release of GFs will be studied using degradation based kinetics, by utilizing collagenase at levels similar to *in vivo*, and characterized to collect baseline data on the influence of GF release on 3D cell cultures. Additonally, I will measure how the addition of the three GFS affect the EC lumen formation complex, as it is critical for proper microvascular formation ensuring its proper function is crucial.

3.3 Specific Aims

Specific Aim 2: Create a GF encapsulated collagen delivery system that will deliver vascular GFs in a temporally controlled manner

Specific Aim 2.1: *Model release rate of VEGF, PDGF and ANG1 encapsulated within collagen hydrogels.* I hypothesize that the release of all three GFs will be occur based on size, and will occur in the following order; first VEGF, then Ang1/PDGF at the same time.

Specific Aim 2.2: *Characterize the effect the GFs have on endothelial cells.* I hypothesize that cells seeded on top of gels that had GFs encapsulated within them will form tubes at a higher rate and invade into the collagen gel deeper than control gels without GFs.

Specific Aim 2.3: *Elucidate the effect that the GFs have on certain endothelial cell lumen formation complex machinery.* I hypothesize that the presence of the GFs will increase the amount of Mt1-mmp active in ECs, and activate down stream effectors of the EC lumen formation complex such as CDC42 and Rac1.

Overall Goal for Specific Aim 2: Create a GF encapsulated collagen delivery system that will deliver vascular GFs in a temporally controlled manner to be one day used in tissue-engineered specimens.

Specific Aim 3: Characterization of endothelial cell behavior to growth factor release in a simulated *in vivo* environment

Specific Aim 3.1: Characterize the ability of endothelial cells encapsulated within collagen gels with or without the presence of GFs, layered on top of dECM hydrogels. *I hypothesize that cells encapsulated within collagen gels with GFs will invade deeper into dECM hydrogels than their control counterparts.*

Specific Aim 3.2: Characterize the ability of ECs seeded on top of collagen gels with or without GFs to migrate through the collagen and dECM hydrogel. *I hypothesize that the ability to migrate through the collagen gel will be significantly increased in gels with encapsulated GFs, but that they will still not migrate through the dECM hydrogel.*

Overall Goal for Specific Aim 3: To recapitulate *in vivo* conditions, a sandwich assay using collagen gels with or without GFs will be layered on top of dECM hydrogels, and

ECs will be seeded on top of the collagen gels, or encapsulated within the collagen gels. This will be used to help characterize the dECM vascularization potential in response to sequential growth factor release.

3.4 Materials and Methods

3.4.1 Collagen Film Synthesis and Characterization

Type I porcine collagen (Advanced BioMatrix, Inc.) was used as the system for sustained GF delivery. Collagen solutions were made per the manufacturer's instructions. Briefly, 0.5 mls of 10X M199 Media (With Hanks salts; Thermo Fisher) was added to 4 mls of collagen solution. The solution pH was then adjusted to 7.2 - 7.6 through the addition of 0.1M NaOH, as needed. Sterile water (0.5 ml) was then added to this base solution, which is maintained at 2-10°C, until use. In the control gels, sterile water was added, and in the GF gels, growth factors were added as listed in the table below (Table 3.1). 150 ul of gel solutions were added into 48-well plates and placed in 37°C to crosslink.

Growth Factor	**VEGF-A**	**PDGF-BB**	**Ang1**
Molecular Weight (kDA)	38.2	28.5	70
Effective dose 50 (ng/ml)	3.1-4.6	3-5	10-40
Concentration (ng/ml)	3.3	3.3	3.3

Table 3.1: Growth Factors used in Studies. Effective dose (ED50) is listed.

3.4.2 Collagen Degradation

To characterize the release profile of the GFs from the collagen gels, rate of collagen degradation was recorded in gels made using the above protocol, with 40,000 p3-5 HUVECs (LONZA, Walkersville, Md). Media was changed and collected and stored at -80°C once a day. Collected media was analyzed for hydroxyproline content (Biovision). Hydroxyproline can be used to measure the amount of collagen in a given sample, as the hydroxyproline amino acid is unique to collagen. This was used in order to measure the rate at which the cells were degrading the collagen, so then an equivalent amount of Type 1 Collagenase could then be used as an *in vitro* model of release.

3.4.2.1 Hydroxyproline Assay Procedure

Assay was performed following manufacturers instructions. Briefly, 100 µls of collected media was hydrolyzed in 100 µls of 12 N HCl at 120°C for 3 hours. Samples were then allowed to cool, and 10 µls of the homogenate was added into a 96 well plate. A standard curve was created using the provided hydroxyproline standard in media and brought to a concentration of 0.1 mg/ml. Subsequently 0, 2, 4, 6, 8,and 10 µls of the 0.1 mg/ml hydroxyproline stock was added into different wells to create standards of 0.2-2 µg/well standards. Both standard and samples were then evaporated to dryness under a vacuum. For the reaction, 100 µls of Chloramine T reagent was added into each sample well and incubated at room temperature for 5 minutes. 100 µls of DMAB reagent to each well and incubated for 90 minutes at 60°C. Immediately afterwards, absorbance was measured at 560 nm in a POLARstar Omega Plate reader (BMG LABtech).

3.4.3 Collagenase Concentration Optimization

The results from the above mentioned hydroxyproline assay were then compared to the hydroxyproline release from gels that were exposed to different concentrations of Type 1 collagenase (Gibco; Figure 3.3). Briefly, Type 1 Collagenase (Gibco) was added onto the collagen gels containing the above-mentioned GFs, in order to mimic the effect of cell based collagen degradation. Collagenase was added on to the gels at vary times after the set "zero" timepoint, to mimic the amount of time it would take for cells to adhere and begin to degrade the matrix. Based on the collected data, a 2-hour delay of the addition of collagenase was sufficient to mimic the time to adherence of the HUVECs.

3.4.4 Growth Factor Release Quantification

Samples from gels that had GFs encapsulated within them, after the addition of 0.05 units/ml of collagenase as determined above, were collected at set time intervals over 22 days and storing them at -20°C throughout the time course of release. An enzyme-linked immunosorbent assay (ELISA) was then performed to quantify the activity of proteins released from collagen films. Each GF was individually run on different ELISA plates.

3.4.4.1 ELISA Procedure

Briefly, each primary antibody (VEGFA- Thermo Fisher, PDGF-BB- R&D Biosystems, ANG1- R&D Biosystems) was added onto Nunc Maxisorp® 96 well plates (Thermo Fisher) at a concentration of 1.25 μg/ml. Primary antibodies were added onto the plates using a coating buffer consisting of 1.5 g Na_2CO_3 2.93 g $NaHCO_3$ into 1 L of distilled

water, at a pH of 9.6, overnight at 4°C. The coated plate wells were then emptied, and gently patted dry on an absorbent towel. Wells were washed 3 times, repeating the drying on an absorbent towel procedure, using a wash buffer consisting of 1xPBS and 0.05% Tween 20 (Sigma Aldrich). Next, 150 µl of a blocking solution (PBS with 1% Bovine Serum Albumin) was added onto the plate for an hour at 37°C. Well plates were washed 4 times. 100 µl of the previously collected samples were added into the well plates. Standards were created for each respective GF, at concentrations of 1.5, 1.0, 0.75, 0.375, 0.1875, 0.09375, and 0 ng/ml, in the media that was used for the initial release experiments above (Endothelial Growth Media- Lonza). Plates were incubated for 90 minutes at 37°C. Well plates were washed 3 times and patted dry. Biotin-conjugated detection antibodies for each respective GF (VEGFA- Thermo Fisher Scientific, PDGFBB- R&D Biosystems, ANG1- R&D Biosystems) were dilute to a concentration of 0.025 µl per antibody, in the above-mentioned wash buffer. 100 µl of each respective solution was added onto their corresponding wells, and plates were then incubated for one hour at 37°C. Well plates were washed 3 times and patted dry. HRP Conjugated Streptavidin Antibody (Thermo Fisher Scientific) was diluted in the wash buffer to a final concentration of 0.05 µg/ml, and 100 µl of the solution was added into each well, and incubated for one hour at 37°C. Well plates were washed 3 times and patted dry. 100 µl of TMB substrate solution (Thermo Fisher Scientific) was added to each well, and incubated at room temperature in the dark for 30 minutes. After 30 minutes, 50 µl of stop solution (Thermo Fisher Scientific) was added onto the wells. Plates were gently tapped to ensure thorough mixing of the stop solution and TMB substrate solution. Plates were measured in a plate reader at 570 nM on a POLARstar Omega Plate reader (BMG LABtech).

3.4.5 HUVEC Cell Behavior Characterization

P3-5 HUVECs were serum starved (0.5%) for 4 hours prior to seeding on collagen gels with or without GFs encapsulated within them. Cells were seeded at 40,000 cells per cm^2 dependent on the culture dish used. After 3, 7, 14, and 21 days post cell seeding gels were collected and fixed with 4% Paraformaldehyde for 15 minutes. Samples were either stored overnight at 37°C or immediately stained. Cells were washed 3x for 5 minutes in 1X PBS after fixation, and subsequently permeabilized for 15 minutes with 0.1% Triton in 1X PBS. Cells were then stained with Fluoresein Phalloidin for 25 minutes, washed, and then DAPI for 10 minutes and one final wash step. Gels were inverted onto a microscope slide and images on a Zeiss Meta Confocal microscope. Z stacks were taken to allow for quantification of invasion to the scaffold.

3.4.6 Cdc42/ Rac1 Activation Assay

3.4.6.1 Cell Lysate Collection

P3-5 HUVECs were serum starved (0.5%) for 4 hours prior to seeding on collagen gels with or without GFs encapsulated within them. Cells were seeded at 40,000 cells per cm^2 dependent on the culture dish used. After 1, 3, 5, 7, 9, 11, and 14 days samples were collected per manufacturers instructions. Both CDC42 and RAC1 assays were conducted using a G-LISA® Activation Assay Biochem Kit- Absorbance based (Cytoskeleton, Inc. Denver, CO). Briefly, gels are removed from the wells and rinsed quickly in ice-cold 1XPBS. Gels are then blotted, and put into a microcentrifuge tube containing 400 µl of ice-cold lysis buffer and protease inhibitors provided by the kit. The gels were then sheared

through 18 gauge needles, and then quickly spun at 14,000 RPM at 4°C. Samples were then snap frozen in liquid nitrogen and stored in -80°C until the rest of the assay was performed.

3.4.6.2 G-LISA® Assay

On the day of the assay, snap frozen lysates were thawed in a room temperature bath. Provided microplates were dissolved in 100 µl of ice-cold water, and then turned over and flicked to remove the solution followed by patting on paper towels. The plate was then returned to ice, and 50 µl of sample cell lysate was added into wells. Blanks and positive controls provided by the kits were added as well. The plate was then shaken on an orbital shaker at 400 rpm for 15 minutes at 4°C. Next, plate was washed with 200 µl of provided wash buffer and removed, and patted on a paper towel. 200 µl of antigen presenting buffer (provided) was then added into the plates for 2 minutes. Antigen presenting buffer was then removed, and wells were washed three times with 200 µl of wash buffer and removed, then patted dry on a paper towel. Anti-CDC42 primary antibody (diluted in antigen presentation buffer) was then added onto each well and incubated on a shaker plate at 400 rpm for 30 minutes at room temperature. After 30 minutes, antibody was washed 3 times with 200 µl wash buffer and removed, and patted dry on a paper towel. Provided secondary antibody was diluted in antibody dilution buffer and 50 µl was added to each well and incubated on a shaker plate at 400 rpm for 30 minutes at room temperature. After 30 minutes, secondary antibody was washed 3 times with 200 µl wash buffer and removed, and patted dry on a paper towel. 70µl of the provided horseradish peroxidase (HRP) reagent was then added into each well and plates were incubated at 37°C for 15 minutes.

140 µl of the provided stop solution was added to each well, and immediately measured at 490 nm using a POLARstar Omega Plate reader (BMG LABtech). CDC42 and RAC1 assays were completed the same way as mentioned above, but using their respective antibody pairs.

3.4.7 MMP14 Activation Assay

3.4.7.1 Cell Lysate Collection

Activity of MMP14 was measured using a SensoLyte® 520 MMP14 Assay kit (fluorimetric; AnaSPEC Fremont, CA). P3-5 HUVECs were serum starved (0.5%) for 4 hours prior to seeding on collagen gels with or without GFs encapsulated within them. Cells were seeded at 40,000 cells per cm^2 dependent on the culture dish used. After 1, 3, 5, 7, 9, 11, and 14 days samples were collected per manufacturers instructions. Briefly, cells were washed with PBS. Assay buffer (provided) with 0.1% Triton-X 100 was added to the cells and incubated at 4°C for 15 minutes. Sample was then collected in a microcentrifuge tube, and incubated at 4°C for 10 minutes. Samples were then centrifuge for 15 minute at 2000 g at 4°C. Supernatant was collected at stored at -80°C until assay was performed.

3.4.7.2 MMP14 Activation Assay

Provided APMA is activated prior to initiation of experiment for 2 hours at 37°C. Samples were thawed and incubated with provided APMA (previously activated at a concentration of 1 mM for 3 hours at 37°C. 50 µl of samples were added into wells of a 96 well plate, along with positive control provided with kit, and substrate control (just assay buffer). 50 µl of MMP14 substrate solution (provided with kit) was then added into all wells, and the

plate was shaken for 30 seconds, and incubated for 60 minutes in the dark at 37°C, then 50 µl of provided stop solution was added to the wells, mixed, and fluorescence intensity was measured at 520 nm on a POLARstar Omega Plate reader (BMG LABtech) .

3.4.8 Sandwich Assay

Sandwich assays were completed forming dECM hydrogels using the following protocol. dECM was created from porcine left ventricles using a previously established protocol. Digested dECM at a concentration of 6 mg/ml was crosslinked with genipin using either 5mM, 7.5 mM, or 10 mM total genipin solution content. dECM-genipin mixtures were pipetted into the wells of a 96-well plate and incubated for 24 hours at 37°C. After 24 hours, gels were rinsed with 1xPBS overnight and exposed to UV light during this time. The following day, gels were rinsed in EGM for 3-2 hour segments, and exposed to UV during that time as well. Subsequently, collagen gels were formed on top of the dECM hydrogels. Briefly, 0.5 mls of 10X M199 Media (With Hanks salts; Thermo Fisher) was added to 4 mls of collagen solution. The solution pH was then adjusted to 7.2 - 7.6 through the addition of 0.1M NaOH, as needed. Approximately 166.6 µls of each GF (VEGF, PDGF, Ang1) at a concentration of 1000 ng/ml (in sterile water) were added into the solution. In the control gels, sterile water was added in the place of the GFs. Solutions were placed in 37°C for one hour to allow for collagen to crosslink. P3-5 HUVECs were serum starved (0.5%) for 4 hours prior to seeding on collagen gels with or without GFs encapsulated within them. Cells were seeded at 40,000 cells per cm^2 dependent on the culture dish used. After 3, 7, 14, and 21 days post cell seeding, gels were collected and fixed with 4% Paraformaldehyde for 15 minutes. Samples were either stored overnight at

37°C or immediately stained. Cells were washed 3x for 5 minutes in 1X PBS after fixation, and subsequently permeabilized for 15 minutes with 0.1% Triton in 1X PBS. Cells were then stained with Fluoresein Phalloidin for 25 minutes, washed, and then DAPI for 10 minutes and one final wash step. Gels were inverted onto a microscope slide and images on a Zeiss Meta Confocal microscope. Z stacks were taken to allow for quantification of invasion to the scaffold.

3.4.9 Statistical Analysis

The statistical analysis of all data was performed using GraphPad Prism 7 (GraphPad Software Inc, La Jolla, CA, USA). Data are presented as mean ± standard deviation unless otherwise stated. Statistical comparison between groups were performed using either a one-way analysis of variance (ANOVA) with Tukey's multiple comparison test (Cell invasion into the collagen gels, Cdc42 activation, dECM hydrogel cell invasion distance) or a unpaired students T-test (all other studies). *p* values less than or equal to 0.05 were considered statistically significant.

3.5 Results

3.5.1 Hydroxyproline Release Assay

In order to fully replicate the degradation of collagen by the cells, the time it took for the cells to be established on the matrix had to be identified. Three different time points were examined, 2 hours, 4 hours, and 6 hours post the simulated cell seeding time to add the collagenase onto the matrices in order to mimic the time it took for the cells to attach and

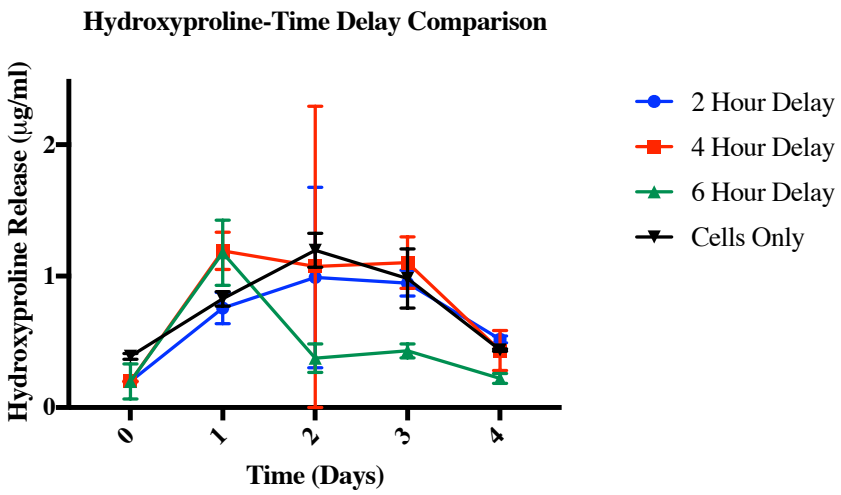

Figure 3.3: Hydroxyproline Time Comparison Release. Collagenase was added on 2, 4, or 6 hours after simulated post cell seeding time. The delay of the collagenase by 2 hours seemed to closely mimic the hydroxyproline release by the cells. Data represent mean +/- SD. N=4 for each group and timepoint.

begin degrading the matrix. As seen in figure 3.3 the differing time addition of the collagenase made a significant difference in the release of hydroxyproline. Since the data showed that the delayed addition of the collagenase by two hours (blue) was the most similar to the hydroxyproline content detected by the cells seeded onto the GF containing gels. The 2-hour delayed collagenase time point was chosen as the *in vitro* model to further confirm the release of hydroxyproline from the cells.

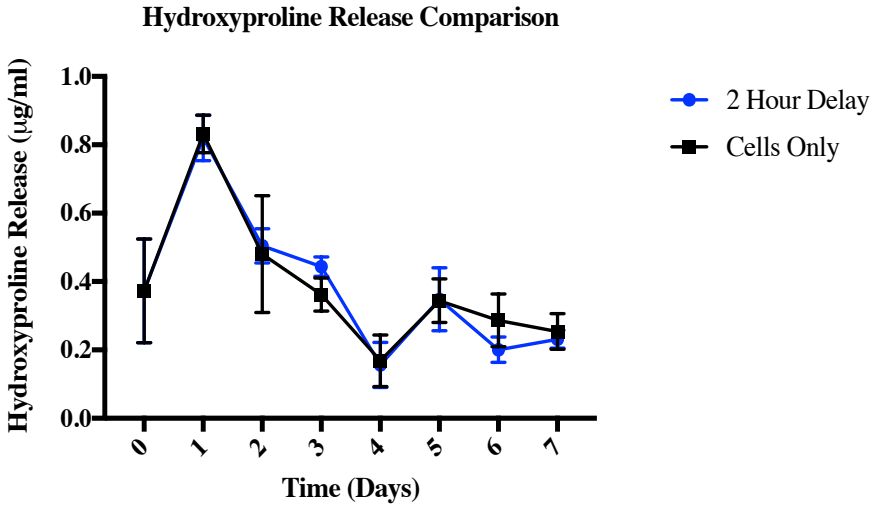

Figure 3.4: 2 hour Collagenase Delay- Hydroxyproline Assay. Comparison of hydroxyproline release over a time period of 7 days. Detection of hydroxyproline was almost identical between the collagenase and cell groups. Data represent mean +/- SD. N=6 for each timepoint

As seen in Figure 3.4 the production of hydroxproline via the degradation of the collagen by either the cells or the type 1 collagenase was almost identical throughout the time course of the release. Therefore, the addition of type 1 collagenase after 2 hours from the initial set time post cell seeding was chosen to proceed forward as the *in vitro* model of GF release.

3.5.2 Growth Factor Release Quantification

The release of the three growth factors VEGF, PDGF, and Ang1 were quantified over 22 days. This was completed to simulate the amount of time that the endothelial cells would be cultured in a decellularized environment. In Figure 3.5, the release is shown to first

happen in VEGF, were sustained release of VEGF is seen, and followed by PDGF 1 day later. Interestingly, Ang1 release was not seen until 7 days after the start of the experiment.

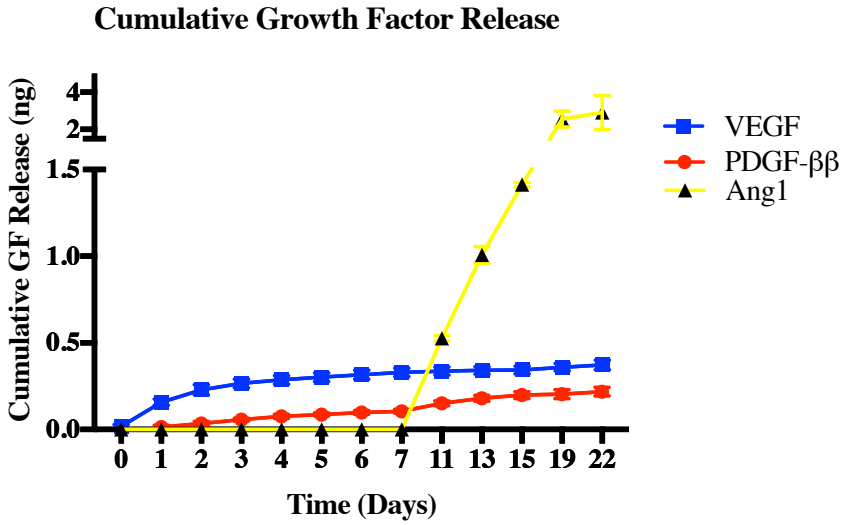

Figure 3.5: Cumulative GF Release. VEGF is released initially, and release is sustained over the entire time period. After 2 days PDGF release is initiated. After a period of 7 days Ang1 is released. Data represent mean +/- SD per group and timepoint.

3.5.3 HUVEC Invasion into the Scaffold

During the first 7 days there was no statistically significant difference between the invasion into the collagen gels between the GF and control groups (Figure 3.6). After 7 days however, there was a statistically significant difference seen. By 21 days, few or no cells were visible within the control gels, but cells and tubules were present in the gels with GFs within them (Figure 3.6).

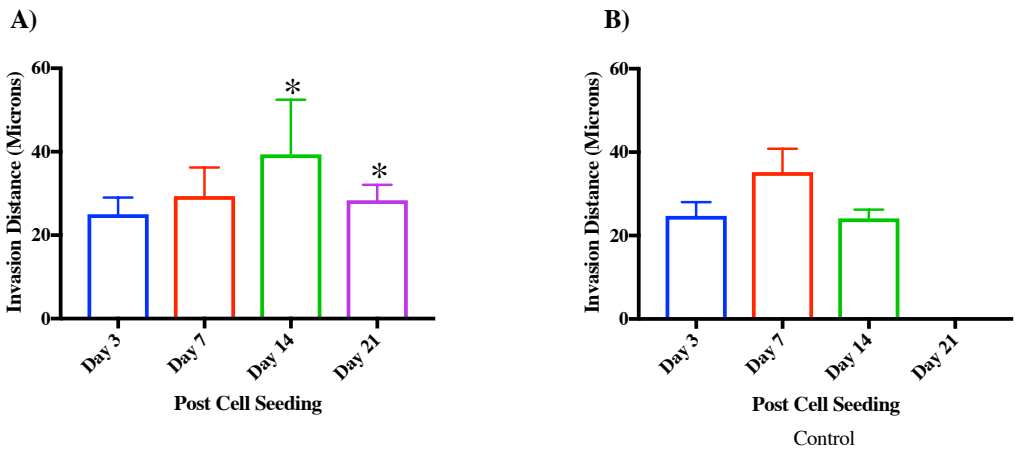

Figure 3.6: Invasion Distance into Collagen. Distance HUVECs invade into collagen scaffolds with GFS (A), and without (B). Data represent mean +/- SD. N=6 for each group and timepoint. *= *p<0.001*

3.5.4 Activation of Endothelial Cell Lumen Formation Complex

The activation of MMP14 was not seen to be different over time in the scaffold. There was no change of between the control and the test group (Figure 3.7). A downstream effector of MMP14, CDC42 a rho-GTPase, was only detected on the first 2 days post cell seeding. On day 2 there was a statistically significant difference between the GF containing gels and

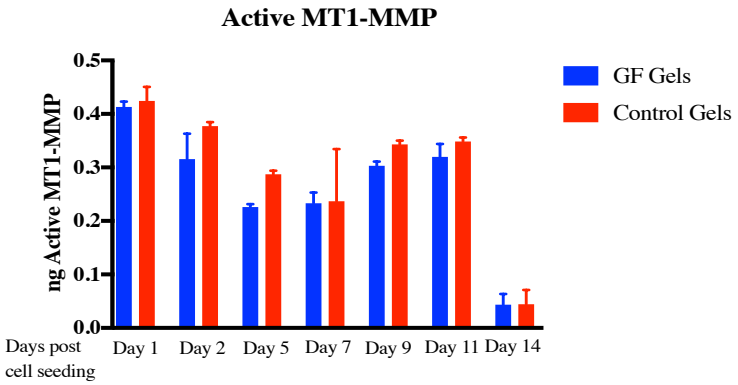

Figure 3.7: Activation of MMP14/MT1MMP. No difference was seen in between the collagen gels containing growth factors vs control gels. Data represent mean +/- SD.

the control gels (Figure 3.8). Rac1, another downstream effector of MMP14 was detected all throughout culture. Interestingly, on day 5 Rac1 activation was activated more than the control gels. Over time however, there was an increase in the activation of Rac1 on days 11 and 14 (Figure 3.9).

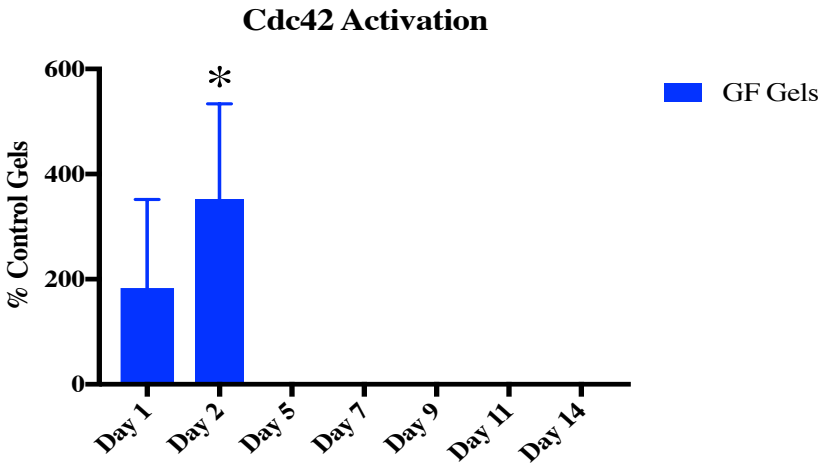

Figure 3.8: Activation of Cdc42. On Day 2 there was a statistically significant difference between the control and the GF groups. Data represent mean +/- SD. N=3 for each group. *= $p<0.05$. Statistics calculated using a 2-way ANOVA.

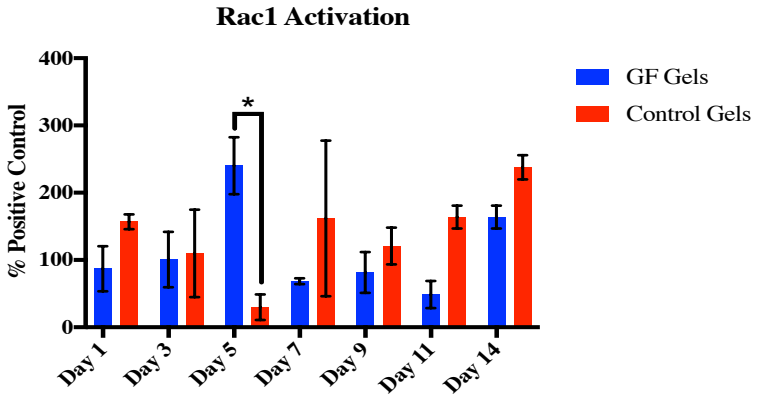

Figure 3.9: Activation of Rac1. No statistically significant differences seen until day 5, when rac1 activation increased in GF containing gels. From day 9 on, Rac1 activation was higher in control gels. Data represent mean +/- SD. N=3 for each group at each timepoint. ***= $p<0.01$

3.5.5 Modeling Decellularized Environment Using dECM Hydrogels

In order to model how cells would behave to this system in a decellularized extracellular matrix environment, dECM hydrogels were utilized. The cells were either encapsulated within the gels, or on top. Over a period of 14 days, there was no statistically significant difference seen between the cells that had been seeded on top of collagen gels with GFs vs the controls (Figure 3.10). However, there was a significant difference seen in cells that had been encapsulated within collagen gels (Figure 3.11).

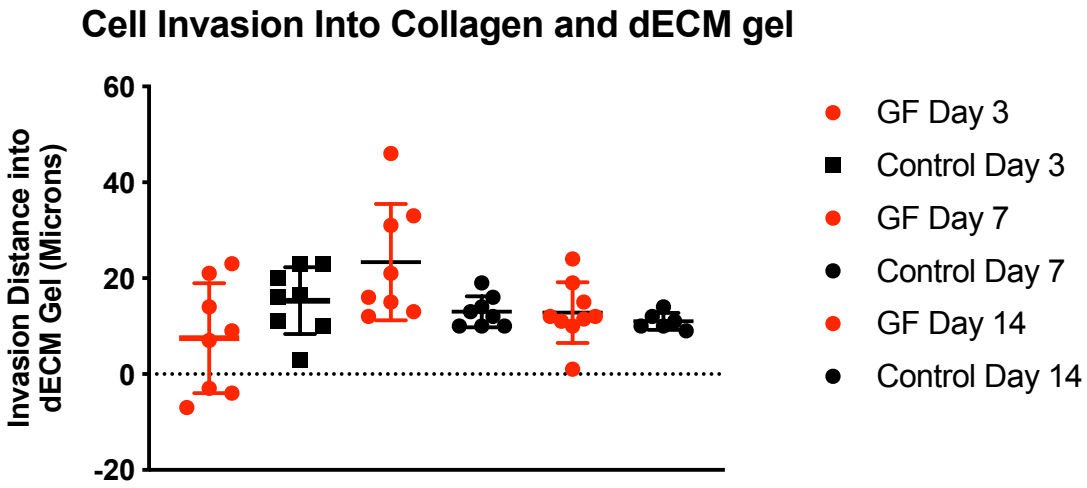

Figure 3.10: Cells on top- Invasion into the dECM. Invasion into the dECM by the endothelial cells over a time course of 14 days. Cells that had been seeded on top of collagen gels with GFs invaded into the dECM hydrogels the same statistically as their control Counter parts. Data represent individual points with means. N=3 for each group. **= $p<0.01$, ***= $p<0.0001$

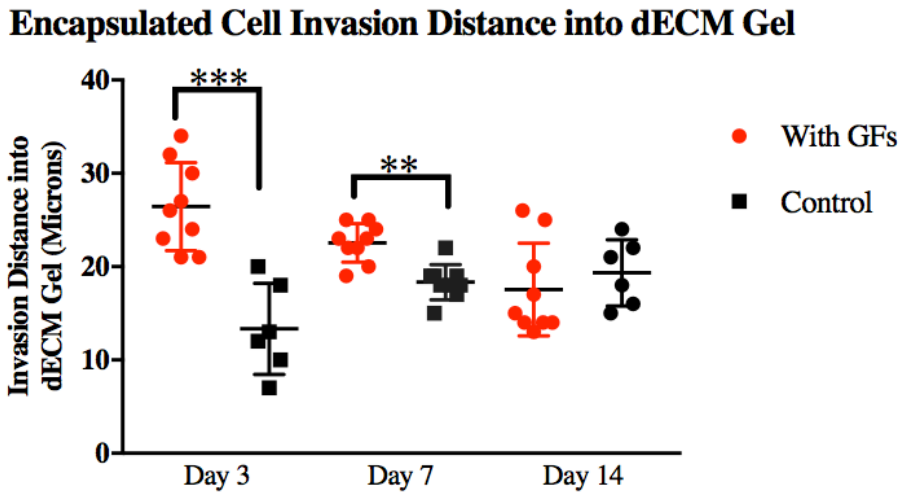

Figure 3.11: Cells Encapsulated- Invasion into the dECM. Invasion into the dECM by the endothelial cells over a time course of 14 days. After 3 days cells that had been seeded in collagen gels with GFs invaded into the dECM hydrogels at a distance greater than their control counterparts. By day 14 this effect was not seen. Data represent individual points with means. N=3 for each group. **= $p<0.01$,

3.6 Discussion

In tissue engineering, insufficient vascularization continues to be one of the leading challenges of the field. Due to oxygen's limited diffusion capacity of ~100-200 μM, metabolically active tissues must have a dense microvascular supply. Synthetic or biologic scaffolding is used in tissue engineering as a surface for cells to grow on. These scaffolds, typically hydrogels, may be either pre-vascularized with cells within them, or acellular with modifications to the scaffold so that it encourages vascular growth into the scaffold itself. Some of the modifications that have been done include encapsulation of bioactive cues, chemical surface modification of scaffolds, and actual physical binding of bioactive

cues to the scaffolds [244, 245]. The goal regardless of what method is used is to encourage angiogenesis, the outgrowth of new vasculature from existing vasculature, either into the scaffold, or if the scaffold is prevascularized, engraft with the host's vasculature. While researchers have thoroughly explored ways to encourage vascular growth into the scaffold, few utilize methods to fully recapitulate *in vivo* angiogenesis.

Angiogenesis is regulated by a complex series of cellular events and growth factors. The basic steps include degradation of the basement membrane, endothelial cell proliferation, migration of endothelial cells, tube formation, vessel fusion and pruning, and stabilization [246]. The initial migration of the endothelial cells is guided by vascular endothelial growth factor A (VEGF-A), as the cells migrate towards this potent stimulus. As more and more cells migrate towards this stimulus and proliferate, vacuoles between to develop within the cells and coalesce to form a lumen [246]. Various intra and extracellular machineries regulate this lumen formation including MT1-MMP (MMP1) and surface integrin's [235]. Finally, maturation and stabilization of the lumens and nearby vessels coalesce to form one tube. These final processes are facilitates by growth factors such as PDGF-ββ and Angiopoietin 1 [242, 243]. All together, angiogenesis is an incredibly complex set of events that occur regularly *in vivo.* In tissue engineering recapitulating this entire cascade of signaling cascades would be difficult and complex to achieve. However, by choosing certain key aspects of the signaling processes, it becomes a less murky goal. Here, in this study, I combined three vascular growth factors, known to be important in angiogenesis, within a collagen scaffold to encourage endothelial cell migration and tube formation.

In this study, I was able to create a system in which the three GFs chosen were released in a manner that was similar to angiogenesis *in vivo.* As seen in figure 3.3, release of the GFs occurred in a sequential order; first VEGF was released, then PDGF- ββ and finally seven days later Ang1, similar to the normal angiogenic events. The release that occurred was due to charge and size of the actual molecules. VEGF-A, is a positively charge growth factor that has a molecular weight of 27 kDa. PDGF-ββ is also positively charged and weights 25.4 kDa. Ang1 has a neutral charge, and weights 72 kDa. As collagen is a negatively charged protein, the charge interactions of VEGF-A and PDGF-ββ are suspected to have been a major predictor of their release behavior. For Ang1, due to the neutral charge, the size most likely determined the release rate.

The endothelial cells response to the release of the growth factors was positive when compared to controls. The presence of the GFs increased the migration into the scaffold and also increased cell survival. In order this system was indeed recapitulating crucial angiogenic events such as lumen formation, machinery involved in the process was examined. Activity of MT1-MMP/MMP14 a matrix metalloproteinase known for its role in lumen formation was examined, and was seen that over the course of 14 days no significant difference was seen in the amount of activation compared to control gels. Initially, it was believed that the scaffold with the GFs encapsulated within them would increase the activation of the matrix metalloproteinase. However, it was concluded that although there was increased migration and cell survival, the GFs were not aberrantly affecting the lumen formation process, in fact, levels of activation was almost identical to controls (Figure 3.7). MT1-MMP/MMP14 activates downstream intracellular signaling

processes that are also implicated in their roles for lumen formation, such as Cdc42, a rho-GTPase. Cdc42 is also activated by VEGF-A, and known to further activate downstream effectors such as Rac1, and cause actin cytoskeletal rearrangement and cell polarity changes [235, 247]. Cdc42 activity was measured as well. Interestingly, it was found that Cdc 42 was only detectable on the first 2 days of culture in cells seeded on collagen gels with GFs (Figure 3.8), and was significantly higher than control gels without GFs. This initial activation was attributed to the point in time when cells are the most motile, and first exposed to the GFs in high amounts, especially VEGF-A. Rac1, another lumen formation complex known constituent also known for cytoskeletal rearrangement was seen to be activated at levels similar to controls until day 5, when GF gels showed much higher activation compared to controls. However, as time progressed such as day 11 and 14, control gels actually showed higher rates of activation. This was attributed to the pro-maturation GFs that were being released at high rates in the GF gels, known for their role in stopping cell migration. I was able to prove that we were not negatively affecting lumen formation machinery by the release of the GFs.

After confirmation that the system positively influence cell behavior the system had to be tested within a model dECM environment. By using a dECM hydrogel system, I could simulate the environment that the encapsulated GFs in collagen and endothelial cells would be exposed to when this system would be later on used in a decellularized scaffold. When the cells were encapsulated within the collagen system with GFs and then this was seeded on top of a dECM hydrogel, migration into the matrix was significantly higher over the first 7 days. By day 14, the invasion into the matrix was the same compared to the

control (Figure 3.10). When cells were seeded on top of the collagen gels with or without GFs encapsulated within them that had then been seeded on top of dECM hydrogels, invasion into the matrix was not statistically different (Figure 3.11). This was attributed to the positive affect that encapsulating cells within a hydrogel during their sol-gel transition has on cell survival and behavior, as well as proximity and exposure to GFs within the hydrogels. dECM hydrogels themselves retain extracellular matrix proteins and growth factors similar to *in vivo* and acts as a potent migration stimulator itself [93]. Further studies into whether cells should be encapsulated within the collagen hydrogels or seeded on top of the gels are necessitated in order to fully elucidate the observed difference in behavior.

3.7 Conclusion

The intent of this design was to recapitulate angiogenic-signaling events that occur *in vivo*. Not only was the system that was created able to do that, it also positively increased cell migration into the matrix. The system was also shown to not effect angiogenic processes in a negative manner, instead increasing activation of lumen formation complex machinery such as Cdc42, without which, has shown to inhibit endothelial cell lumen formation [239]. This collagen encapsulated growth factor system was created for use within decellularized scaffolds to help encourage microvascular growth and overall cell coverage within these scaffolds. By utilizing a 3D dECM hydrogel to model a decellularized environment, I showed that the encapsulation of ECs within collagen that has GFs encapsulated within it encourages migration into the dECM. The exciting results indicate that this system may be beneficial and help encourage microvascular growth within

decellularized specimens. Further studies into the utilization of the system in an actual scaffold within lumens of a decellularized matrix should be completed to fully elucidate the role in which this GF delivery system can be used.

4 CONCLUSION

4.1 Angiogenic Growth Factors Encourage Vascularization in dECM

As human life expectancy continues to increase with newer technologies aimed at keeping the population healthier longer, age related diseases and trauma to internal organs increases. When damage from the previously mentioned diseases occur that is severe enough, a transplant may be necessitated. Currently, across all donor organ waiting lists, the list for those awaiting transplant far exceeds the availble donor organs. Over time donor organ availability has plateued, while those needing a transplant has continued to exponentially grow [248] (Figure 4.1). To alleviate this apparent discrepency alternatives to donor organ transplantation has been researched, and a new field of research took center stage.

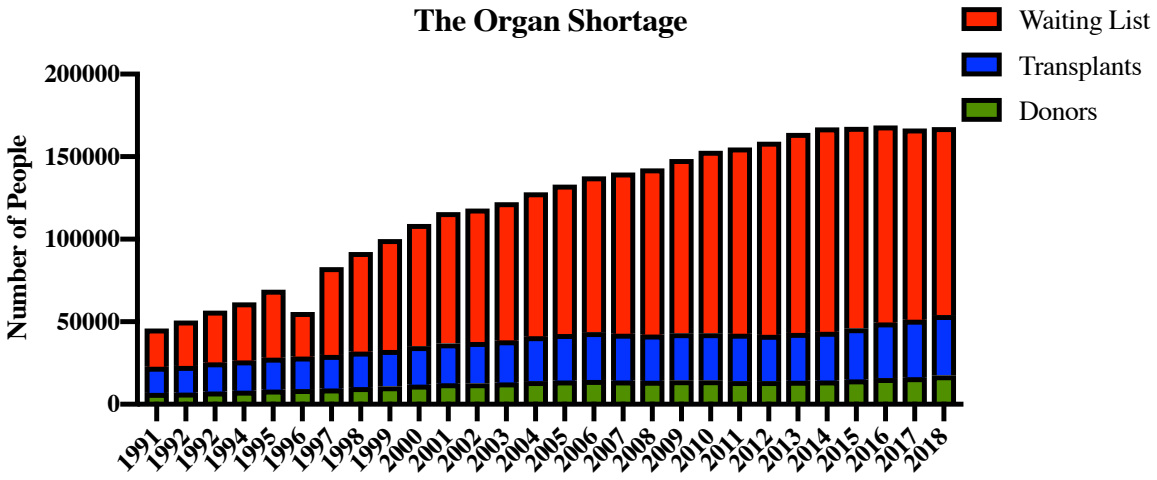

Figure 4.1: Transplant Donors, Waiting List, and Recipients. Data taken from OPTN.org.

Regenerative medicine is a broad field of study whose main goal is to either replace or repair damaged tissues. This damage may arise from congenital defects, trauma, or age related diseases. In order to accomplish this goal of replacing damaged tissue, a scaffold is most often used as a method to either replace a piece of damaged tissue, either delivered acellular or seeded with cells. This scaffolding is used as a physical mechanical support to the tissue, or as a method of delivering bioactive cues that can stimulate repair, or act as a delivery method for new cells to repopulate a damaged area. The scaffolding chose however, must be able to recapitulate the tissue that is to be replaced both mechanically, and environmentally. Biomaterials used as a scaffolding may be either syntheic and biologic in origin, but few can fully mimic the complex *in vivo* environment. Decellularized organs have emerged as a new scaffold, where a cadaveric organ's own cells are removed leaving the extracellular matrix behind. However, as noted in Chapter 1b, the microvasculature is also removed. This renders decellularized organs an almost perfect choice as a replacement organ, but still not completely ideal. There are however, methods to encourage vascularization of these scaffolds as mentioned in Chapter 1b. Because of the significant need to vascularize decellularized scaffolds at a faster rate, I decided to focus my research on a method to increase the vascularization of said scaffolds by delivery angiogenic growth factors to the scaffold.

The first step was working on the model environment that would be used as a subsitute for the decellularized scaffold. Since the use of a full acellular organ scaffold was beyond the scope of the work described here, a smaller *in vitro* model system needed to be utilized. In chapter 2, I used a known cardiac decellularized extracellular matrix protocol, and added a

crosslinker in to create more mechanically stiff gels. Without the addition of the crosslinker, genipin, the gels would be virtually impossible to handle and not an ideal model system. Upon further research into the literature, it was discovered that the protocol to actually make these hydrogels was somewhat customizable for the desired application. In one of the processeing steps, the dECM is digested in a pepsin and HCl solution. Throughout the literature, there is not a consensus over the length of time utilized for this step. Should it be until the tissue is solubilized? Or does it need to be longer? Curious about this, I decided to dive deeper into whether a specific digestion time would actually affect cell behavior and material strength. As time progresses, the protein fragments in the solution should become smaller, and theoretically this should affect the final hydrogel characteristics because of the smaller peptide pieces that are then being recrosslinked together. The final hydrogel of a dECM solution that had been digested longer than a solution that had been digested for a shorter amount of time, should be a completely different environment for the cells. It would follow then, that this difference in cell microenvironment would then affect cell behavior such as differentiation. Following previously completed research, hADSCs were chosen as a stem cell model system since they have been previously shown to differentiate towards cardiac lineages on cardiac hydrogels. To test this further, β4 and β5 integrins were blocked on cell surfaces. This was done to elucidate whether this different material composition was indeed affecting cell differentiation, and were chosen based on their roles in recognition of known cardiac differntiation influencers Laminin and Fibronectin. The hypothesis was that these would show us the significance of the different protein profiles. Because of the different laminin and fibronectin amounts that was seen on the Mass Spec data, I further was interested in

this. Upon first experimentation, it was found that the blocking of these integrins actually led to an upregulation of certain cardiac genes when compared to collagen controls. A further dive into the literature revealed that the previous work has shown that blocking of beta 5 integrin actually has led to an upregluation of beta 1 integrin signaling [212]. Because of the importance of beta 1 integrin to cardiac differentiation, I then hypothesized that this cardiac gene expression upregulation was attributable to the increase in the beta 1 integrin signaling activity. The beta 1 integrin activity was analyzed using an antibody that detects active beta 1 integrin, HUTS4, and was shown to be active more in the integrin blocked groups, than their control counterparts. This data gave us evidence of not only the importance of beta 1 integrin signalling in cardiac development, but also how cardiac differentiation can be potentially upregulated.

4.2 New Methods to Vascularize Acellular Cardiac Scaffolds

In acellular cardiac scaffolds re-endothelialization of the scaffolds is impertive for their therapeutic use. First, full coverage of the ECM is required in order to prevent thrombosis from occuring. Second, the endothelial cells must be able to migrate out of the higher order vascular conduit branchs, and form microvasculature (Figure 4.2). In my research, after the model decellularized environment was successfully made and characterized, attention was then turned to making the growth factor delivery vehicle. Because of the short half-life of most bioactive molecules, bolus delivery methods are not optimial. Therefore, encapsulation within a scaffold was chosen as the method of delivery. I used type 1

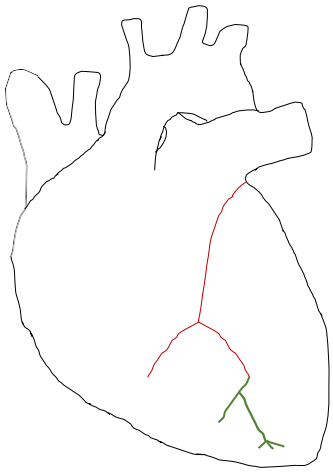

Figure 4.2: New Vascular Growth in a Decellularized Scaffold. Representation of new vasculature growing out of existing vasculature in acellular cardiac scaffold. Red- Exsisting vasculature, and Green- New vasculature outgrowth.

porcine collagen as it is the most abundant in the cardiac matrix and is easily accessible I chose known angiogenic growth factors VEGF-A, PDGF-BB, and Ang1, to be released from the scaffold based on charge and size. In chapter 3, I characterized the release of these growth factors from collagenous scaffolds over the course of 22 days. In recellularization of cardiac scaffolds, the time to re-endothelialze the scaffold is typically ~14 days, which was the intended time course of the experiment. I found that the release of the growth factors was similar to what the timecourse of release is *in vivo.* By mimicing angiogenic signaling cascades, the system is attempting to create a environment similar to *in vivo* with the desire of causing correct cell behavior and microvascular growth. I made sure to ensure that critical angiogenesis machinery such as the endothelial cell lumen formation complex was not abbherently affecting this. The endothelial cell lumen formation complex is responsible for the beginning stages of vessel formation, specifically

when the endothelial cells are colaescing with another endothelial cell outgrowth from another area in the body to form a microvasculature. If this process did not work correctly, no fluid would be able to travel through, it would essentially act as a plug.

In acellular cardiac scaffolds re-endothelialization of the scaffolds is impertive for their use. As mentioned previously, naked vascular conduits cause thrombosis when blood makes contact with those surfaces [62]. Therefore the inclusion of potent cell growth bioactive molecules such as VEGF-A is crucial. Because of this fact, and the main end goal of having microvascular outgrowth out of the exisisting larger order vascular conduits, migration through either the collagen or dECM hydrogels were a critical endpoint. In Chapter 3, I examined the invasion of the cells into both the collagenous scaffolds and the collagen scaffolds that had been made on top of the dECM hydrogels. I found that the cells that had been encapsulated within the top collagen gels with growth factors invaded into the dECM hydrogel that was on bottom, more than the their non GF counterparts (Figure 3.11, Figure 4.3). The reason why it was tested against it's non growth factor counterparts is that the dECM itself should be a potent mitogen, as the ECM is full of bioactive cues. It showed evidence that the presence of the growth factors helped increase the migratory behahavior of the endothelial cells- a critical endpoint for these studies. This gave us the crucial evidence that the presence of the GFs would not only help the ECs migrate into the scaffolds, but would also still exhibit a normal EC phenotype

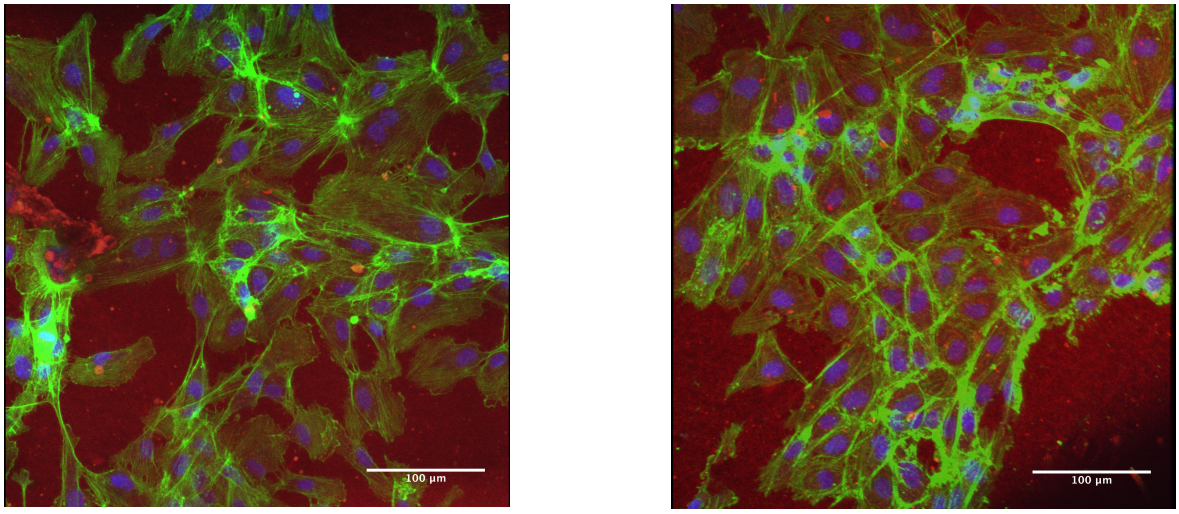

Figure 4.3: Cells Encapsulated- Invasion into the dECM Images. Endothelial cells ecapsulated within collagen gels with GFs (right) and without GFs (left), that were seeded on top of dECM hydrogels. Green- Actin, Blue, Dapi, Red, auto fluorescence from Genipin hydrogels

4.3 Summary

The central goal of this dissertation was to deliver growth factors to a cardiac decellularized extracellular matrix environment to increase microvascular growth. In order to mimic the complex cardiac decellularized matrix environment, in chapter 2 I developed a cardiac hydrogel system crosslinked with a low-cytotoxic crosslinker genipin, and examined the material characteristics. I showed that the digestion time of the dECM in the enzyme pepsin affected the final material characteristics, and also influenced cell behavior. First, I showed that gelation of the dECM, or the time it takes for the material to form a gel, was the lowest when the dECM had been digested the least amount of time. Additionally, I showed that the degradation kinetics was affected by the digestion time, as dECM that had been digested for the least amount of time took the most time to degrade.

Finally, the storage modulus was also affected my the digestion length, with the second longest digestion time showing the highest material strength.

In the rest of chapter 2, I delved into how the digestion length affected the differentiation of the hADSCs towards a cardiomyocyte lineage. I showed that the least digestion time led to a increase in cardiac phenotypic genes, more than likely due to a environement that is more similar to *in vivo.* To follow that up and examine whether certain proteins were influencing the differentiation, two integrins β4 and β5 were blocked and shown to cause an even further upregulation of cardiac phenotypic genes. This was hypothesized to be attributed to the integrin crosstalk and increased activity of a known cardiac influencing integrin- β1.

In chapter 3, I show that the combination of three angiogenic growth factors (VEGF-A, PDGF- ββ, and Ang1) in a collagen hydrogel release in a fashion that mimics the natural angiogenic cascade of events. Further, this release of growth factors encourages cell migration and invasion into the collagen scaffold- a critical endpoint. Additionally, in chapter 3 I show that the EC lumen formation complex, crucial for the formation of functional vasculature, was not damaged or downregulated by the addition of the GFs. Cdc 42, a rho-GTPase component of the lumen formation complex was shown to be upregulated compared to our control gels without GFs within them, and was attributed to the release of the VEGF-A intially. Collectively, the data presented in chapter 3 show evidence that the combination of the three GFs positively influence endothelial cells and encourage neovascularization behavior. Finally in chapter 3, I combined the dECM

hydrogel that I had developed from chapter 2 with my collagen containing GF system and examined the invasion of cells into the scaffold. I found that the cells encapsulated within the collagen hydrogels with GFs will be the most optimal condition to proceed with further research. In this condition, cells invaded into the matrix deeper compared to controls. Overall, the work done here establishes the first ever study into how decellularized cardiac extracellular matrix hydrogel digestion affects material behavior and also how that change in behavior influences both parenchymal and stem cells. Additionally, the work done here establishes a model to be used that may increase the vascularization in decellularized scaffolds- a feat that could potentially make these organs a “off the shelf” functional organ.

LITERATURE CITED

1. Kassebaum, N.J., et al., *Global, regional, and national disability-adjusted life-years (DALYs) for 315 diseases and injuries and healthy life expectancy (HALE), 1990–2015: a systematic analysis for the Global Burden of Disease Study 2015.* The Lancet, 2016. **388**(10053): p. 1603-1658.

2. Mortality, G.B.D. and C. Causes of Death, *Global, regional, and national life expectancy, all-cause mortality, and cause-specific mortality for 249 causes of death, 1980-2015: a systematic analysis for the Global Burden of Disease Study 2015.* Lancet (London, England), 2016. **388**(10053): p. 1459-1544.

3. Cohn, J.N., *Continue what we are doing to treat HF, but do it better.* Nature Reviews Cardiology, 2013. **11**: p. 69.

4. Yancy, C.W., et al., *2017 ACC/AHA/HFSA Focused Update of the 2013 ACCF/AHA Guideline for the Management of Heart Failure: A Report of the American College of Cardiology/American Heart Association Task Force on Clinical Practice Guidelines and the Heart Failure Society of America.* 2017. **136**(6): p. e137-e161.

5. Wilhelm, M.J., *Long-term outcome following heart transplantation: current perspective.* J. Thorac. Dis., 2015. **7**(3): p. 549-551.

6. Longnus, S.L., et al., *Heart transplantation with donation after circulatory determination of death.* Nature Reviews Cardiology, 2014. **11**: p. 354.

7. Wang, B., et al., *Establishing Early Functional Perfusion and Structure in Tissue Engineered Cardiac Constructs.* Critical reviews in biomedical engineering, 2015. **43**(5-6): p. 455-471.

8. Kaiser, N.J. and K.L.K. Coulombe, *Physiologically inspired cardiac scaffolds for tailored in vivo function and heart regeneration.* Biomedical Materials (Bristol, England), 2015. **10**(3): p. 034003-034003.

9. Iozzo, R.V. and L. Schaefer, *Proteoglycan form and function: A comprehensive nomenclature of proteoglycans.* Matrix Biol., 2015. **42**: p. 11-55.

10. Engel, J. and M. Chiquet, *An Overview of Extracellular Matrix Structure and Function*, in *The Extracellular Matrix: an Overview*. 2011, Springer, Berlin, Heidelberg. p. 1-39.

11. Badylak, S.F., D.O. Freytes, and T.W. Gilbert, *Extracellular matrix as a biological scaffold material: Structure and function.* Acta Biomater, 2009. **5**(1): p. 1-13.

12. Frantz, C., K.M. Stewart, and V.M. Weaver, *The extracellular matrix at a glance.* J. Cell Sci., 2010. **123**(Pt 24): p. 4195-4200.

13. Rienks, M., et al., *Myocardial Extracellular Matrix: An Ever-Changing and Diverse Entity.* Circulation Research, 2014. **114**(5): p. 872-888.

14. Mouw, J.K., G. Ou, and V.M. Weaver, *Extracellular matrix assembly: a multiscale deconstruction.* Nature Reviews Molecular Cell Biology, 2014. **15**: p. 771.

15. Hynes, R.O., *The extracellular matrix: not just pretty fibrils.* Science (New York, N.Y.), 2009. **326**(5957): p. 1216-1219.

16. Brizzi, M.F., G. Tarone, and P. Defilippi, *Extracellular matrix, integrins, and growth factors as tailors of the stem cell niche.* Current Opinion in Cell Biology, 2012. **24**(5): p. 645-651.

17. Kim, S.-H., J. Turnbull, and S. Guimond, *Extracellular matrix and cell signalling: the dynamic cooperation of integrin, proteoglycan and growth factor receptor.* Journal of Endocrinology, 2011. **209**(2): p. 139-151.

18. Bowers, S.L.K., I. Banerjee, and T.A. Baudino, *The extracellular matrix: at the center of it all.* J. Mol. Cell. Cardiol., 2010. **48**(3): p. 474-482.

19. Taylor, D.A., et al., *Decellularized matrices in regenerative medicine.* Acta Biomater, 2018. **74**: p. 74-89.

20. Rana, D., et al., *Development of decellularized scaffolds for stem cell-driven tissue engineering.* Journal of Tissue Engineering and Regenerative Medicine, 2017. **11**(4): p. 942-965.

21. Zaman, M.H., et al., *Computational Model for Cell Migration in Three-Dimensional Matrices.* Biophysical Journal, 2005. **89**(2): p. 1389-1397.

22. Gaudet, C., et al., *Influence of Type I Collagen Surface Density on Fibroblast Spreading, Motility, and Contractility.* Biophysical Journal, 2003. **85**(5): p. 3329-3335.

23. Ott, H.C., et al., *Perfusion-decellularized matrix: using nature's platform to engineer a bioartificial heart.* Nature Medicine, 2008. **14**(2): p. 213-221.

24. Guyette, J.P., et al., *Bioengineering Human Myocardium on Native Extracellular Matrix.* Circulation Research, 2015.

25. Hodgson, M.J., et al., *Extracellular Matrix from Whole Porcine Heart Decellularization for Cardiac Tissue Engineering*, in *Decellularized Scaffolds and Organogenesis: Methods and Protocols*, K. Turksen, Editor. 2018, Springer New York: New York, NY. p. 95-102.

26. Kitahara, H., et al., *Heterotopic transplantation of a decellularized and recellularized whole porcine heart.* Interactive CardioVascular and Thoracic Surgery, 2016.

27. Rieder, E., et al., *Decellularization protocols of porcine heart valves differ importantly in efficiency of cell removal and susceptibility of the matrix to recellularization with human vascular cells.* The Journal of Thoracic and Cardiovascular Surgery, 2004. **127**(2): p. 399-405.

28. Courtman, D.W., et al., *Development of a pericardial acellular matrix biomaterial: Biochemical and mechanical effects of cell extraction.* Journal of Biomedical Materials Research, 1994. **28**(6): p. 655-666.

29. Gittenberger-de Groot, A.C., et al., *Histological evaluation of decellularised porcine aortic valves: matrix changes due to different decellularisation methods ☆.* European Journal of Cardio-Thoracic Surgery, 2005. **27**(4): p. 566-571.

30. Wainwright, J.M., et al., *Preparation of cardiac extracellular matrix from an intact porcine heart.* Tissue Eng Part C Methods, 2010. **16**(3): p. 525-32.

31. Akhyari, P., et al., *The Quest for an Optimized Protocol for Whole-Heart Decellularization: A Comparison of Three Popular and a Novel Decellularization Technique and Their Diverse Effects on Crucial Extracellular Matrix Qualities.* Tissue Engineering Part C: Methods, 2011. **17**(9): p. 915-926.

32. Robertson, M.J., et al., *Optimizing Recellularization of Whole Decellularized Heart Extracellular Matrix.* Plos One, 2014. **9**(2).

33. Lee, P.-F., et al., *Inverted orientation improves decellularization of whole porcine hearts.* Acta Biomater., 2017. **49**: p. 181-191.

34. Crapo, P.M., T.W. Gilbert, and S.F. Badylak, *An overview of tissue and whole organ decellularization processes.* Biomaterials, 2011. **32**(12): p. 3233-3243.

35. Garreta, E., et al., *Tissue engineering by decellularization and 3D bioprinting.* Materials Today, 2017. **20**(4): p. 166-178.

36. Zahmati, A.H.A., et al., *Chemical Decellularization Methods and Its Effects on Extracellular Matrix.* Internal Medicine and Medical Investigation Journal, 2017. **2**(3): p. 76-83.

37. Gratzer, P.F., R.D. Harrison, and T. Woods, *Matrix Alteration and Not Residual Sodium Dodecyl Sulfate Cytotoxicity Affects the Cellular Repopulation of a Decellularized Matrix.* Tissue Engineering, 2006. **12**(10): p. 2975-2983.

38. Cebotari, S., et al., *Detergent decellularization of heart valves for tissue engineering: toxicological effects of residual detergents on human endothelial cells.* Artif. Organs, 2010. **34**(3): p. 206-210.

39. Keane, T.J., I.T. Swinehart, and S.F. Badylak, *Methods of tissue decellularization used for preparation of biologic scaffolds and in vivo relevance.* Methods, 2015. **84**: p. 25-34.

40. Sarig, U., et al., *Thick Acellular Heart Extracellular Matrix with Inherent Vasculature: A Potential Platform for Myocardial Tissue Regeneration.* Tissue Engineering. Part A, 2012. **18**(19-20): p. 2125-2137.

41. Gilpin, A. and Y. Yang, *Decellularization Strategies for Regenerative Medicine: From Processing Techniques to Applications %J BioMed Research International.* 2017. **2017**: p. 13.

42. University of Arizona College of Medicine, D.o.S.D.o.C.S.T.A.Z. and Z. Khalpey, *Acellular porcine heart matrices: whole organ decellularization with 3D-Bioscaffold & vascular preservation.* Transl. Res., 2017.

43. Lynch, A.P. and M. Ahearne, *Strategies for developing decellularized corneal scaffolds.* Experimental Eye Research, 2013. **108**: p. 42-47.

44. *Culture of Specific Cell Types*, in *Culture of Animal Cells*.

45. Olsen, J.V., S.-E. Ong, and M. Mann, *Trypsin Cleaves Exclusively C-terminal to Arginine and Lysine Residues.* 2004. **3**(6): p. 608-614.

46. Merna, N., et al., *Optical imaging predicts mechanical properties during decellularization of cardiac tissue.* Tissue Eng. Part C Methods, 2013. **19**(10): p. 802-809.

47. Remlinger, N.T., P.D. Wearden, and T.W. Gilbert, *Procedure for decellularization of porcine heart by retrograde coronary perfusion.* J. Vis. Exp., 2012(70): p. e50059.

48. Methe, K., et al., *An alternative approach to decellularize whole porcine heart.* BioResearch open access, 2014. **3**(6): p. 327-338.

49. Seo, Y., Y. Jung, and S.H. Kim, *Decellularized heart ECM hydrogel using supercritical carbon dioxide for improved angiogenesis.* Acta Biomater, 2017.

50. Seo, Y., Y. Jung, and S.H. Kim, *Decellularized heart ECM hydrogel using supercritical carbon dioxide for improved angiogenesis.* Acta Biomater., 2017.

51. Sawada, K., et al., *Cell removal with supercritical carbon dioxide for acellular artificial tissue.* 2008. **83**(6): p. 943-949.

52. Payam, A., et al., *Characterization of the Epicardial Adipose Tissue in Decellularized Human-Scaled Whole Hearts: Implications for the Whole-Heart Tissue Engineering.* 2018. **24**(7-8): p. 682-693.

53. Zhou, P. and W.T. Pu, *Recounting Cardiac Cellular Composition.* Circulation research, 2016. **118**(3): p. 368-370.

54. Pinto, A.R., et al., *Revisiting Cardiac Cellular Composition.* 2016. **118**(3): p. 400-409.

55. Bergmann, O., et al., *Dynamics of Cell Generation and Turnover in the Human Heart.* Cell, 2015. **161**(7): p. 1566-1575.

56. Garreta, E., et al., *Myocardial commitment from human pluripotent stem cells: Rapid production of human heart grafts.* Biomaterials, 2016. **98**: p. 64-78.

57. Guyette, J.P., et al., *Bioengineering Human Myocardium on Native Extracellular Matrix.* Circ. Res., 2016. **118**(1): p. 56-72.

58. Hülsmann, J., et al., *A novel customizable modular bioreactor system for whole-heart cultivation under controlled 3D biomechanical stimulation.* Journal of Artificial Organs, 2013. **16**(3): p. 294-304.

59. Ng, S.L.J., et al., *Lineage restricted progenitors for the repopulation of decellularized heart.* Biomaterials, 2011. **32**(30): p. 7571-7580.

60. Lu, T.Y., et al., *Repopulation of decellularized mouse heart with human induced pluripotent stem cell-derived cardiovascular progenitor cells.* Nat Commun, 2013. **4**: p. 2307.

61. Yasui, H., et al., *Excitation propagation in three-dimensional engineered hearts using decellularized extracellular matrix.* Biomaterials, 2014. **35**(27): p. 7839-7850.

62. Robertson, M.J., et al., *Optimizing Recellularization of Whole Decellularized Heart Extracellular Matrix.* PLoS ONE, 2014. **9**(2): p. e90406.

63. Narmoneva, D.A., et al., *Endothelial cells promote cardiac myocyte survival and spatial reorganization: implications for cardiac regeneration.* Circulation, 2004. **110**(8): p. 962-968.

64. Weymann, A., et al., *Bioartificial Heart: A Human-Sized Porcine Model – The Way Ahead.* PLoS ONE, 2014. **9**(11): p. e111591.

65. VeDepo, M.C., et al., *Recellularization of decellularized heart valves: Progress toward the tissue-engineered heart valve.* J. Tissue Eng., 2017. **8**: p. 2041731417726327.

66. Wang, B., et al., *Fabrication of Cardiac Patch with Decellularized Porcine Myocardial Scaffold and Bone Marrow Mononuclear Cells.* Journal of biomedical materials research. Part A, 2010. **94**(4): p. 1100-1110.

67. Siddiqui, R.F., J.R. Abraham, and J. Butany, *Bioprosthetic heart valves: modes of failure.* Histopathology, 2009. **55**(2): p. 135-144.

68. Bloomfield, P., *Choice of heart valve prosthesis.* Heart (British Cardiac Society), 2002. **87**(6): p. 583-589.

69. Manji, R.A., et al., *The future of bioprosthetic heart valves.* The Indian journal of medical research, 2012. **135**(2): p. 150-151.

70. Schmidt, D., U.A. Stock, and S.P. Hoerstrup, *Tissue engineering of heart valves using decellularized xenogeneic or polymeric starter matrices.* Philosophical transactions of the Royal Society of London. Series B, Biological sciences, 2007. **362**(1484): p. 1505-1512.

71. Dohmen, P.M., et al., *Is there a possibility for a glutaraldehyde-free porcine heart valve to grow?* Eur. Surg. Res., 2006. **38**(1): p. 54-61.

72. Baraki, H., et al., *Orthotopic replacement of the aortic valve with decellularized allograft in a sheep model.* Biomaterials, 2009. **30**(31): p. 6240-6246.

73. Brown, J.W., et al., *Performance of the CryoValve® SG human decellularized pulmonary valve in 342 patients relative to the conventional CryoValve at a mean follow-up of four years.* The Journal of Thoracic and Cardiovascular Surgery, 2010. **139**(2): p. 339-348.

74. Brown, J.W., et al., *Performance of SynerGraft Decellularized Pulmonary Homograft in Patients Undergoing a Ross Procedure.* The Annals of Thoracic Surgery, 2011. **91**(2): p. 416-423.

75. Singelyn, J.M., et al., *Naturally derived myocardial matrix as an injectable scaffold for cardiac tissue engineering.* Biomaterials, 2009. **30**(29): p. 5409-16.

76. Lim, P.S., et al., *Repair of left ventricular aneurysm with acellular dermis graft: A case report.* Journal of cardiology cases, 2012. **6**(2): p. e42-e44.

77. Robinson, K.A., et al., *Extracellular Matrix Scaffold for Cardiac Repair.* 2005. **112**(9_supplement): p. I-135-I-143.

78. Svystonyuk, D., et al., *ACELLULAR EXTRACELLULAR MATRIX SCAFFOLD REPROGRAMS CARDIAC FIBROBLASTS AND PROMOTES ADAPTIVE CARDIAC REMODELING AND REPAIR.* Canadian Journal of Cardiology, 2017. **33**(10): p. S49-S50.

79. Chen, W.C.W., et al., *Decellularized zebrafish cardiac extracellular matrix induces mammalian heart regeneration.* 2016. **2**(11): p. e1600844.

80. Majeed, A., et al., *Photo-oxidized bovine pericardium in congenital cardiac surgery: single-centre experience.* Interactive CardioVascular and Thoracic Surgery, 2016. **24**(2): p. 240-244.

81. Woo, J.S., M.C. Fishbein, and B. Reemtsen, *Histologic examination of decellularized porcine intestinal submucosa extracellular matrix (CorMatrix) in pediatric congenital heart surgery.* Cardiovasc. Pathol., 2016. **25**(1): p. 12-17.

82. Seif-Naraghi, S., et al., *Fabrication of biologically derived injectable materials for myocardial tissue engineering.* Journal of visualized experiments : JoVE, 2010(46): p. 2109.

83. Gaetani, R., J. Ungerleider, and K. Christman, *Acellular Injectable Biomaterials for Treating Cardiovascular Disease*. 2016. p. 309-325.

84. Wang, R.M. and K.L. Christman, *Decellularized myocardial matrix hydrogels: In basic research and preclinical studies.* Advanced Drug Delivery Reviews, 2016. **96**: p. 77-82.

85. Wassenaar, J.W., G.R. Boss, and K.L. Christman, *Decellularized skeletal muscle as an in vitro model for studying drug-extracellular matrix interactions.* Biomaterials, 2015. **64**: p. 108-114.

86. Suarez, S.L., et al., *Intramyocardial injection of hydrogel with high interstitial spread does not impact action potential propagation.* Acta Biomaterialia, 2015. **26**: p. 13-22.

87. Gaetani, R., et al., *Cardiac-Derived Extracellular Matrix Enhances Cardiogenic Properties of Human Cardiac Progenitor Cells.* Cell Transplantation, 2016. **25**(9): p. 1653-1663.

88. Singelyn, J.M., et al., *Catheter-deliverable hydrogel derived from decellularized ventricular extracellular matrix increases endogenous cardiomyocytes and preserves cardiac function post-myocardial infarction.* J Am Coll Cardiol, 2012. **59**(8): p. 751-63.

89. Seif-Naraghi, S.B., et al., *Safety and Efficacy of an Injectable Extracellular Matrix Hydrogel for Treating Myocardial Infarction.* Science Translational Medicine, 2013. **5**(173): p. 173ra25.

90. Wassenaar, J.W., et al., *Evidence for Mechanisms Underlying the Functional Benefits of a Myocardial Matrix Hydrogel for Post-MI Treatment.* Journal of the American College of Cardiology, 2016. **67**(9): p. 1074-1086.

91. Saldin, L.T., et al., *Extracellular matrix hydrogels from decellularized tissues: Structure and function.* Acta biomaterialia, 2017. **49**: p. 1-15.

92. Stoppel, W.L., et al., *Elastic, silk-cardiac extracellular matrix hydrogels exhibit time-dependent stiffening that modulates cardiac fibroblast response.* 2016. **104**(12): p. 3058-3072.

93. Spang, M.T. and K.L. Christman, *Extracellular matrix hydrogel therapies: In vivo applications and development.* Acta Biomaterialia, 2018. **68**: p. 1-14.

94. Grover, G.N., N. Rao, and K.L. Christman, *Myocardial matrix-polyethylene glycol hybrid hydrogels for tissue engineering.* Nanotechnology, 2014. **25**(1): p. 014011-014011.

95. Williams, C., et al., *Cardiac extracellular matrix-fibrin hybrid scaffolds with tunable properties for cardiovascular tissue engineering.* Acta biomaterialia, 2015. **14**: p. 84-95.

96. Efraim, Y., et al., *Biohybrid cardiac ECM-based hydrogels improve long term cardiac function post myocardial infarction.* Acta Biomater, 2017. **50**: p. 220-233.

97. Stoppel, W.L., et al., *Anisotropic silk biomaterials containing cardiac extracellular matrix for cardiac tissue engineering.* Biomedical materials (Bristol, England), 2015. **10**(3): p. 034105-034105.

98. Singelyn, J.M., et al., *Catheter-deliverable hydrogel derived from decellularized ventricular extracellular matrix increases endogenous cardiomyocytes and preserves cardiac function post-myocardial infarction.* J. Am. Coll. Cardiol., 2012. **59**(8): p. 751-763.

99. *Identifier: NCT02305602; A Phase I, Open-label Study of the Effects of Percutaneous Administration of an Extracellular Matrix Hydrogel, VentriGel, Following Myocardial Infarction*. 2014.

100. Ferris, C.J., et al., *Biofabrication: an overview of the approaches used for printing of living cells.* Appl. Microbiol. Biotechnol., 2013. **97**(10): p. 4243-4258.

101. Kim, B.S., et al., *Decellularized extracellular matrix: a step towards the next generation source for bioink manufacturing.* Biofabrication, 2017. **9**(3): p. 034104.

102. Jang, J., et al., *3D printed complex tissue construct using stem cell-laden decellularized extracellular matrix bioinks for cardiac repair.* Biomaterials, 2017. **112**: p. 264-274.

103. Jang, J., et al., *Tailoring mechanical properties of decellularized extracellular matrix bioink by vitamin B2-induced photo-crosslinking.* Acta Biomaterialia, 2016. **33**: p. 88-95.

104. Pati, F., et al., *Printing three-dimensional tissue analogues with decellularized extracellular matrix bioink.* Nat. Commun., 2014. **5**: p. 3935.

105. Daar, A.S. and H.L. Greenwood, *A proposed definition of regenerative medicine.* J Tissue Eng Regen Med, 2007. **1**(3): p. 179-84.

106. Mason, C. and P. Dunnill, *A brief definition of regenerative medicine.* Regen Med, 2008. **3**(1): p. 1-5.

107. Gilbert, T.W., T. Sellaro, and S. Badylak, *Decellularization of tissues and organs.* Biomaterials, 2006. **27**(19): p. 3675.

108. Scarritt, M.E., N.C. Pashos, and B.A. Bunnell, *A review of cellularization strategies for tissue engineering of whole organs.* Front Bioeng Biotechnol, 2015. **3**: p. 43.

109. Kanematsu, A., et al., *Bladder regeneration by bladder acellular matrix combined with sustained release of exogenous growth factor.* J Urol, 2003. **170**(4 Pt 2): p. 1633-8.

110. Baptista, P., et al., *The use of whole organ decellularization for the generation of a vascularized liver organoid.* Hepatology, 2011. **53**(2): p. 604-617.

111. Caralt, M., et al., *Optimization and critical evaluation of decellularization strategies to develop renal extracellular matrix scaffolds as biological templates for organ engineering and transplantation.* Am J Transplant, 2015. **15**(1): p. 64-75.

112. Stabler, C.T., et al., *Revascularization of decellularized lung scaffolds: principles and progress.* Am J Physiol Lung Cell Mol Physiol, 2015. **309**(11): p. L1273-85.

113. Vunjak Novakovic, G., et al., *Challenges in Cardiac Tissue Engineering.* Tissue Engineering Part B: Reviews, 2010. **16**(2): p. 169-187.

114. Lesman, A., L. Gepstein, and S. Levenberg, *Vascularization shaping the heart.* Ann N Y Acad Sci, 2010. **1188**: p. 46-51.

115. Novosel, E., C. Kleinhans, and P. Kluger, *Vascularization is the key challenge in tissue engineering.* Advanced drug delivery reviews, 2011. **63**(4): p. 300-311.

116. Auger, F.A., L. Gibot, and D. Lacroix, *The pivotal role of vascularization in tissue engineering.* Annu Rev Biomed Eng, 2013. **15**: p. 177-200.

117. Folkman, J. and M. Hochberg, *Self-regulation of growth in three dimensions.* J Exp Med, 1973. **138**(4): p. 745-53.

118. Baiguera, S. and D. Ribatti, *Endothelialization approaches for viable engineered tissues.* Angiogenesis, 2013. **16**(1): p. 1-14.

119. Clark, E.R. and E.L. Clark, *Microscopic observations on the growth of blood capillaries in the living mammal.* American Journal of Anatomy, 1939. **64**(2): p. 251-301.

120. Bergers, G. and S. Song, *The role of pericytes in blood-vessel formation and maintenance.* Neuro-Oncology, 2005. **7**(4): p. 452-464.

121. *Collagen cross-linking: current status and future directions.* J. Ophthalmol., 2012. **2012**.

122. Coffin, J.D., et al., *Angioblast differentiation and morphogenesis of the vascular endothelium in the mouse embryo.* Developmental Biology, 1991. **148**(1): p. 51-62.

123. Shibuya, M., *Vascular Endothelial Growth Factor (VEGF) and Its Receptor (VEGFR) Signaling in Angiogenesis: A Crucial Target for Anti- and Pro-Angiogenic Therapies.* Genes & Cancer, 2011. **2**(12): p. 1097-1105.

124. *Safety and efficacy of an injectable extracellular matrix hydrogel for treating myocardial infarction.* Sci. Transl. Med., 2013. **5**.

125. Malik, N. and M.S. Rao, *A Review of the Methods for Human iPSC Derivation.* Methods in molecular biology (Clifton, N.J.), 2013. **997**: p. 23-33.

126. Ito, K. and T. Suda, *Metabolic requirements for the maintenance of self-renewing stem cells.* Nat. Rev. Mol. Cell Biol., 2014. **15**(4): p. 243-256.

127. Gonzalez, F. and D. Huangfu, *Mechanisms underlying the formation of induced pluripotent stem cells.* Wiley Interdiscip Rev Dev Biol, 2016. **5**(1): p. 39-65.

128. Asahara, T., et al., *Isolation of putative progenitor endothelial cells for angiogenesis.* Science, 1997. **275**(5302): p. 964-7.

129. Zhou, L., et al., *In vitro evaluation of endothelial progenitor cells from adipose tissue as potential angiogenic cell sources for bladder angiogenesis.* PLoS One, 2015. **10**(2): p. e0117644.

130. Sen, S., et al., *Endothelial progenitor cells: novel biomarker and promising cell therapy for cardiovascular disease.* Clin Sci (Lond), 2011. **120**(7): p. 263-83.

131. Nagao, R.J., et al., *Ultrasound-guided photoacoustic imaging-directed re-endothelialization of acellular vasculature leads to improved vascular performance.* Acta Biomater, 2015.

132. Zhou, P., et al., *Decellularization and Recellularization of Rat Livers With Hepatocytes and Endothelial Progenitor Cells.* Artif Organs, 2015.

133. Constantinescu, A., et al., *Recellularization potential assessment of Wharton's Jelly-derived endothelial progenitor cells using a human fetal vascular tissue model.* In Vitro Cell Dev Biol Anim, 2014. **50**(10): p. 937-44.

134. Song, J.J., et al., *Regeneration and experimental orthotopic transplantation of a bioengineered kidney.* Nat Med, 2013. **19**(5): p. 646-51.

135. Wang, Z., et al., *Rapid vascularization of tissue-engineered vascular grafts in vivo by endothelial cells in co-culture with smooth muscle cells.* Journal of Materials Science: Materials in Medicine, 2012. **23**(4): p. 1109-1117.

136. Cao, L. and D.J. Mooney, *Spatiotemporal control over growth factor signaling for therapeutic neovascularization.* Advanced Drug Delivery Reviews, 2007. **59**(13): p. 1340-1350.

137. Kanematsu, A., et al., *Collagenous matrices as release carriers of exogenous growth factors.* Biomaterials, 2004. **25**(18): p. 4513-20.

138. Lee, K., E.A. Silva, and D.J. Mooney, *Growth factor delivery-based tissue engineering: general approaches and a review of recent developments.* J R Soc Interface, 2011. **8**(55): p. 153-70.

139. Zhou, L., et al., *Coadministration of platelet-derived growth factor-BB and vascular endothelial growth factor with bladder acellular matrix enhances smooth muscle regeneration and vascularization for bladder augmentation in a rabbit model.* Tissue Eng Part A, 2013. **19**(1-2): p. 264-76.

140. Loai, Y., et al., *Bladder tissue engineering: tissue regeneration and neovascularization of HA-VEGF-incorporated bladder acellular constructs in*

mouse and porcine animal models. J Biomed Mater Res A, 2010. **94**(4): p. 1205-15.

141. Bär, A., et al., *The pro-angiogenic factor CCN1 enhances the re-endothelialization of biological vascularized matrices in vitro.* Cardiovascular Research, 2010. **85**(4): p. 806-813.

142. Zavan, B., R. Cortivo, and G. Abatangelo, *Hydrogels and Tissue Engineering*, in *Hydrogels: Biological Properties and Applications*. 2009, Springer Milan: Milano. p. 1-8.

143. Câmara, F.V., & Ferreira, L. J. , *Hydrogels: synthesis, characterization and applications*, in *Synthesis, Characterization, and applications*, F.V. Câmara and a.L.J. Ferreira, Editors. 2012, Nova Science Publishers, Inc. p. 388.

144. Nicodemus, G. and S. Bryant, *Cell Encapsulation in Biodegradable Hydrogels for Tissue Engineering Applications.* Tissue Engineering Part B: Reviews, 2008. **14**(2): p. 149-165.

145. Andrejecsk, J.W., et al., *Controlled protein delivery in the generation of microvascular networks.* Drug Deliv Transl Res, 2015. **5**(2): p. 75-88.

146. Tan, Q., et al., *Controlled release of chitosan/heparin nanoparticle-delivered VEGF enhances regeneration of decellularized tissue-engineered scaffolds.* Int J Nanomedicine, 2011. **6**: p. 929-42.

147. Xiong, Q., et al., *A nanomedicine approach to effectively inhibit contracture during bladder acellular matrix allograft-induced bladder regeneration by sustained delivery of vascular endothelial growth factor.* Tissue Eng Part A, 2015. **21**(1-2): p. 45-52.

148. Tan, Q., et al., *Controlled release of chitosan/heparin nanoparticle-delivered VEGF enhances regeneration of decellularized tissue-engineered scaffolds.* Int. J. Nanomedicine, 2011. **6**: p. 929-942.

149. Liang, Y. and K.L. Kiick, *Heparin-functionalized polymeric biomaterials in tissue engineering and drug delivery applications.* Acta Biomater, 2014. **10**(4): p. 1588-600.

150. Sakiyama-Elbert, S.E., *Incorporation of heparin into biomaterials.* Acta Biomater, 2014. **10**(4): p. 1581-7.

151. Domouzoglou, E.M., et al., *Fibroblast growth factors in cardiovascular disease: The emerging role of FGF21.* American Journal of Physiology - Heart and Circulatory Physiology, 2015. **309**(6): p. H1029-H1038.

152. Brudno, Y., et al., *Enhancing microvascular formation and vessel maturation through temporal control over multiple pro-angiogenic and pro-maturation factors.* Biomaterials, 2013. **34**(36): p. 9201-9.

153. Mendis, S., et al., *World Health Organization definition of myocardial infarction: 2008-09 revision.* Int J Epidemiol, 2011. **40**(1): p. 139-46.

154. Thygesen, K., et al., *Third universal definition of myocardial infarction.* J Am Coll Cardiol, 2012. **60**(16): p. 1581-98.

155. Weerasinghe, P., et al., *A model for cardiomyocyte cell death: Insights into mechanisms of oncosis.* Experimental and Molecular Pathology, 2013. **94**(1): p. 289-300.

156. Buja, L.M., *Myocardial ischemia and reperfusion injury.* Cardiovascular Pathology, 2005. **14**(4): p. 170-175.

157. Jones, R.H., et al., *Coronary Bypass Surgery with or without Surgical Ventricular Reconstruction.* New England Journal of Medicine, 2009. **360**(17): p. 1705-1717.

158. Haeck, M.L.A., et al., *Treatment options in end-stage heart failure: where to go from here?* Netherlands Heart Journal, 2012. **20**(4): p. 167-175.

159. Oni-Orisan, A. and D. Lanfear, *Pharmacogenomics in Heart Failure: Where Are We Now and How Can We Reach Clinical Application.* Cardiology in review, 2014. **22**(5): p. 193-198.

160. Agnetti, G., et al., *New Insights in the Diagnosis and Treatment of Heart Failure.* BioMed Research International, 2015. **2015**: p. 265260.

161. Jakovljevic, D.G., et al., *Left Ventricular Assist Device as a Bridge to Recovery for Patients With Advanced Heart Failure.* Journal of the American College of Cardiology, 2017. **69**(15): p. 1924-1933.

162. Akin, S., et al., *Haemolysis as a first sign of thromboembolic event and acute pump thrombosis in patients with the continuous-flow left ventricular assist device HeartMate II.* Netherlands Heart Journal, 2016. **24**(2): p. 134-142.

163. Gerds, H.Z.R., et al., *The diagnosis of left ventricular assist device thrombosis.* Netherlands Heart Journal, 2015. **23**(7-8): p. 389-391.

164. Nabeebaccus, A., S. Zheng, and A.M. Shah, *Heart failure—potential new targets for therapy.* British Medical Bulletin, 2016. **119**(1): p. 99-110.

165. Bernardo, B.C. and B.C. Blaxall, *From Bench to Bedside: New approaches to therapeutic discovery for heart failure.* Heart, lung & circulation, 2016. **25**(5): p. 425-434.

166. Dib, N., D.A. Taylor, and E.B. Diethrich, *Stem Cell Therapy and Tissue Engineering for Cardiovascular Repair: From Basic Research to Clinical Applications*. 2006: Springer.

167. Wang, Y., et al., *Degradable PLGA Scaffolds with Basic Fibroblast Growth Factor: Experimental Studies in Myocardial Revascularization.* Texas Heart Institute Journal, 2009. **36**(2): p. 89-97.

168. Badylak, S.F., D. Taylor, and K. Uygun, *Whole-organ tissue engineering: decellularization and recellularization of three-dimensional matrix scaffolds.* Annu Rev Biomed Eng, 2011. **13**: p. 27-53.

169. Johnson, T.D., R.L. Braden, and K.L. Christman, *Injectable ECM Scaffolds for Cardiac Repair.* Methods in molecular biology (Clifton, N.J.), 2014. **1181**: p. 109-120.

170. Singelyn, J.M. and K.L. Christman, *Modulation of Material Properties of a Decellularized Myocardial Matrix Scaffold.* Macromolecular Bioscience, 2011. **11**(6): p. 731-738.

171. Singelyn, J.M. and K.L. Christman, *Injectable Materials for the Treatment of Myocardial Infarction and Heart Failure: The Promise of Decellularized Matrices.* Journal of Cardiovascular Translational Research, 2010. **3**(5): p. 478-486.

172. Wang, B., et al., *Myocardial scaffold-based cardiac tissue engineering: application of coordinated mechanical and electrical stimulations.* Langmuir, 2013. **29**(35): p. 11109-17.

173. Rajabi, S., et al., *Human embryonic stem cell-derived cardiovascular progenitor cells efficiently colonize in bFGF-tethered natural matrix to construct contracting humanized rat hearts.* Biomaterials, 2018. **154**: p. 99-112.

174. Wang, B., et al., *Fabrication of cardiac patch with decellularized porcine myocardial scaffold and bone marrow mononuclear cells.* Journal of Biomedical Materials Research Part A, 2010. **94A**(4): p. 1100-1110.

175. Yang, M., et al., *Favorable effects of the detergent and enzyme extraction method for preparing decellularized bovine pericardium scaffold for tissue engineered heart valves.* Journal of Biomedical Materials Research Part B: Applied Biomaterials, 2009. **91B**(1): p. 354-361.

176. Brown, B.N. and S.F. Badylak, *Extracellular matrix as an inductive scaffold for functional tissue reconstruction.* Translational research : the journal of laboratory and clinical medicine, 2014. **163**(4): p. 268-285.

177. Badylak, S.F., *Xenogeneic extracellular matrix as a scaffold for tissue reconstruction.* Transplant Immunology, 2004. **12**(3–4): p. 367-377.

178. Seif-Naraghi, S.B., et al., *Design and Characterization of an Injectable Pericardial Matrix Gel: A Potentially Autologous Scaffold for Cardiac Tissue Engineering.* Tissue Engineering Part A, 2010. **16**(6): p. 2017-2027.

179. Jakus, A.E., et al., *"Tissue Papers" from Organ-Specific Decellularized Extracellular Matrices.* Adv Funct Mater, 2017. **27**(3).

180. Shridhar, A., et al., *Composite Bioscaffolds Incorporating Decellularized ECM as a Cell-Instructive Component Within Hydrogels as In Vitro Models and Cell Delivery Systems.* Methods Mol Biol, 2017.

181. Beachley, V., et al., *Extracellular matrix particle-glycosaminoglycan composite hydrogels for regenerative medicine applications.* J Biomed Mater Res A, 2018. **106**(1): p. 147-159.

182. Sun, D., et al., *Novel decellularized liver matrix-alginate hybrid gel beads for the 3D culture of hepatocellular carcinoma cells.* Int J Biol Macromol, 2018. **109**: p. 1154-1163.

183. Brown, A.L., et al., *Development of a Model Bladder Extracellular Matrix Combining Disulfide Cross-Linked Hyaluronan with Decellularized Bladder Tissue.* Macromolecular Bioscience, 2006. **6**(8): p. 648-657.

184. Wolf, M.T., et al., *A hydrogel derived from decellularized dermal extracellular matrix.* Biomaterials, 2012. **33**(29): p. 7028-7038.

185. Sawkins, M.J., et al., *Hydrogels derived from demineralized and decellularized bone extracellular matrix.* Acta Biomaterialia, 2013. **9**(8): p. 7865-7873.

186. Young, D.A., et al., *Injectable hydrogel scaffold from decellularized human lipoaspirate.* Acta Biomaterialia, 2011. **7**(3): p. 1040-1049.

187. Rane, A.A., et al., *Increased infarct wall thickness by a bio-inert material is insufficient to prevent negative left ventricular remodeling after myocardial infarction.* PLoS One, 2011. **6**(6): p. e21571.

188. Jorge-Herrero, E., et al., *Influence of different chemical cross-linking treatments on the properties of bovine pericardium and collagen.* Biomaterials, 1999. **20**(6): p. 539-45.

189. Ma, B., et al., *Crosslinking strategies for preparation of extracellular matrix-derived cardiovascular scaffolds.* Regen Biomater, 2014. **1**(1): p. 81-9.

190. Jayakrishnan, A. and S.R. Jameela, *Glutaraldehyde as a fixative in bioprostheses and drug delivery matrices.* Biomaterials, 1996. **17**(5): p. 471-84.

191. Gaudière, F., et al., *Genipin-Cross-Linked Layer-by-Layer Assemblies: Biocompatible Microenvironments To Direct Bone Cell Fate.* Biomacromolecules, 2014. **15**(5): p. 1602-1611.

192. Jianliang, Z., et al., *Promoting endothelialization on decellularized porcine aortic valve by immobilizing branched polyethylene glycolmodified with cyclic-RGD peptide: an in vitro study.* Biomedical Materials, 2015. **10**(6): p. 065014.

193. Fiejdasz, S., et al., *Biopolymer-based hydrogels as injectable materials for tissue repair scaffolds.* Biomed Mater, 2013. **8**(3): p. 035013.

194. Wang, C., et al., *Cytocompatibility study of a natural biomaterial crosslinker—Genipin with therapeutic model cells.* Journal of Biomedical Materials Research Part B: Applied Biomaterials, 2011. **97B**(1): p. 58-65.

195. Qiu, J., et al., *In vitro Investigation on the Biodegradability and Biocompatibility of Genipin Cross-linked Porcine Acellular Dermal Matrix with Intrinsic Fluorescence.* ACS Applied Materials & Interfaces, 2013. **5**(2): p. 344-350.

196. Zhou, X., et al., *Genipin cross-linked type II collagen/chondroitin sulfate composite hydrogel-like cell delivery system induces differentiation of adipose-derived stem cells and regenerates degenerated nucleus pulposus.* Acta Biomater, 2018. **71**: p. 496-509.

197. Sundararaghavan, H.G., et al., *Genipin-induced changes in collagen gels: correlation of mechanical properties to fluorescence.* J Biomed Mater Res A, 2008. **87**(2): p. 308-20.

198. Hwang, Y.J., et al., *Effect of genipin crosslinking on the optical spectral properties and structures of collagen hydrogels.* ACS Appl Mater Interfaces, 2011. **3**(7): p. 2579-84.

199. Matcham, S. and K. Novakovic, *Fluorescence Imaging in Genipin Crosslinked Chitosan-Poly(vinyl pyrrolidone) Hydrogels.* Polymers, 2016. **8**(11).

200. Butler, M.F., Y.-F. Ng, and P.D.A. Pudney, *Mechanism and kinetics of the crosslinking reaction between biopolymers containing primary amine groups and genipin.* Journal of Polymer Science Part A: Polymer Chemistry, 2003. **41**(24): p. 3941-3953.

201. Dimida, S., et al., *Genipin-cross-linked chitosan-based hydrogels: Reaction kinetics and structure-related characteristics.* Journal of Applied Polymer Science, 2015. **132**(28).

202. Muzzarelli, R.A.A., et al., *Genipin-Crosslinked Chitosan Gels and Scaffolds for Tissue Engineering and Regeneration of Cartilage and Bone.* Marine Drugs, 2015. **13**(12): p. 7314-7338.

203. Yang, G., et al., *Assessment of the characteristics and biocompatibility of gelatin sponge scaffolds prepared by various crosslinking methods.* Sci Rep, 2018. **8**(1): p. 1616.

204. Jeffords, M.E., et al., *Tailoring material properties of cardiac matrix hydrogels to induce endothelial differentiation of human mesenchymal stem cells.* ACS Appl Mater Interfaces, 2015. **7**(20): p. 11053-61.

205. Elder, S., et al., *Evaluation of genipin for stabilization of decellularized porcine cartilage.* Journal of Orthopaedic Research, 2016. **35**(9): p. 1949-1957.

206. Sa, S., L. Wong, and K.E. McCloskey, *Combinatorial fibronectin and laminin signaling promote highly efficient cardiac differentiation of human embryonic stem cells.* BioResearch open access, 2014. **3**(4): p. 150-161.

207. Israeli-Rosenberg, S., et al., *Integrins and integrin-associated proteins in the cardiac myocyte.* Circulation research, 2014. **114**(3): p. 572-586.

208. Ross, R.S., *Molecular and mechanical synergy: cross-talk between integrins and growth factor receptors.* Cardiovascular Research, 2004. **63**(3): p. 381-390.

209. Czyz, J., et al., *Loss of beta 1 integrin function results in upregulation of connexin expression in embryonic stem cell-derived cardiomyocytes.* The International Journal Of Developmental Biology, 2005. **49**(1): p. 33-41.

210. Schroer, A.K. and W.D. Merryman, *Mechanobiology of myofibroblast adhesion in fibrotic cardiac disease.* Journal of cell science, 2015. **128**(10): p. 1865-1875.

211. Maitra, N., et al., *Expression of α and β integrins during terminal differentiation of cardiomyocytes.* Cardiovascular Research, 2000. **47**(4): p. 715-725.

212. Wang, L., et al., *Degradation of Internalized αvβ5 Integrin Is Controlled by uPAR Bound uPA: Effect on β1 Integrin Activity and α-SMA Stress Fiber Assembly.* PLOS ONE, 2012. **7**(3): p. e33915.

213. Rangappa, S., et al., *Transformation of adult mesenchymal stem cells isolated from the fatty tissue into cardiomyocytes.* The Annals of Thoracic Surgery, 2003. **75**(3): p. 775-779.

214. Oedayrajsingh-Varma, M., et al., *Adipose tissue-derived mesenchymal stem cell yield and growth characteristics are affected by the tissue-harvesting procedure.* Cytotherapy, 2006. **8**(2): p. 166-177.

215. Baghalishahi, M., et al., *Cardiac extracellular matrix hydrogel together with or without inducer cocktail improves human adipose tissue-derived stem cells differentiation into cardiomyocyte–like cells.* Biochemical and Biophysical Research Communications, 2018. **502**(2): p. 215-225.

216. Sonnenberg, S.B., et al., *Delivery of an engineered HGF fragment in an extracellular matrix-derived hydrogel prevents negative LV remodeling post-myocardial infarction.* Biomaterials, 2015. **45**: p. 56-63.

217. Mousavi, S.J. and M. Hamdy Doweidar, *Role of Mechanical Cues in Cell Differentiation and Proliferation: A 3D Numerical Model.* PLOS ONE, 2015. **10**(5): p. e0124529.

218. Hogrebe, N.J. and K.J. Gooch, *Direct influence of culture dimensionality on human mesenchymal stem cell differentiation at various matrix stiffnesses using a fibrous self-assembling peptide hydrogel.* Journal Of Biomedical Materials Research. Part A, 2016. **104**(9): p. 2356-2368.

219. van Dijk, A., et al., *Differentiation of human adipose-derived stem cells towards cardiomyocytes is facilitated by laminin.* Cell and Tissue Research, 2008. **334**(3): p. 457-467.

220. Tan, G., et al., *Differential effect of myocardial matrix and integrins on cardiac differentiation of human mesenchymal stem cells.* Differentiation, 2010. **79**(4): p. 260-271.

221. *European Commission. Background document: Public Consultation 'Science 2.0': Science in Transition. Directorates-General for Research and Innovation (RTD) and Communications Networks, content and Technology (CONNECT). 2014.* http://ec.europa.eu/research/consultations/science-2.0/background.pdf.Accessed *05/09/2015.*

222. Bonnans, C., J. Chou, and Z. Werb, *Remodelling the extracellular matrix in development and disease.* Nature reviews. Molecular cell biology, 2014. **15**(12): p. 786-801.

223. Lu, P., et al., *Extracellular matrix degradation and remodeling in development and disease.* Cold Spring Harbor perspectives in biology. **3**(12): p. a005058.

224. Sarker, M.D., et al., *3D biofabrication of vascular networks for tissue regeneration: A report on recent advances.* J Pharm Anal, 2018. **8**(5): p. 277-296.

225. Sun, X., W. Altalhi, and S.S. Nunes, *Vascularization strategies of engineered tissues and their application in cardiac regeneration.* Advanced Drug Delivery Reviews, 2016. **96**: p. 183-194.

226. Tang-Quan, K.R., et al., *Whole Cardiac Tissue Bioscaffolds*, in *Cardiac Extracellular Matrix: Fundamental Science to Clinical Applications*, E.G. Schmuck, P. Hematti, and A.N. Raval, Editors. 2018, Springer International Publishing: Cham. p. 85-114.

227. Hussein, K.H., et al., *Heparin-gelatin mixture improves vascular reconstruction efficiency and hepatic function in bioengineered livers.* Acta Biomaterialia, 2016. **38**: p. 82-93.

228. Bao, J., et al., *Hemocompatibility improvement of perfusion-decellularized clinical-scale liver scaffold through heparin immobilization.* Scientific reports, 2015. **5**: p. 10756-10756.

229. Nakatsu, M.N., et al., *Angiogenic sprouting and capillary lumen formation modeled by human umbilical vein endothelial cells (HUVEC) in fibrin gels: the role of fibroblasts and Angiopoietin-1 ☆*. Microvascular Research, 2003. **66**(2): p. 102-112.

230. Carmeliet, P., *Mechanisms of angiogenesis and arteriogenesis.* Nature Medicine, 2000. **6**(4): p. 389.

231. Chang, J.H., et al., *Matrix metalloproteinase 14 modulates signal transduction and angiogenesis in the cornea.* Surv Ophthalmol, 2015.

232. Davis, G.E., P.R. Norden, and S.L. Bowers, *Molecular control of capillary morphogenesis and maturation by recognition and remodeling of the extracellular matrix: functional roles of endothelial cells and pericytes in health and disease.* Connect Tissue Res, 2015. **56**(5): p. 392-402.

233. Page-McCaw, A., A.J. Ewald, and Z. Werb, *Matrix metalloproteinases and the regulation of tissue remodelling.* Nat Rev Mol Cell Biol, 2007. **8**(3): p. 221-33.

234. Eisenach, P.A., et al., *MT1-MMP regulates VEGF-A expression through a complex with VEGFR-2 and Src.* J Cell Sci, 2010. **123**(Pt 23): p. 4182-93.

235. Sacharidou, A., et al., *Endothelial lumen signaling complexes control 3D matrix-specific tubulogenesis through interdependent Cdc42- and MT1-MMP-mediated events.* Blood, 2010. **115**(25): p. 5259-69.

236. Sacharidou, A., A.N. Stratman, and G.E. Davis, *Molecular mechanisms controlling vascular lumen formation in three-dimensional extracellular matrices.* Cells Tissues Organs, 2012. **195**(1-2): p. 122-43.

237. Davis, G.E., W. Koh, and A.N. Stratman, *Mechanisms controlling human endothelial lumen formation and tube assembly in three-dimensional extracellular matrices.* Birth Defects Research Part C: Embryo Today: Reviews, 2007. **81**(4): p. 270-285.

238. Iruela-Arispe, M.L. and G.E. Davis, *Cellular and Molecular Mechanisms of Vascular Lumen Formation.* Developmental Cell, 2009. **16**(2): p. 222-231.

239. Bayless, K.J. and G.E. Davis, *The Cdc42 and Rac1 GTPases are required for capillary lumen formation in three-dimensional extracellular matrices.* Journal of Cell Science, 2002. **115**(6): p. 1123-1136.

240. Dragoni, S., et al., *Vascular Endothelial Growth Factor Stimulates Endothelial Colony Forming Cells Proliferation and Tubulogenesis by Inducing Oscillations in Intracellular Ca2+ Concentration.* Stem Cells, 2011. **29**(11): p. 1898-1907.

241. Egorova, A.D., et al., *Endothelial colony-forming cells show a mature transcriptional response to shear stress.* In Vitro Cellular & Developmental Biology-Animal, 2012. **48**(1): p. 21-29.

242. Evrard, S.M., et al., *The profibrotic cytokine transforming growth factor-beta1 increases endothelial progenitor cell angiogenic properties.* J Thromb Haemost, 2012. **10**(4): p. 670-9.

243. Thurston, G., et al., *Leakage-resistant blood vessels in mice transgenically overexpressing angiopoietin-1*. Science, 1999. **286**(5449): p. 2511-4.

244. Song, M., Y. Zhou, and Y. Liu, *VEGF heparinized-decellularized adipose tissue scaffolds enhance tissue engineering vascularization in vitro.* RSC Advances, 2018. **8**(59): p. 33614-33624.

245. Subbiah, R. and R.E. Guldberg, *Materials Science and Design Principles of Growth Factor Delivery Systems in Tissue Engineering and Regenerative Medicine.* 2019. **8**(1): p. 1801000.

246. Adair, T.H., *Angiogenesis*. 2011, [San Rafael, Calif.] :: Morgan & Claypool Life Sciences.

247. Kiosses, W.B., et al., *A Dominant-Negative p65 PAK Peptide Inhibits Angiogenesis.* 2002. **90**(6): p. 697-702.

248. Boatman, J.A. and D.M. Vock, *Estimating the causal effect of treatment regimes for organ transplantation.* Biometrics, 2018. **74**(4): p. 1407-1416.

APPENDIX I

Manuscripts accepted for publication:

"Whole Cardiac Bioscaffolds"

Manuscripts in preparation/submission:

"Characterization of dECM hydrogel and influence on cell behavior and differentiation"

"Vascularizing decellularized tissues- Current understandings and future directions"